UNIVERSITY OF SIENA

DEPARTMENT OF MEDICAL BIOTECHNOLOGIES

PhD COURSE IN MEDICAL BIOTECHNOLOGIES

SECTION OF MICROBIOLOGY AND VACCINES

XXXV CYCLE

Antimicrobial and antibiofilm activity of drug combinations and violet-blue light against clinically relevant bacterial pathogens causing airway infections

Supervisor:
Prof.ssa Lucia Pallecchi

PhD candidate:
Felice Valzano

Academic year 2021/2022

FOREWORD

This PhD thesis is divided in seven sections: background, aim of the PhD research project, results and discussion, conclusions and perspectives, bibliography, my PhD activities, and annexes. The annexes include the research papers that have been published in international scientific journals in relation to the thesis work.

CONTENTS

PART I – BACKGROUND

PART II – AIM OF THE PhD PROJECT

PART III – RESULTS AND DISCUSSION

PART I

BACKGROUND

1. Biofilm-related respiratory tract infections

Pulmonary diseases, such as cystic fibrosis (CF), chronic obstructive pulmonary disease (COPD), non-CF bronchiectasis, and ventilator-associated pneumonia (VAP), are usually characterized by irreversible decline in lung function, compromised immune system, decreased mucus clearance, and alteration of the physiological environment. These disfunctions create conditions promoting bacterial invasion and infection in the host. Bacteria can survive in the respiratory tract by switching from the planktonic to the biofilm mode of growth, which provides tolerance to the inflammatory defence mechanisms and antibiotic therapy. In fact, biofilm colonization has been demonstrated to be responsible for both acute and chronic events in airway infections and is a real challenge in clinical practice (Ciofu *et al.*, 2022; Lebeaux *et al.*, 2014; Bjarnsholt, 2013).

1.1 Biofilm lifestyle, tolerance and resistance

Bacterial pathogens causing pulmonary infections tend to grow in biofilms and may eventually lead to chronic infection. In contrast to planktonic motile bacteria, which appear as segregated cells, bacteria existing in biofilm appear as an aggregated microbial community of sessile cells embedded in an extracellular polymeric substances (EPS) matrix (Bjarnsholt, 2013; Davies, 2003). Biofilms appear as cellular cluster or microcolonies, whose formation is regulated by intercellular small messenger molecules, (i.e., acylated homoserine lactones, AHLs), that are used for a cell-cell communication process, namely quorum sensing (QS), which in turn regulates gene expression based on the bacterial density (Bjarnsholt, 2013; Davies, 2003).

Five stages have been identified in biofilm development (Figure 1): i) reversible early attachment, where planktonic cells adhere to the surface through reversible van der Waals forces; ii) irreversible late attachment, where bacteria tightly attach to the surface through fimbrial and non-fimbrial adhesins and begin producing EPS; iii) early maturation stage where biofilm takes form and consists of microcolonies immersed in EPS; iv) biofilm maturation stage, characterized by microcolonies separated by open water channels that act as circulatory system; v) dispersion stage, where mature biofilm begins to release planktonic cells and bacterial aggregates (Bjarnsholt, 2013; Davies, 2003).

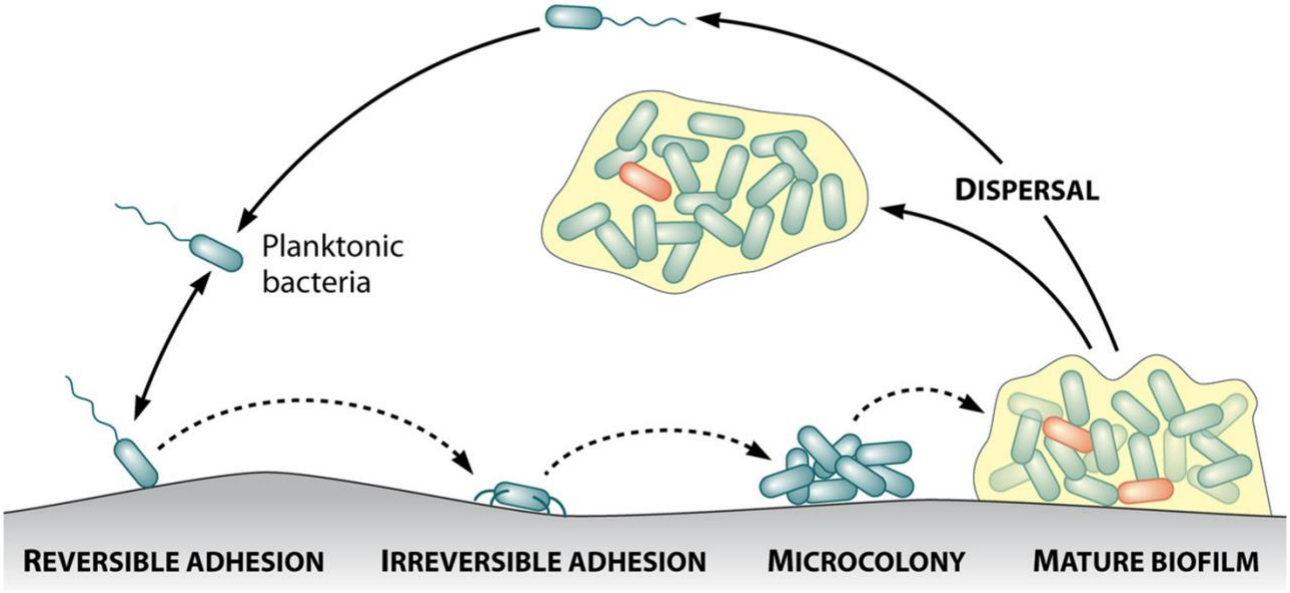

Figure 1. Five stages of biofilm development. Adapted from Lebeaux *et al.* (Lebeaux *et al.*, 2014).

Biofilms have been always associated with recurrent and chronic infections. Unlike planktonic cells, generally implicated in acute infections and better responsive to antimicrobial agent treatments (because of their faster growth rates and higher metabolic activity), biofilms are responsible of chronic infections difficult to treat due to their tolerance and/or resistance to antimicrobials and host immune response (Ciofu *et al.*, 2022; Lebeaux *et al.*, 2014; Bjarnsholt, 2013).

Tolerance to host defences, such as polymorphonuclear leukocytes (PMNs), complement system and antibodies, is related to the presence of the EPS matrix: not only PMNs are unable to phagocytise bacterial aggregates larger than their own size, but also the matrix exopolysaccharides (i.e., Psl and alginate) protect biofilms from opsonization and killing by PMNs and macrophages. Proteolytic enzymes produced by *P. aeruginosa* biofilm and the O-acetylation of alginate are other two strategies to defend biofilm from the complement system. Additionally, the production of rhamnolipids responsible of cellular necrosis and tissue damage lead to the failure of the PMNs-mediated killing (Ciofu *et al.*, 2022; Lebeaux *et al.*, 2014; Bjarnsholt, 2013).

However, the persistence of chronic infection could be better explained by tolerance mechanisms to antimicrobials. In fact, the EPS matrix reduce or delay the antibiotic diffusion across the biofilm (demonstrated for some antibiotics that may be trapped by the EPS matrix, such as tobramycin, polymyxins and glycopeptides) and, consequently, biofilm cells activate adaptive stress responses that further contribute to tolerance (Ciofu *et al.*, 2022; Lebeaux *et al.*, 2014; Bjarnsholt, 2013). On the other hand, a stratified bacterial physiology in biofilms, due to a spatial distribution of nutrients

and oxygen, corresponds to stratified layers of susceptibility (Figure 2): while at the air-liquid interface there is a subpopulation of metabolically active and fast-growing cells that consumes oxygen, a subpopulation of metabolically inactive and slow-growing or non-growing cells are located in the deep layers of the biofilm where survive under anoxic conditions. Consequently, the low metabolic activity of these bacterial cells can be translated into low antibiotic target production and activity, affecting the activity of different types of antibiotics (Ciofu *et al.*, 2022; Lebeaux *et al.*, 2014; Bjarnsholt, 2013). Similarly, the intense oxygen consumption mediated by PMNs accumulated at the site of infection, lead to bacteria to adapt to slow growth and anaerobic lifestyles. Indeed, slow-growing biofilms, such as those formed by *P. aeruginosa*, *Stenotrophomonas maltophilia*, *Staphylococcus aureus*, *Achromobacter xylosoxidans* and *Streptococcus pneumoniae*, have been described in respiratory secretions obtained from patients with chronic lung infection (Ciofu *et al.*, 2022; Lebeaux *et al.*, 2014). Moreover, there is a subpopulation (<1% of bacterial population) of dormant and non-dividing cells, namely persister cells, that lacks genetic resistance determinants and survive to high doses of antibiotics. These are described as tolerant but not resistant cells since when stress is removed can revert to fast-dividing cells, causing relapse of the biofilm infection while displaying the original, non-persister antibiotic susceptible profile (Ciofu *et al.*, 2022; Lebeaux *et al.*, 2014).

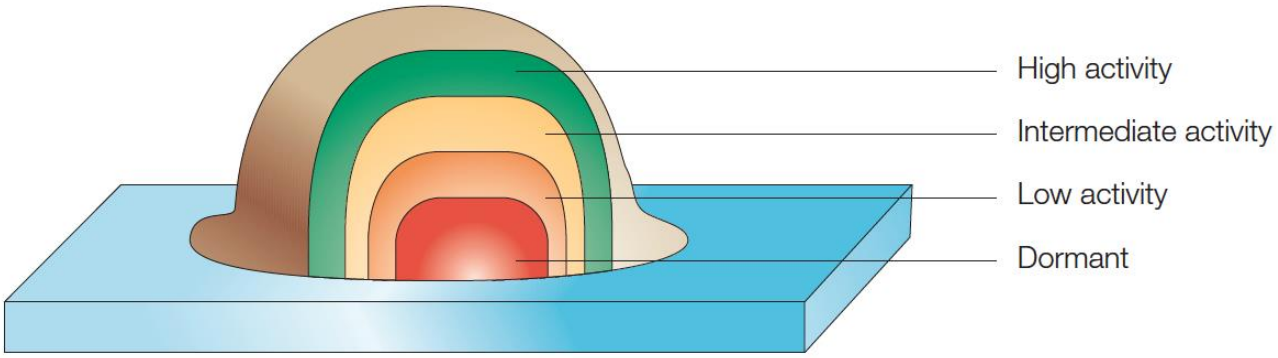

Figure 2. Approximative metabolic activity in a biofilm microcolony (Davies, 2003).

Other adaptation mechanisms are involved in the tolerance to antimicrobials, including: i) the stringent response, which alters cellular physiology causing biofilm tolerance to fluoroquinolones, meropenem and gentamycin by preventing the accumulation of reactive oxygen species (ROSs); ii) the SOS response, which repairs DNA by oxidative damage leading to β-lactams, fluoroquinolones or aminoglycosides tolerance; iii) adaptative resistance, following polymyxins or β-lactams exposure, which triggers temporary upregulation of resistance genes, such as those involved in the activation of

two-component systems (e.g., *pmrAB*), multidrug efflux pumps (e.g., *mexAB-oprM*) or β-lactamases (Ciofu *et al.*, 2022; Lebeaux *et al.*, 2014).

In contrast to tolerance, acquired resistance (AMR) is not transient, and is caused by either chromosomal mutations and/or acquisition of resistance genes by horizontal gene transfer (HGT). Firstly, impaired antibiotic diffusion through the matrix (as discussed above) exposes some biofilm areas to sub-inhibitory concentrations of antibiotics, thus facilitating the selection of resistant mutants (Ciofu *et al.*, 2022; Lebeaux *et al.*, 2014). In this respect, the development of *P. aeruginosa* mutants with quinolones resistance due to the upregulation of efflux pumps in biofilms it has been reported (Ahmed *et al.*, 2020; Frimodt-Møller *et al.*, 2018). At the same time, HGT may be favoured inside biofilm due to the close distance between cells embedded in the matrix. In fact, high rates of conjugation have been demonstrated *in vitro* in *S. aureus* and *Klebsiella pneumoniae* biofilms in comparison to planktonic cultures (Savage *et al.*, 2013; Hennequin *et al.*, 2012).

1.2 Cystic fibrosis and chronic biofilm infection

Biofilm-associated infections represent the main life threat for patients with CF. In such patients, the malfunction of the chloride channel leads to decreased volume of the paraciliary fluid in the lower respiratory tract and impaired mucus detachment from the submucosal gland ducts, thus interfering with mucociliary clearance and leading to defective host defence against respiratory bacterial infections (Ciofu *et al.*, 2015). *P. aeruginosa* is among the most common bacterial species involved in respiratory tract infection in CF patients and can be found in up to 80% of adults. The ability of *P. aeruginosa* to form biofilms is thought to be the primary reason for its survival and persistence in the CF lung (Figure 3A, 3B and 3C) (Ciofu *et al.*, 2015). Other pathogens such as *Burkholderia cepacia* complex, *S. aureus*, *S. maltophilia*, and *A. xylosoxidans* have also been shown to be able to grow as biofilms in CF airways, thus contributing to the CF morbidity and mortality (Figure 3D, 3E and 3F) (Ciofu *et al.*, 2015).

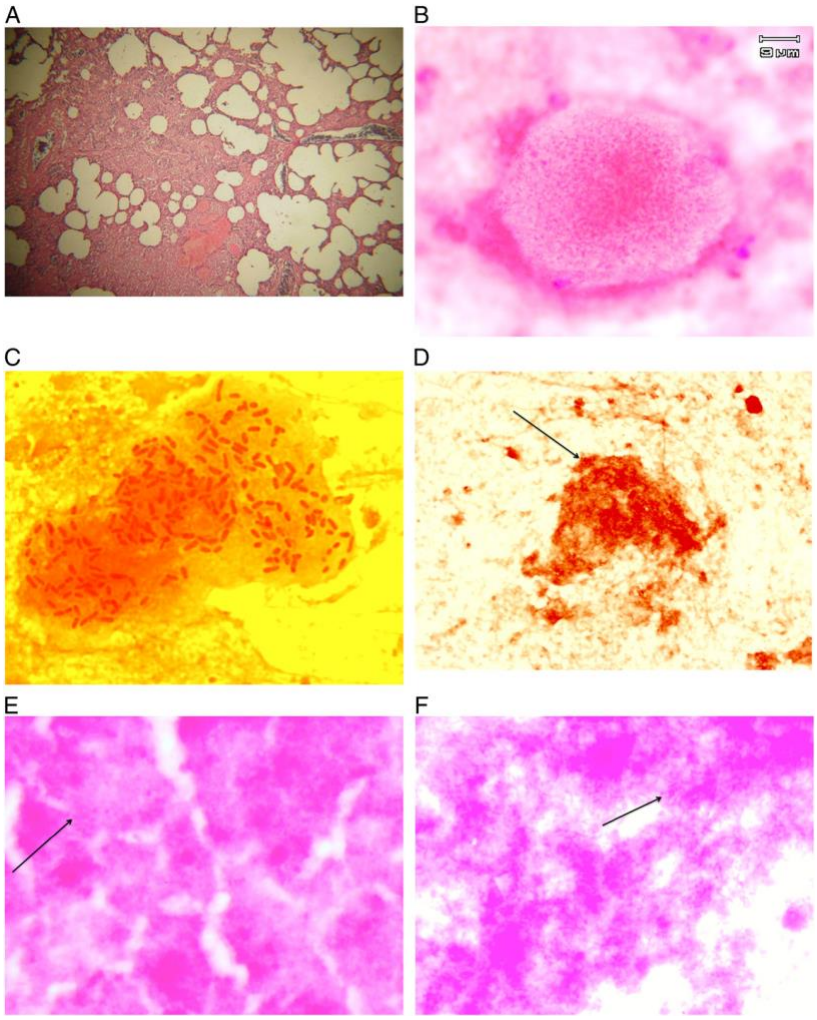

Figure 3. Biofilms of CF-related pathogens in the lungs of patients with cystic fibrosis. A) Mucoid biofilm of *P. aeruginosa* in an alveolar sac surrounded by severely inflamed tissue (PMNs, pneumonia) (HE stain ×100). B) *P. aeruginosa* biofilm in a detached lung alveole in sputum from a CF patient suffering from chronic lung infection (Gram-stained smear, ×1000 magnification). C) *P. aeruginosa* biofilm in sputum from a cystic fibrosis patient suffering from chronic lung infection (Gram-stained smear, ×1000 magnification). D) *A. xylodoxidans* biofilm in sputum from a CF patient suffering from chronic lung infection (Gram-stained smear, ×400 magnification). E) *B. multivorans* biofilm in sputum from a CF patient suffering from chronic lung infection (Gram-stained smear, ×1000 magnification). F) *S. maltophilia* biofilm in sputum from a CF patient suffering from chronic lung infection (Gram-stained smear, ×1000 magnification) (Ciofu *et al.*, 2015).

The *P. aeruginosa* infection starts from the paranasal sinuses which are colonized before the lower airways. *P. aeruginosa*, therefore, adapts to the upper airways and forms biofilms from where it repeatedly colonizes the lower airways leading successively to chronic lung infection (Høiby *et al.*, 2017; Fothergill *et al.*, 2014). The lower airways consist of the conductive zone (at the bronchioles level) where the mucosa is ciliated and where sputum is produced, and the respiratory zone (at the alveoli levels) where there are not cilia and sputum production (Høiby *et al.*, 2017). During lung infections, PMNs are recruited from the alveolar capillaries and transported to the conductive zone where cause oxygen consumption, ROSs formation and, additionally, DNA and proteases release. The chronic inflammation triggered by *P. aeruginosa* biofilms is therefore dominated by PMNs in both the respiratory zone and the conductive zone inside sputum. In the respiratory zone, this leads to tissue damage and loss of lung function, whereas in the conductive zone it leads to obstruction of the airways. Here the sputum becomes also viscid and anaerobic due to the consumption of oxygen by PMNs (Høiby *et al.*, 2017).

All these physiologically stressful conditions, in addition to intra/interspecies competition and high concentrations of antibiotics used to treat infection, drive *P. aeruginosa* microevolution, characterized by the acquisition of mutations followed by the selection of clones better adapted for long-term colonization of the airways (Rossi *et al.*, 2021). In most patients, the primary colonizing bacterium (clone) persists and dominates for extended periods of time, although other patients may be colonized in the long-term by more than one *P. aeruginosa* strain, which coexist stably. The invasion by new clones coming from other patients can occur frequently, but in most cases the adapted residing bacterial population keeps the invaders out (Rossi *et al.*, 2021). Nonetheless, phenotypic features associated with the clone adaptation include: i) flagella downregulation, which enables evasion of immune system recognition and phagocytosis; ii) lipid A modifications, causing reduced phagocyte recruitment and lower proinflammatory cytokine production; iii) expression of the denitrification operons (i.e., *nar*, *nir*, *nor*, *nos* operons), which allow to respond to the PMNs-mediate oxygen limitation and consequently to grow in anaerobic environment (Rossi *et al.*, 2021; Malhotra *et al.*, 2019; Ciofu *et al.*, 2015). In addition, the exposure to neutrophil-derived antimicrobials (e.g., antimicrobial peptides) is responsible of mutations in genes involved in DNA repair (i.e., *mutS* and *mutL*) associated with the occurrence of "hypermutator" populations of *P. aeruginosa* exhibiting reduced virulence and increased antibiotic resistance, thus conferring advantages to the whole populations (Rossi *et al.*, 2021; Malhotra *et al.*, 2019; Ciofu *et al.*, 2015).

Further phenotypic changes involving *P. aeruginosa* during chronic infection of the CF lungs include the overproduction of exopolysaccharides (i.e., Psl, Pel, and alginate), the major components of the

biofilm EPS matrix conferring resistance to antibiotics and innate immune effectors. In particular, the overproduction of alginate is responsible for the emergence of mucoid *P. aeruginosa* strains, which are associated with the transition to chronic infection, severe bronchiectasis, and accelerated lung function decline (Rossi *et al.*, 2021; Malhotra *et al.*, 2019; Ciofu *et al.*, 2015). Mucoidy offers to *P. aeruginosa* several advantages *in vivo*, including: (i) antibiotic and phagocytosis resistance, (ii) ability to inhibit PMNs chemotaxis, (iii) biofilm-like characteristics and (iv) evasion of immune detection by flagella downregulation (Malhotra *et al.*, 2019).

1.3 Other chronic lung diseases

Other chronic lung diseases, such as COPD, non-CF bronchiectasis and VAP, are all characterized by a cycle of events promoting impaired mucociliary clearance and retention of airway secretions, even though each one with a different aetiology. For example, in the setting of COPD, the exposition to noxious gases (e.g., cigarette smoke) impairs normal breathing and/or destructs the lung parenchyma (Mammen and Sethi, 2016; Hassett *et al.*, 2014; Beasley *et al.*, 2012), whereas in non-CF bronchiectasis, an initial airways injury (i.e., either because of severe infection or mechanical injury) together with immune or autosomal disorders can be the cause of a change in the muscular and elastic components of the bronchial wall, which become distorted and enlarged (Marsh *et al.*, 2022; Flume *et al.*, 2018; Chalmers and Hill, 2013). Instead, in patients admitted into intensive care units (ICU) and receiving mechanical ventilation, the insertion of an endotracheal tube (ETT) lead to the accumulation of tracheobronchial secretions, because of the disruption of the cough reflex, other than facilitate the inoculation of endogenous oropharyngeal bacteria in the low airway tract (Papazian *et al.*, 2020; Fernández-Barat and Torres, 2016; Gil-Perotin *et al.*, 2012). These events disrupt the host's defences, due to the inability of the airways to clear mucus, facilitating the colonization of bacteria and rendering the airways more susceptible to establishment of chronic infection. As consequence, the persistence of bacterial pathogens incites an inflammatory response that results in a further injury and pathological remodelling of the airways, allowing further bacterial persistence and proliferation. This circle of chronic infection and inflammation contributes to the progressive lung damage and loss of function characteristic of such respiratory diseases (Flume *et al.*, 2018; Mammen and Sethi, 2016) (Figure 4).

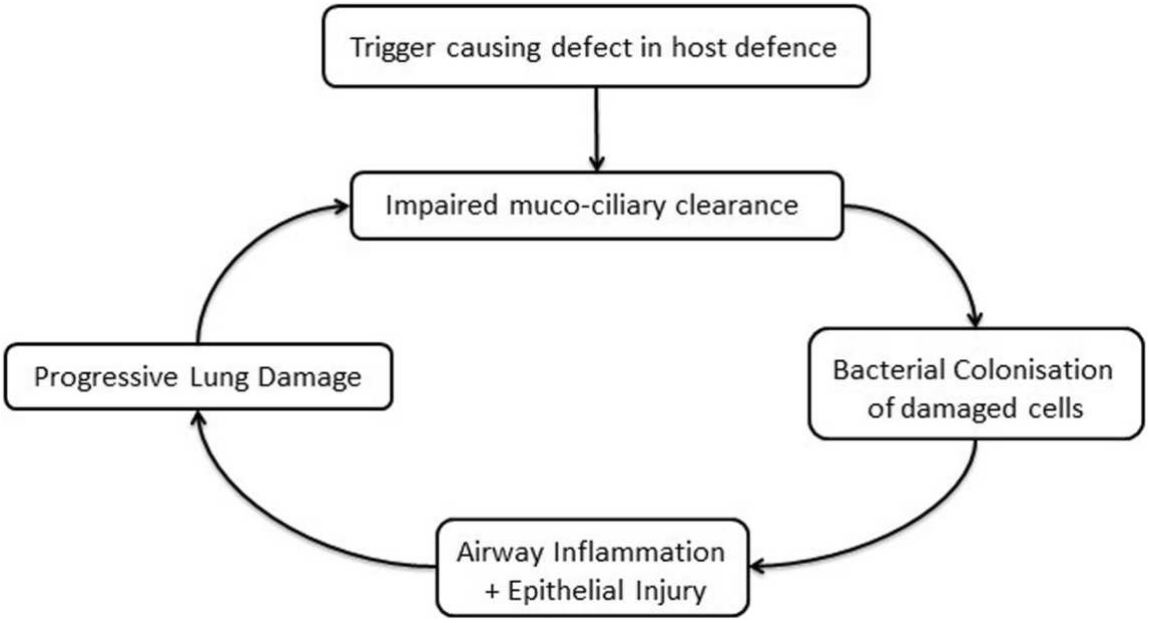

Figure 4. The vicious cycle hypothesis based on Peter Cole's original description (Mitchelmore *et al.*, 2018).

In general, the most common pathogenic bacteria associated with COPD and non-CF bronchiectasis include *Haemophilus influenzae*, *S. pneumoniae*, and *Moraxella catarrhalis* However, the bacterial flora varies with disease severity as Gram-negative organisms, such as *P. aeruginosa*, are more commonly detected in patients with more severe airflow obstruction. In fact, it has been reported that *P. aeruginosa* infection is associated with worse lung function, more exacerbations and increased mortality in patients with COPD and bronchiectasis not due to CF (Marsh *et al.*, 2022; Flume *et al.*, 2018; Mammen and Sethi, 2016; Hassett *et al.*, 2014; Chalmers and Hill, 2013; Beasley *et al.*, 2012). Additionally, similarly to CF, *P. aeruginosa* persistent infections are usually caused by a single clone showing increased antibiotic resistance, lowered motility, and greater mucoid biofilm production (Hassett *et al.*, 2014). In fact, mucoid *P. aeruginosa* strains are commonly isolated from chronically colonized COPD patients and the alginate production is considered a biomarker for the biofilm mode of growth of *P. aeruginosa* in the thick COPD airway mucus (Hassett *et al.*, 2014). On the other hand, it has recently been demonstrated biofilm presence in bronchoalveolar lavage from children with non-CF bronchiectasis, thus confirming the relevant role of the biofilm in the pathophysiological cascade and treatment responses of such a disease (Marsh *et al.*, 2022).

Concerning ICU-ventilated patients, biofilms can develop rapidly following intubation, with well-organized structures detectable within 24 hours (Fernández-Barat and Torres, 2016; Gil-Perotin *et al.*, 2012). Evidences also report that the same microorganisms causing VAP are found in the ETT biofilm, thus demonstrating the microbial link between airway colonization, biofilm formation and

VAP development. This could be due to the use of mechanical ventilation or invasive techniques (e.g., bronchoscopy or tracheal aspiration), which allow biofilm to easily reach the distal tracheobronchial tree, thus contributing to the development of VAP (Fernández-Barat and Torres, 2016; Gil-Perotin *et al.*, 2012). Usual microorganisms involved in early-onset VAP (≤4 days of intubation) are *H. influenzae*, *Enterobacter cloacae* and *Streptococcus* spp., while *P. aeruginosa*, *Acinetobacter baumannii* and *S. aureus* are involved in late-onset VAP, where are responsible of microbial persistence, treatment failure and relapse episodes, other than represent a VAP risk factor in colonized patients (Fernández-Barat and Torres, 2016; Gil-Perotin *et al.*, 2012).

2. Pathogens

2.1 *Pseudomonas aeruginosa*

P. aeruginosa is a Gram-negative aerobe/facultative anaerobe found ubiquitously in soil and aquatic environments. Metabolically may use nitrite or nitrate as terminal electron acceptor under anoxic conditions, including those within the CF lung. It is also capable of three forms of motility, which include flagellum-dependent swimming, flagellum- and pilus-dependent swarming, and pilus-dependent twitching, allowing to colonize different environments. All these features contribute to the pathogenicity *P. aeruginosa*, which is also the leading pathogen infecting adult CF patients and for this reason the most studied model system (Malhotra *et al.*, 2019).

The worldwide spreading of multidrug (MDR) and pan-drug resistant (PDR) strains makes *P. aeruginosa* infections a serious threat (Pang *et al.*, 2019). The development of resistance to a wide range of antibiotics is mainly due to a combination of intrinsic, acquired and/or adaptive resistance mechanisms including: i) low permeability of the outer membrane (due to loss or reduced expression of OprD porin, leading to carbapenems and cephalosporins resistance); ii) overexpression of efflux pumps (i.e., MexAB-OprM, responsible for efflux of nearly all β-lactams and fluoroquinolones, and MexXY-OprM, expelling aminoglycosides); iii) and the production of antibiotic inactivating enzymes (i.e., AmpC β-lactamase and extended-spectrum β-lactamases, implicated in the resistance to wide range of β-lactams) (Pang *et al.*, 2019). In addition, acquired resistance of *P. aeruginosa* can occur by HGT of plasmid-carried resistance genes (e.g., *mcr-1* gene, conferring resistance to colistin, and genes encoding carbapenemases), or mutational changes (e.g., those within the fluoroquinolone targets, such as DNA gyrase and topoisomerase IV-encoding genes *gyrA*, *gyrB*, *parC* and *parE*) (Pang *et al.*, 2019). All these resistance mechanisms are clinically important not only due to their activity

on a wide range of antibiotics, but also for their worldwide prevalence. For example, the spread of carbapenemase-producing *P. aeruginosa* strains is a growing concern, with carbapenemases-encoding genes found in all continents (Tenover *et al.*, 2022). Also, the recent findings about colistin-resistant *P. aeruginosa* strains producing different β-lactamases led to a global attention since colistin is used to treat extensively drug resistant (XDR) strains (Chen *et al.*, 2022). Another important aspect is the ability of *P. aeruginosa* to acquire and lose resistance in the presence and absence of colistin, respectively. This can be caused by multiple mutations regulatory proteins, such as the two-component systems (i.e., PhoP-PhoQ, PmrA-PmrB, CprRCprS, and ParR-ParS) (Lee *et al.*, 2016). Such an adaptational resistance is associated with the addition of 4-amino-L-arabinose (L-Ara4N) to the phosphate groups within the lipid A moiety of LPS and it has been related to the colistin treatment of CF patients (Moskowitz *et al.*, 2012). Moreover, as mentioned above, the most important mechanisms of adaptative resistance in *P. aeruginosa* involve the biofilm formation, which increase its ability to cause persistent infection by protecting the bacteria against host defences and antibiotic treatments (Ciofu *et al.*, 2022; Malhotra *et al.*, 2019; Ciofu *et al.*, 2015).

2.2 *Stenotrophomonas maltophilia*

S. maltophilia is an environmental Gram-negative microorganism, obligate aerobe, rod shaped and motile with a few polar flagella. It has recently emerged as an important nosocomial pathogen causing serious human infections, such as respiratory tract infections (pneumonia and acute exacerbations of COPD) and blood stream infections (Mojica *et al.*, 2022; Brooke, 2012). Risk factors for *S. maltophilia* infection include underlying malignancy, the presence of indwelling devices (e.g., catheters), chronic respiratory disease, prolonged antibiotic use and long-term hospitalization or admission to ICU (Mojica *et al.*, 2022; Brooke, 2012). Indeed, this pathogen has been identified on the surfaces of materials used in intravenous cannulae, prosthetic devices, and nebulizers. *S. maltophilia* is often co-isolated with other microorganisms (e.g., *P. aeruginosa*, *S. aureus*, *Burkholderia* species) in respiratory samples obtained from CF patients, where it contributes to the chronic infection of the airways. In addition, its interaction with other microorganisms can worse the prognosis of the infection. For instance, *P. aeruginosa* and *S. maltophilia* can produce polymicrobial biofilms in the CF lungs, thus contributing to a higher mortality rate (Mojica *et al.*, 2022; Brooke, 2012).

S. maltophilia is intrinsically resistant to a wide range of antibiotics (e.g., β-lactams, fluoroquinolones, tetracyclines, chloramphenicol, aminoglycosides, polymyxins, and trimethoprim/sulfamethoxazole). The low membrane permeability together with the presence of

chromosomally encoded MDR efflux pumps, β-lactamases, and antibiotic-modifying enzymes all contribute to its intrinsic antibiotic resistance (Mojica *et al.*, 2022; Brooke, 2012). In this regard, the increasing reports of isolates resistant to trimethoprim/sulfamethoxazole, historically the drug of choice for treatment of *S. maltophilia*, are concerning (Mojica *et al.*, 2022).

Clinical management is further complicated by the shortcomings of available antimicrobial susceptibility tests and the lack of standardized susceptibility breakpoints for most antibiotics. In fact, the antimicrobial susceptibility methods for *S. maltophilia* have been adapted from *P. aeruginosa* (i.e., broth microdilution), despite these organisms display growth, susceptibility, and intrinsic resistance mechanisms differences (Mojica *et al.*, 2022). Additionally, in contrast to CLSI, which has defined MIC breakpoints for ceftazidime, levofloxacin, minocycline, trimethoprim/sulfamethoxazole, ticarcillin/clavulanate, chloramphenicol, and cefiderocol, EUCAST defines MIC and disc breakpoints for trimethoprim/sulfamethoxazole. Lastly, FDA only recognizes ceftazidime breakpoints (Mojica *et al.*, 2022). The lack of breakpoints arises because there are many unknowns in the *in vitro* microbiological, clinical and PK/PD data typically used to establish breakpoints. Consequently, this issue can negatively impact on patient management.

2.3 *Staphylococcus aureus*

S. aureus is a Gram-positive often present asymptomatically on different parts of the human body as commensal. This colonization significantly increases the chances of infections by providing a reservoir of the pathogen. In fact, the affected individuals in most cases are infected by the *S. aureus* strain that they usually carry as a commensal. It can affect the bloodstream, skin and soft tissues, and lower respiratory tract, other than can cause infections related to medical instrumentation, as well as endocarditis and osteomyelitis (Guo *et al.*, 2020; Lakhundi and Zhang, 2018). Infections associated with higher mortality rates are those due to methicillin-resistant *S. aureus* (MRSA) strains, producing an altered penicillin-binding protein (PBP) associated with decreased affinity for most semisynthetic penicillins. Vancomycin has historically been the drug of choice and sometimes the last resort for the treatment of serious MRSA infections, providing empirical coverage and definitive therapy. However, its increased use has already led to vancomycin-intermediate *S. aureus* (VISA) as well as vancomycin-resistant *S. aureus* (VRSA) in certain parts of the world (Guo *et al.*, 2020; Lakhundi and Zhang, 2018). There are also several studies that have reported *S. aureus* strains from CF patients showing high resistance levels to antibiotics usually active against MRSA and VRSA strains (Boudet *et al.*, 2021; Antonelli *et al.*, 2016; Long *et al.*, 2014). This is a worrying aspect since *S. aureus* is the first pathogens detectable in the airways of young CF patients and with the highest prevalence at an

early age. Already among children younger than two years of age its prevalence exceeds 50%, reaching its peak value in the early teenage years at a prevalence of almost 80% (CFF, 2019) (Figure 5). In young patients with CF, the presence of *S. aureus* is associated with increased inflammatory activity in the airways, worse lung function, and increased hospitalization. With the progression of the disease, the replacement of *S. aureus* by *P. aeruginosa* occurs as a common process (Figure 5), albeit in adult CF patients *S. aureus* prevalence remains at about 40% (Rumpf *et al.*, 2021). There is a special *S. aureus* phenotype associated with chronic infection in CF patients, namely "small colony variants" (SCVs), which show slow growth rates and increased antibiotic resistance. Moreover, similarly to *P. aeruginosa*, biofilm formation has been described as an important virulence trait and mechanism for the adaptation of *S. aureus* in CF airways, as it facilitates immune evasion and helps to protect the pathogen from antibiotic treatment. Additionally, there is still absence of accepted therapeutic guidelines for the treatment of *S. aureus* in CF patients, both internationally and nationally, due to the shortage in valid studies and reliable data in this respect (Rumpf *et al.*, 2021).

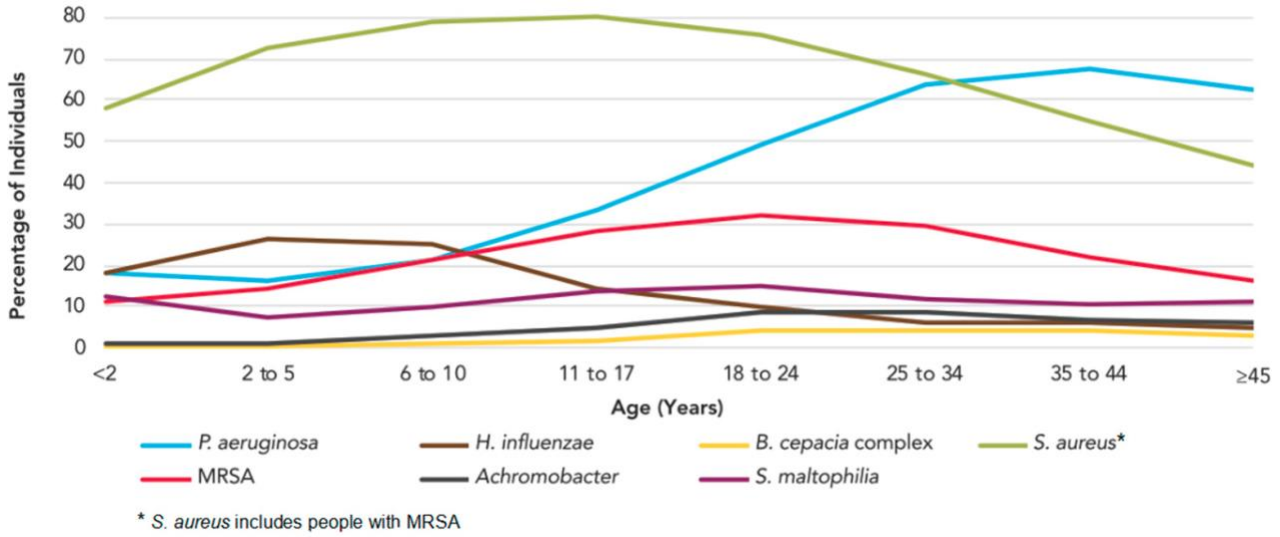

Figure 5. Age-dependent prevalence of different bacteria in CF patients based on the data of 31.199 patients (CFF, 2019).

3. *In vitro* and *in vivo* biofilm models

Biofilms have been studied for decades using various *in vitro* models for both high throughput screening and in-depth investigations. The most common methods used for high throughput screening are the static microtiter plate assay (O'Toole and Kolter, 1998) and the Calgary Biofilm Device (Ceri *et al.*, 1999). These assays are used to test for biofilm growth dispersal, direct killing, and anti-virulence. More comprehensive investigations of such parameters rely on continuous flow cell systems, bacterial colonies on agar plates, drip flow reactors, or rotating reactors (Azeredo *et al.*,

2017; Bjarnsholt, 2013). Despite the reproducible use of these *in vitro* systems, they fail to mimic the complexity of the host environment. Indeed, *in vivo* biofilms have structural and chemical characteristics different from most *in vitro* biofilms, in addition to the presence of host defences, which play an important role in the pathophysiology of biofilm infections (Azeredo *et al.*, 2017; Bjarnsholt, 2013). For this reason, *in vivo* models of many biofilm-related infections have been developed, such as animal models of chronic diseases (e.g.: chronic wounds, implant-related infections, CF, otitis media) (Bjarnsholt, 2013). In general, such models reflect the interaction between bacterial pathogens and host immune response, although the long-term inflammatory response and substantial antibiotic treatment is difficult to mimic. In the CF lung, this interplay can last up to 30 years and is known to result in the development of both phenotypic and genotypic variants of the infecting bacteria. Therefore, animal models for chronic *P. aeruginosa* lung infection are repeatedly exposed to bacteria to mimic persistent infections, although tends to have a limited lifetime (McCarron *et al.*, 2021; Bjarnsholt, 2013). However, the *in vivo* models show some important limitations, including: i) time and resource consuming, due to an extensive phenotype characterization necessary for any animal model; ii) early mortality of the model, which is often the case for many CF animal models; iii) and irreproducibility and poor recapitulation of human conditions, in particular for mouse models (McCarron *et al.*, 2021). Nonetheless, there are circumstances where *in vitro* systems are better suited to answering a particular research question (e.g., to select the most effective drugs to be tested thereafter in a dynamic model reproducing pharmacokinetic variations and to evaluate drug combinations, as well as innovative therapeutic options).

3.1 *In vitro m*odels mimicking cystic fibrosis lung infections

The most physiologically relevant method to study CF infections would be to use sputum obtained directly from CF patients, albeit it is inconsistent in composition, highly variable and affected by patient's infection stage at the time of collection. Furthermore, commercially available growth media lack of key components usually found in the CF lung environment and involved in microbial pathogenesis and biofilm formation (Aiyer and Manos, 2022). Consequently, artificial sputum medium (ASM) has been created to mimic the average composition of CF sputum and to provide a replicable, biologically relevant formulation that may be used for the *in vitro* investigation of microbial physiology, biofilm development, antibiotic susceptibility, and interspecies interactions in the context of CF. ASM key components are mucin and extracellular DNA (eDNA), which are responsible for bacterial microcolony and biofilm formation *in vivo*, while also providing the high viscosity environment characteristic in CF (Aiyer and Manos, 2022).

Neve *et al.* outlined nine distinct formulations, whose components have been established over the years from concentrations reported in literature for nutrients identified in CF sputum (Neve *et al.*, 2021). Although each of the nine ASM formulations is distinct in composition, experimental conclusions from different ASM claim to provide depictions of pathogen growth and physiology that are reflective of observations made from patient samples (Neve *et al.*, 2021).

ASM shows several advantages that make it an eligible model for studying CF infections, including: i) cost-effectiveness and simplicity to reproduce the CF lung milieu; ii) adaptability to the addition of host cell layers, thus providing an opportunity to conduct long-term adaptation experiments (Wijers *et al.*, 2016); iii) usefulness to determine effective drug concentrations, since mucin in sputum is recognized to bind antibiotics, thus reducing free drug levels and affecting biofilm susceptibility (Huang *et al.*, 2015); iv) suitability to study the most relevant respiratory pathogens in CF (i.e., *P. aeruginosa*, *Burkholderia spp.*, *S. maltophilia*, *A. xylosoxidans*) (Aiyer and Manos, 2022; Neve *et al.*, 2021; Jaiyesimi *et al.*, 2021; Willsey *et al.*, 2019).

4. Antibiofilm strategies

Current antibiofilm approaches may act through the following ways: i) by preventing bacterial adhesion (e.g., coating surfaces of implanted devices with Ti/Ag nanoparticles, antibiotics and/or antimicrobials, inhibiting the EPS production or binding EPS components on the microbial surfaces); ii) by inducing biofilm dispersal (e.g., using EPS matrix-degrading enzymes, or interfering with c-di-GMP pathway or quorum sensing, both strategies requiring co-administration alongside antibiotics); and iii) the eradication of the preformed biofilm (e.g., using high antibiotic concentrations for extended incubation periods) (Verderosa *et al.*, 2019; Koo *et al.*, 2017).

Targeting the mechanisms involved in the biofilm tolerance and resistance to the immune system and antimicrobials (see paragraph 1.1) is an attractive strategy to improve established treatment principles. In this respect, a very promising perspective, although still at an early stage of development, is the use of molecules active against persister cells (e.g., antimicrobial peptides) (Verderosa *et al.*, 2019; Koo *et al.*, 2017). However, the use of such strategies shows a limited efficacy, is still under investigation or difficult to translate into the clinic. In addition, the development of resistance, the recalcitrance to treatment and the ability of dispersed biofilm cells to spread the infection require that the above-reported agents are co-administered alongside antibiotics.

4.1 Treatments of pulmonary infections

In respiratory tract infections antibiotics alone are unable to eradicate biofilm infection, not only because of biofilm resistance, but also owing to dispersion limitations of antibiotics posed by the biofilm EPS matrix. Conversely, combined antibiotic therapies seem to be better than monotherapy, although high dosages are necessary to disrupt biofilms, since microbes usually reside deep in the lung where only a small proportion of systemically absorbed antimicrobial agents can access. However, oral or parenteral administration of antimicrobial agents at high dosages is often not desirable due to their high systemic toxicity. For this reason, the inhaled route of administration is preferred and represents the standard of care for the management of several chronic respiratory infections, including *P. aeruginosa* infection in CF patients (Manos, 2021; Taccetti *et al.*, 2021).

Aerosolized antibiotics offer advantages over systemic therapy (oral or intravenous), since relatively high concentrations of the drug can be delivered directly to the airways, thus improving the pharmacokinetic/pharmacodynamic indices and reducing systemic toxicity. In fact, daily inhaled antibiotics are currently used to reduce the risk of pulmonary exacerbations in CF adults with chronic *P. aeruginosa* infection (Manos, 2021; Taccetti *et al.*, 2021).

Most therapeutic options are focused on the main pathogen responsible for chronic respiratory colonization in patients with CF, COPD, and non-CF bronchiectasis (i.e., *P. aeruginosa*), but there is a significant interest in developing novel inhaled antibiotic treatments for other respiratory pathogens other than *P. aeruginosa* (i.e., *S. maltophilia*, *B. cepacia* and *S. aureus*). At present, colistin, tobramycin, aztreonam lysine and, more recently, levofloxacin represent the most commonly used inhaled antibiotics for the management of CF infections. Other inhaled antibiotics, such as the fosfomycin/tobramycin inhalation solution and amikacin liposome inhalation suspension, are currently being introduced into CF treatment regimens (Manos, 2021; Taccetti *et al.*, 2021). Nevertheless, there is no clear recommendation on how to select the most appropriate inhaled antibiotic based on different patient characteristics. It has been proposed that alternating antibiotics monthly might reduce development of further resistance improving the clinical outcome. Unfortunately, long-term efficacy data are unavailable, and the maximum length of the studies varies from 6 to 24 months. Moreover, the long-term use of inhaled antibiotics can cause local side effects for some CF patients. Finally, while lung function can be improved and exacerbations reduced, bacterial eradication is unlikely to be achieved, due to the presence of MDR strains and persister cells along with poor antibiotic penetration of biofilm aggregates (Manos, 2021; Taccetti *et al.*, 2021). Therefore, the development of alternative inhalable antimicrobials is desirable.

4.2 *N*-acetylcysteine

Apart from antibiotics, several different compounds have been investigated *in vitro* for their potential to reduce biofilm formation. For example, non-steroidal anti-inflammatory drugs and mucolytics have been shown to have inhibitory effects on biofilm production (Manos, 2021; Taccetti *et al.*, 2021). Among these, *N*-acetylcysteine (NAC), a mucolytic and antioxidant agent, is commonly administered together with antibiotics for the treatment of lower respiratory tract infections, because it provides sulfhydryl groups, which may hydrolyse disulphide bonds within mucin making the mucus less viscous (Guerini *et al.*, 2022; Blasi *et al.*, 2016). *In vitro* studies have also reported that NAC may exert antimicrobial and antibiofilm activity against several CF relevant pathogens, including *P. aeruginosa*, *S. maltophilia*, *B. cepacia*, *A. xylosoxidans* and *S. aureus* (Guerini *et al.*, 2022; Shen *et al.*, 2020; Pollini *et al.*, 2018b; Zhao and Liu, 2010). It has been suggested that such activities could be related to: i) competitive inhibition of cysteine utilization; ii) reaction of the NAC sulfhydryl group with bacterial proteins; and iii) perturbation of the intracellular redox equilibrium with potential indirect effects on cell metabolism and intracellular signal transduction pathways (Blasi *et al.*, 2016). The previously reported activity of NAC against preformed biofilms could be related either to perturbation of microbial physiology or to a direct effect of NAC in affecting biofilm matrix architecture (e.g., by chelation of calcium and magnesium or interaction with crucial components in the matrix) (Blasi *et al.*, 2016). Therefore, the hypothesized multifactorial activity of NAC against microbial biofilms represents a strength for its potential use as an antibiofilm agent in combination with antibiotics.

4.3 Light-based antimicrobial approaches

The observation that antibiotics are not unequivocally effective in eradicating biofilms, in addition to the worldwide dissemination of MDR and PDR bacterial pathogens, has led to an increased interest in non-antibiotic therapies. A promising and innovative approach to kill pathogenic bacteria is the use of several wavelengths of light, in particular those in the region of visible light (within the spectrum of 400 to 760 nm) (Hamblin and Abrahamse, 2019; Wang *et al.*, 2017). Unlike wavelengths outside of the visible spectrum, such as ultraviolet radiation, known to possess a high antimicrobial activity but damaging host cells, visible light may have a broad-spectrum activity and a low risk of causing host damage (Hamblin and Abrahamse, 2019; Wang *et al.*, 2017).

4.3.1 Antimicrobial photodynamic inactivation

Antimicrobial photodynamic inactivation (aPDI) can be defined as a photodynamic therapy (PDT) method that specifically uses light for the treatment of infectious diseases. It is based on the generation of cytotoxic reactive oxygen species (ROSs) by the combined action of visible light, oxygen and a photosensitizer (PS). The PSs are molecules able to absorb and transfer energy or electrons (after light absorption) to molecular oxygen for the generation of ROSs which in turns can destroy several microbial targets (e.g., proteins, lipids, and nucleic acids), thus leading to bacterial cell death (Wainwright *et al.*, 2017). The antibacterial effect of visible light it is possible because of the presence inside bacteria of endogenous PSs, named porphyrins. Different porphyrin subtypes have been identified as the primary microbial PSs responsible for bacterial photokilling, including protoporphyrin, coproporphyrin, or uroporphyrin (Hamblin and Abrahamse, 2019; Wang *et al.*, 2017). In particular, such molecules strongly absorb light at about 400 to 420 nm, which is the region of violet-blue light (VBL). In fact, VBL has consistently been reported to be the most antimicrobial light and has been shown to exert an antibiofilm activity against important nosocomial pathogens (Martegani *et al.*, 2020; Ferrer-Espada *et al.*, 2020; Rupel *et al.*, 2019; Halstead *et al.*, 2016; Wang *et al.*, 2016; Amin *et al.*, 2016). In addition to its antibacterial efficacy, VBL is not as harmful to the host tissues as to other wavelengths, since the concentration of porphyrins within bacteria is far greater than those present within mammalian cells, and because the mammalian cells have more sophisticated antioxidant processes compared to bacterial cells (Hamblin and Abrahamse, 2019; Wang *et al.*, 2017). Moreover, there are *in vitro* evidence showing a lack or limited bacterial resistance after the VBL treatment in *P. aeruginosa* and *A. baumannii* (Amin *et al.*, 2016; Zhang *et al.*, 2014). Therefore, the use of VBL may allow for the development of more convenient and safer therapeutic options for the treatment of biofilm-related chronic infections.

However, application of PDT to the treatment of lung infections is considered an impossible task because of the need to deliver light to the whole of the bronchi surface and possibly the 700 million pulmonary alveoli. Irradiation of the lungs from the outside of the body cannot be considered due to the poor penetration of light in human tissues. The use of fiber optics or modified bronchoscopes would be highly invasive and costly and would not guarantee the whole illumination of the infected lung regions.

4.3.2 Light4Lungs project

Light4Lungs (acronym for Inhalable Aerosol Light Source for Controlling Drug-Resistant Bacterial Lung Infections), a four-year Horizon 2020 FET Open project, addresses the problem of antimicrobial

resistance in the treatment of chronic lung infections, such as CF and hospital-acquired lung infections (https://cordis.europa.eu/project/id/863102; https://light4lungs.eu). The aim of this project is to develop a novel therapeutic scheme for the treatment of lung infections, based on inhalable light-emitting particles exciting bacterial porphyrins (i.e., endogenous PSs) and consequently killing the bacteria via the photodynamic effect (i.e., local production of cytotoxic ROSs by the combined action of light, endogenous PS, and oxygen).

The project encompasses a multidisciplinary approach for: i) the design, synthesis, characterization, and testing of inhalable light-emitting particles; ii) development of the method for delivery to the lungs; iii) and evaluation of the treatment parameters in relevant clinical models. The results of the project will be useful for patients with chronic respiratory tract infections, caused by MDR bacteria.

The first part of the project relies on the potential antimicrobial activity of light against *in vitro* planktonic and biofilm cultures of clinically relevant pathogens involved in chronic pulmonary diseases (e.g., *P. aeruginosa* and *S. aureus*), aimed at predicting the *in vivo* action spectrum of photokilling. This step includes the choice of the most effective wavelength, corresponding to the expected absorption peaks of the bacterial porphyrins, among different wavelengths of the visible spectrum (380-700 nm), for bacterial photokilling.

PART II

AIM OF THE PhD

RESEARCH PROJECT

The first general objective of the PhD research project was to investigate the potential antimicrobial and antibiofilm activity of NAC alone and in combination with colistin against *Stenotrophomonas maltophilia* and *Pseudomonas aeruginosa* strains, most of which isolated from cystic fibrosis (CF) patients. The transcriptomic response of planktonic cultures of a representative CF strain to NAC exposure was also examined.

On the other hand, the potential *in vitro* activity of violet-blue light (415 nm) against planktonic and biofilm cultures of both clinical isolates from CF and reference strains of *P. aeruginosa* and *Staphylococcus aureus*, was investigated. Such a research study was part of the follow-up activities of the Light4Lungs project aimed at develops a novel antimicrobial therapy for the treatment of chronic lung infections using inhalable light sources.

In detail, the following specific topics are discussed:

- *in vitro* activity of NAC alone and in combination with colistin against *S. maltophilia* and *P. aeruginosa*;
- transcriptomic response to NAC exposure of a *P. aeruginosa* strain from CF;
- *in vitro* photokilling activity of light at 415 nm against *P. aeruginosa* and *S. aureus*.

PART III

RESULTS AND DISCUSSION

1. *In vitro* activity of NAC alone and in combination with colistin against *Stenotrophomonas maltophilia* and *Pseudomonas aeruginosa*

RELATED PUBLICATIONS:

- Ciacci N, Boncompagni SR, Valzano F, Cariani L, Aliberti S, Blasi F, Pollini S, Rossolini GM, Pallecchi L. *In Vitro* Synergism of Colistin and *N*-acetylcysteine against *Stenotrophomonas maltophilia*. *Antibiotics*. 2019 8(3):101.

- Valzano F, Boncompagni SB, Micieli M, Di Maggio T, Di Pilato V, Colombini L, Santoro F, Pozzi G, Rossolini GM, Pallecchi L. Activity of *N*-Acetylcysteine Alone and in Combination with Colistin against *Pseudomonas aeruginosa* Biofilms and Transcriptomic Response to *N*-Acetylcysteine Exposure. *Microbiol Spectr.* 2022 10(4):e0100622.

In vitro studies have revealed that NAC may exhibit some intrinsic antimicrobial and antibiofilm activity against several clinically relevant pathogens (including Gram-positive and Gram-negative bacteria) (Guerini *et al.*, 2020; Shen *et al.*, 2020; Pollini *et al.*, 2018b; Zhao and Liu, 2010). The concentrations at which the antimicrobial and antibiofilm activities of NAC have been observed were usually higher than those achievable by systemic administration routes (i.e., oral, intramuscular, or intravenous). However, NAC can be administered topically, either by nebulization or direct instillation, and reach at the site of infection the higher concentrations needed for the antimicrobial and antibiofilm activity, thus both avoiding that the drug is metabolized by liver and intestines and paving the way for enhanced antibiotic action within the lung (Blasi *et al.*, 2016). On the other hand, it has been previously demonstrated that NAC does not negatively affect the activity of the major antibiotic classes, except for carbapenems (Landini *et al.*, 2016; Rodríguez-Beltrán *et al.*, 2015). In this perspective, and by virtue of its multiple beneficial effects and high tolerability, a renewed interest in the potential therapeutic efficacy of topical NAC has recently emerged, especially for the management of cystic fibrosis (CF) and other chronic respiratory diseases (e.g., COPD and non-CF bronchiectasis) (Blasi *et al.*, 2016).

Colistin represents a last-resort antibiotic for the treatment of infections caused by MDR Gram-negative bacteria. Inhaled colistin has been increasingly used for the treatment of difficult-to-treat respiratory tract infections (Karaiskos *et al.*, 2017), both in CF and non-CF patients, because it allows achieving high lung concentrations while reducing nephrotoxicity and neurotoxicity (Vardakas *et al.*, 2018; Boisson *et al.*, 2017). In addition, colistin in combination with NAC has been recently shown to exert a relevant antimicrobial and antibiofilm synergistic activity against colistin-resistant *A. baumannii* strains (Pollini *et al.*, 2018a), highlighting the potential efficacy of this combination in the treatment of pulmonary infections caused by biofilm-associated Gram-negative pathogens.

For these reasons, a wide study was carried out to evaluate the potential antimicrobial and antibiofilm activity of NAC in combination with colistin against the two most common non-fermenting Gram-negative respiratory pathogens in CF patients, such as *S. maltophilia* and *P. aeruginosa*. To perform the experiments, NAC stock solutions at 100 g/L were prepared immediately before use, by dissolving the powder in sterile distilled water, adjusting pH to 6.5-6.8 with NaOH, and then sterilizing final solutions by filtration.

1.1 Synergism of NAC-colistin combinations against *Stenotrophomonas maltophilia* planktonic cultures

To evaluate the potential synergism between NAC and colistin against planktonic cultures of *S. maltophilia*, checkerboard assay was performed as described previously (Bonapace *et al.*, 2002). Such an investigation was carried out with a total of 18 *S. maltophilia* (including isolates from CF and trimethoprim-sulfamethoxazole resistant strains), which were the same as in a previous study (Pollini *et al.*, 2018b). Among the strains tested, 13 were categorized as colistin-resistant (MIC range 4–>256 mg/L), while the remaining strains were categorized as colistin-susceptible (MIC range 0.125–1 mg/L) (Table 1), according to the colistin clinical breakpoints for *P. aeruginosa*. The ranges of colistin concentrations tested were 0.003–4 mg/L and 0.25–256 mg/L for colistin-susceptible and colistin-resistant strains, respectively. The NAC range tested was 500–32,000 mg/L for all strains, considering the high drug concentrations potentially achievable by topical administration. Checkerboard results were interpreted through the assessment of the Fractional Inhibitory Concentration Index (FICI), which considers a combination effectively synergistic, partially synergistic, indifferent, or antagonistic when the obtained value is ≤0.5, >0.5–≤1, >1–4.0, or >4.0, respectively.

Overall, NAC and colistin in combination showed a notable synergistic activity against the 13 colistin-resistant strains (FICI ≤0.5) (Table 1, grey shading). Conversely, an undetectable synergistic

activity has been reported for the 5 colistin-susceptible strains, although a trend toward colistin MIC decrease was observed in the presence of increasing NAC concentrations (Table 1). Interestingly, in the presence of NAC 8,000 mg/L, colistin MICs for all the colistin-resistant strains lowered to ≤1 mg/L (below the susceptibility breakpoint of *P. aeruginosa* and *A. baumannii*), thus suggesting that NAC could affect the mechanisms of acquired colistin resistance, potentially restoring a susceptible phenotype (Table 1).

Table 1. Colistin MICs (mg/L) in the presence of increasing NAC concentrations for the 18 *S. maltophilia* clinical isolates investigated in this study.

Strain	MIC		COL MICs (mg/L) associated to increasing NAC concentrations (mg/L)						
	NAC (mg/L)	COL (mg/L)	500	1,000	2,000	4,000	8,000	16,000	32,000
Z63	32,000	>256	32	16	2	1	0.5	≤0.25	≤0.25
Z64	32,000	64	64	32	16	1	1	0.5	0.25
Z119	32,000	32	32	16	8	4	1	1	≤0.25
Z128	16,000	32	32	32	16	2	1	≤0.25	≤0.25
Z117	32,000	16	32	32	16	1	1	≤0.25	≤0.25
Z129	32,000	16	32	16	16	2	1	0.5	≤0.25
Z65	32,000	8	16	8	4	1	≤0.25	≤0.25	≤0.25
Z118	16,000	8	2	2	2	1	≤0.25	≤0.25	≤0.25
Z130	32,000	8	16	8	2	1	1	0.5	≤0.25
Z131	32,000	8	16	8	4	2	1	0.5	≤0.25
Z132	32,000	8	16	8	2	1	1	0.5	≤0.25
Z157	32,000	8	32	32	8	2	1	1	≤0.25
Z155	16,000	4	4	4	2	1	1	≤0.25	≤0.25
Z116	32,000	1	1	1	1	1	0.5	0.25	≤0.003
Z156	16,000	0.25	0.5	0.5	0.25	0.25	0.06	≤0.003	≤0.003
Z120	16,000	0.25	0.5	0.5	0.25	0.25	0.06	≤0.003	≤0.003
Z66	16,000	0.25	0.25	0.25	0.25	0.125	0.125	≤0.003	≤0.003
Z133	32,000	0.125	0.25	0.25	0.125	0.125	0.125	≤0.003	≤0.003

MIC, minimum inhibitory concentration; NAC, *N*-acetylcysteine; COL, colistin.
MIC values corresponding to synergism (based on FICI values) are shown with grey shading.

To investigate the synergy dynamics of colistin in combination with NAC against planktonic cells in exponential growth phase, time-kill assays were carried out according to CLSI guidelines (CLSI M026-A, 1999). For this purpose, the colistin-resistant strains Z131 and Z157, and the colistin-susceptible strain Z66 were selected, according to previously obtained checkerboard results and to their significant clinical relevance in terms of origin (i.e., from CF patients) and colistin susceptibility. Two colistin concentrations (2 and 8 mg/L for the colistin-resistant strains, 0.25 and 0.5 mg/L for the colistin-susceptible strain) and three NAC concentrations (1,600, 3,200 and 8,000 mg/L) were tested alone and in combination. Data were obtained from at least two independent experiments, with two replicates per condition per experiment.

Results of time-kill assays performed with the colistin-resistant strains, Z131 and Z157, showed a concentration-dependent potentiation by NAC of the activity of colistin at 2 and 8 mg/L (i.e., concentrations easily achievable with an inhaled formulation, and 0.25× and 1× MIC of colistin for these strains, respectively) (Table 2). In particular, eradication of the starting inoculum (i.e., absence of regrowth after 48 hours of incubation) was achieved for the tested strains with combinations of NAC at 8,000 mg/L and colistin at 2 or 8 mg/L, albeit at different time points (Table 2). Concerning the colistin-susceptible strain (Z66), complete eradication of the starting inoculum was obtained after 4 hours already with NAC at 3,200 mg/L plus colistin at 0.25 mg/L (i.e., 1× MIC) (Table 3). Similar results were obtained in experiments performed with colistin at 0.5 mg/L (i.e., 2× MIC), although combination including NAC at 3,200 mg/L was responsible for a remarkable decrease in viable cells after 8 hours of incubation, followed by regrowth (Table 3).

Overall, time-kill assay results showed a notable concentration-dependent effect of NAC in potentiating the activity of colistin, confirming the synergy observed with checkerboard assays and thus supporting the notion that NAC could restore the activity of colistin against colistin-resistant strains at concentrations achievable following nebulized administration of the two drugs. These findings are in accordance with what was previously reported for colistin-resistant *A. baumanii* isolates (Pollini *et al.*, 2018a).

Table 2. Antimicrobial activity of colistin alone and in combination with NAC against colistin-resistant *S. maltophilia* Z131 and Z157 grown in exponential-phase planktonic cultures subjected to time-kill assays.

Strain	Time (hours)	Antimicrobial activity		Antimicrobial synergistic combinations					
				COL 2 mg/L			COL 8 mg/L		
		COL 2 mg/L	COL 8 mg/L	NAC 1,600 mg/L	NAC 3,200 mg/L	NAC 8,000 mg/L	NAC 1,600 mg/L	NAC 3,200 mg/L	NAC 8,000 mg/L
Z131	4	>	>>	–	+	+	–	–	+
	6	>	>>	–	+	+	–	+	+
	8	>	>>	–	+	+	–	+	+
	24	RG	RG	–	RG	+	–	RG	+
	48	RG	RG	–	RG	+	–	RG	+
Z157	4	>	>>	–	–	–	–	–	–
	6	>	>>	–	–	–	–	–	+
	8	>	>>	–	+	+	–	–	+
	24	RG	RG	–	RG	+	–	–	+
	48	RG	RG	–	RG	+	–	–	+

NAC, *N*-acetylcysteine; COL, colistin; >, bacteriostatic effect (i.e., reduction of <3 log of the starting inoculum); >>, bactericidal effect (i.e., decrease of ≥3 log of the starting inoculum); +, antimicrobial synergism; –, no antimicrobial synergism; RG, regrowth of the starting inoculum.
Data about the activity of NAC at 1,600, 3,200 and 8,000 mg/L are not reported due to the absence of antimicrobial effect. NAC-colistin combinations leading to eradication of the starting inoculum are shown with grey shading.

Table 3. Antimicrobial activity of colistin alone and in combination with NAC against colistin-susceptible *S. maltophilia* Z66 grown in exponential-phase planktonic cultures subjected to time-kill assays.

Strain	Time (hours)	Antimicrobial activity		Antimicrobial synergistic combinations					
				COL 0.25 mg/L			COL 0.5 mg/L		
		COL 0.25 mg/L	COL 0.5 mg/L	NAC 1,600 mg/L	NAC 3,200 mg/L	NAC 8,000 mg/L	NAC 1,600 mg/L	NAC 3,200 mg/L	NAC 8,000 mg/L
Z66	4	–	>	+	+	+	+	+	+
	6	–	>	+	+	+	+	+	+
	8	–	>	+	+	+	+	+	+
	24	–	RG	RG	+	+	+	+	+
	48	–	RG	RG	+	+	+	RG	+

NAC, *N*-acetylcysteine; COL, colistin; >, bacteriostatic effect (i.e., reduction of <3 log of the starting inoculum); >>, bactericidal effect (i.e., decrease of ≥3 log of the starting inoculum); +, antimicrobial synergism; –, no antimicrobial effect or antimicrobial synergism; RG, regrowth of the starting inoculum.
Data about the activity of NAC at 1,600, 3,200 and 8,000 mg/L are not reported due to the absence of antimicrobial effect. NAC-colistin combinations leading to eradication of the starting inoculum are shown with grey shading.

1.2 Antibiofilm activity of NAC-colistin combinations against *Stenotrophomonas maltophilia*

To investigate the potential synergism of NAC in combination with colistin against preformed biofilms, the Nunc-TSP lid system (i.e., a standardized *in vitro* biofilm model) was used (Harrison *et al.*, 2010). The study was carried out with all the 18 *S. maltophilia* strains used in checkerboard assays (see part III, paragraph 1.1). Biofilms grown for 24 hours were challenged with nine NAC-colistin combinations (i.e., colistin at 8, 32, and 128 mg/L; NAC at 1,600, 8,000 and 16,000 mg/L, alone or in combination) and biofilm mass was evaluated after 24 hours of exposure by viable cell count (i.e., by disruption of biofilms by sonication, and determination of CFU/peg). Data were obtained in at least two independent experiments, with at least six replicates per condition per experiment.

Results of biofilm susceptibility testing showed a NAC-mediated dose-dependent potentiation of the antibiofilm activity of colistin against the majority of *S. maltophilia* strains tested (Table 4). In particular, combinations including NAC at 16,000 mg/L were the most synergistic against all colistin-resistant strains, except for *S. maltophilia* Z155, which was so susceptible to such a NAC concentration that no synergism was visible (Table 4). In addition, the synergism observed with the strains Z131 and Z157 subjected to NAC at 8,000 mg/L plus colistin at 8,000 mg/L was in accordance with what observed in time-kill assays performed with planktonic cells, although did not lead to biofilm eradication (Tables 2 and 4), probably due to the markedly different physiological state of planktonic and biofilm-associated cells. With respect to colistin-susceptible strains, *S. maltophilia* Z156 was the only one where synergism was evident. For the remaining four strains, in two cases a trend toward a dose-dependent antibiofilm effect of NAC in combination with colistin was detected, while in the other two the colistin concentrations were probably high to appreciate a synergy. In fact, for the strain Z133 lower colistin concentrations were necessary to observe NAC and colistin synergism (Table 4 and 5).

Overall, these data demonstrated a remarkable antibiofilm synergistic activity of colistin plus NAC, particularly evident in colistin-resistant strains, thus supporting the hypothesis that NAC, at concentrations likely to be achievable by inhaled formulations, could revert colistin resistance phenotype in *S. maltophilia*.

Table 4. Antibiofilm activity of colistin alone and in combination with NAC against the 18 *S. maltophilia* clinical isolates investigated in this study.

Strain	Antibiofilm activity			Antibiofilm synergistic combinations								
				COL 8 mg/L			COL 32 mg/L			COL 128 mg/L		
	COL 8 mg/L	COL 32 mg/L	COL 128 mg/L	NAC 1,600 mg/L	NAC 8,000 mg/L	NAC 16,000 mg/L	NAC 1,600 mg/L	NAC 8,000 mg/L	NAC 16,000 mg/L	NAC 1,600 mg/L	NAC 8,000 mg/L	NAC 16,000 mg/L
Z63	–	+	+	–	–	+	–	–	–	–	–	–
Z64	–	–	–	–	–	+	–	+	+	–	+	+
Z119	–	–	+	–	+	+	–	–	–	×	–	–
Z128	–	–	+	–	–	+	–	+	+	–	–	–
Z117	–	–	–	–	–	–	–	+	+	–	+	+
Z129	–	–	+	–	–	–	–	+	+	–	–	–
Z65	–	–	+	–	–	–	–	+	+	–	–	–
Z118	–	–	+	–	–	+	–	–	+	–	–	–
Z130	–	–	+	–	–	–	–	+	+	–	–	–
Z131	–	–	+	–	+	+	–	+	+	×	–	–
Z132	–	–	–	+	+	+	+	+	+	+	+	+
Z157	–	–	–	+	+	–	+	+	+	+	+	+
Z155	–	–	+	–	–	–	–	–	–	–	–	–
Z116	–	+	+	–	–	–	–	–	–	–	–	–
Z156	–	–	+	–	+	+	–	+	+	–	–	–
Z120	–	+	+	–	–	–	–	–	–	–	–	–
Z66	+	+	+	–	–	–	–	–	–	–	–	–
Z133	+	+	+	–	–	–	–	–	–	–	–	–

NAC, *N*-acetylcysteine; COL, colistin; +, antibiofilm effect or antibiofilm synergism; –, no antibiofilm effect or antibiofilm synergism.; ×, paradoxical effect (i.e., increasing of biofilm growth in presence of NAC-colistin combinations in comparison to colistin alone).

The presence or not of antibiofilm effect or antibiofilm synergism and paradoxical effect is in accordance with statistical analysis ($p \leq 0.05$). Data about the activity of NAC at 1,600, 8,000 and 16,000 mg/L are not reported here due to the absence of antibiofilm effect (except for *S. maltophilia* Z155 and Z66 where NAC at 16,000 mg/L showed a high antibiofilm activity). Colistin alone or NAC-colistin combinations leading to biofilm eradication are shown with grey shading.

Table 5. Antibiofilm activity of colistin alone and in combination with NAC against colistin-susceptible *S. maltophilia* Z33.

Strain	Antibiofilm activity			Antibiofilm synergistic combinations								
				COL 1.6 mg/L			COL 2 mg/L			COL 4 mg/L		
	COL 1.6 mg/L	COL 2 mg/L	COL 4 mg/L	NAC 1,600 mg/L	NAC 8,000 mg/L	NAC 16,000 mg/L	NAC 1,600 mg/L	NAC 8,000 mg/L	NAC 16,000 mg/L	NAC 1,600 mg/L	NAC 8,000 mg/L	NAC 16,000 mg/L
Z133	–	–	–	–	–	–	–	–	+	+	+	+

NAC, *N*-acetylcysteine; COL, colistin; +, antibiofilm effect or antibiofilm synergism; –, no antibiofilm effect or antibiofilm synergism.
The presence or not of antibiofilm effect or antibiofilm synergism is in accordance with statistical analysis ($p \leq 0.05$). Data about the activity of NAC at 1,600, 8,000 and 16,000 mg/L are not reported here due to the absence of antibiofilm effect. NAC-colistin combinations leading to biofilm eradication are shown with grey shading.

1.3 Antibiofilm activity of NAC-colistin combinations against *Pseudomonas aeruginosa*

To evaluate the potential antibiofilm activity of NAC alone and in combination with colistin against preformed biofilms of *P. aeruginosa*, a first investigation was carried out with 17 strains, most of which showing MDR phenotype (n=11) and being from CF patients (n=15). Biofilms grown for 24 hours were challenged with NAC at 8,000 mg/L (i.e., concentration likely achievable by topical administration) and different colistin concentrations (i.e., from 2 to 32 mg/L, according to preliminary experiments carried out to select colistin concentrations to be tested and the colistin MIC for each strain), alone and in combination. The *in vitro* biofilm model and the procedure for the evaluation of biofilm mass after drugs exposition were the same used in similar experiments performed with *S. maltophilia* strains (see part III, paragraph 1.2). Data were obtained in at least three independent experiments, with at least twelve replicates per condition per experiment.

Results of biofilm susceptibility testing showed a limited and strain-dependent activity of NAC alone (i.e., 8,000 mg/L). In particular, a decrease between ≥0.2 and ≥1 log CFU/peg compared to control was observed with 7 colistin-susceptible strains (Table 6), while with *P. aeruginosa* PAO1 and M42 a biofilm increasing compared to control was evident (i.e., paradoxical effect). With the remaining strains, no antibiofilm effect of NAC alone was detected, highlighting that the NAC activity is not related to phenotypic or genotypic features of the strains tested. Conversely, colistin seemed to have more activity than NAC against both the colistin-susceptible (n=7) and the colistin-resistant strains (n=3), but lower than that observed in combination with NAC at 8,000 mg/L (Table 6). Major effects were visible with three colistin-susceptible strains (i.e., *P. aeruginosa* M4, M7, M32) where colistin was found to determine a reduction of biofilm viable cells between ≥1 and ≥4 log CFU/peg (Table 6), such that did not allow to observe synergism with NAC in two cases (see below). A paradoxical effect was also visible with *P. aeruginosa* Z34 (i.e., increase of >0.5 log CFU/peg compared to the control) (Table 6). The mechanisms accounting for this phenomenon remain unclear and deserve further investigation.

A relevant synergism of NAC-colistin combinations (i.e., NAC at 8000 mg/L plus colistin at 2 to 32 mg/L) was observed with the majority of strains studied (including the three colistin-resistant ones), except for *P. aeruginosa* M4 and M32, whose biofilms were extremely susceptible to colistin (as above-mentioned) (Table 6). Noteworthy, NAC at 8,000 mg/L plus colistin at 8 mg/L eradicated the biofilm cultures of *P. aeruginosa* Z154 (i.e., a mucoid strain isolated from CF). (Table 6).

Additionally, NAC enhanced colistin activity against all colistin-resistant strains, also at sub-MIC concentrations (i.e., 1/64 the MIC of colistin for *P. aeruginosa* FC237) (Table 6).

Biofilm susceptibility assays with the artificial sputum medium (ASM) model (which resemble the chemical composition of CF lung environment) were further carried out in order to confirm antibiofilm synergism of NAC-colistin combinations observed in the Nunc-TSP lid system. For this purpose, two colistin-susceptible strains from CF were selected according to their different phenotypic and genotypic features (i.e., *P. aeruginosa* Z154, mucoid, MDR, ST412, O-type 6; *P. aeruginosa* Z34, nonmucoid, MDR, ST17, O-type 1). Biofilms grown for 24 hours in ASM were subjected to NAC at 8,000 mg/L and colistin at 64 mg/L (colistin concentrations lower or higher than 64 mg/L did not show evident antibiofilm activity or led to biofilm eradication also in absence of NAC, respectively). After 24 hours of exposure, biofilm mass was determined following the same protocol described for the Nunc-TSP lid system (see above).

Results showed a clear synergism of NAC at 8,000 mg/L in combination with colistin at 64 mg/L against *P. aeruginosa* Z154 and Z34 grown in the ASM biofilm model. Unlike the Nunc-TSP lid system, a higher colistin concentration (i.e., 32× MIC of colistin for these strains) was necessary to observe such a synergism in the ASM model (Table 7), probably due to colistin interactions with ASM components (i.e., mucin and extracellular DNA) (Huang *et al.*, 2015). In addition, in such a model NAC alone did not show antibiofilm activity against *P. aeruginosa* Z154 (Table 7), suggesting a probable limited activity of NAC against preformed *P. aeruginosa* biofilms *in vivo*.

Taken together, these data indicated a NAC-mediated potentiation of the antibiofilm activity of colistin against a wide panel of *P. aeruginosa* strains, both colistin-susceptible and colistin-resistant, showing different features in terms of mucoidy, antimicrobial resistance pattern, and MLST and O-type. These results are in accordance with data previously obtained in *A. baumanii* (Pollini *et al.*, 2018a) and *S. maltophilia* (see part III, paragraph 1.2). In addition, antibiofilm synergism of NAC-colistin combinations against *P. aeruginosa* strains was confirmed in an environment mimicking the composition of the CF mucus, thus making such a combination a promising therapeutic option.

Table 6. Antibiofilm activity of NAC at 8,000 mg/L alone or in combination with colistin against the 17 *P. aeruginosa* clinical isolates investigated in this study.

Strain	MIC		Drug concentrations tested		Antibiofilm activity					
					NAC		COL		NAC + COL	
	NAC (mg/L)	COL (mg/L)	NAC (mg/L)	COL (mg/L)	ΔLog CFU/peg		ΔLog CFU/peg		ΔLog CFU/peg	
PAO1	64,000	2	8,000	8	- 1.50	×	- 0.07	–	1.01	+
Z33	16,000	1	8,000	4	0.24	+	0.23	+	0.96	+
Z34	64,000	2	8,000	8	- 0.24	–	- 0.54	×	0.70	+
Z35	16,000	1	8,000	4	0.60	+	0.10	–	2.19	+
Z152	8,000	2	8,000	4	0.39	+	0.08	–	0.90	+
Z154	16,000	2	8,000	8	1.37	+	0.33	–	4.85	+
M1	16,000	2	8,000	4	- 0.02	–	0.75	–	2.19	+
M4	32,000	2	8,000	4	0.50	–	4.14	+	5.45	–
M7	64,000	2	8,000	8	- 0.02	–	2.41	+	5.01	+
M13	32,000	1	8,000	4	0.61	+	0.59	+	4.39	+
M19	64,000	1	8,000	8	0.72	+	0.47	+	3.16	+
M25	16,000	2	8,000	8	0.29	+	0.00	–	4.80	+
M32	16,000	2	8,000	8	0.18	–	1.77	+	4.52	–
M42	32,000	2	8,000	2	- 0.40	×	- 0.15	–	3.74	+
FC237	64,000	512	8,000	8	- 0.50	–	1.04	+	2.04	+
FC238	64,000	8	8,000	32	0.08	–	0.38	+	5.48	+
FZ99	64,000	4	8,000	32	- 0.36	–	1.19	+	3.65	+

MIC, minimum inhibitory concentration; NAC, *N*-acetylcysteine; COL, colistin; CFU, colony forming units; +, antibiofilm effect or antibiofilm synergism; –, no antibiofilm effect or antibiofilm synergism; ×, paradoxical effect (i.e., increasing of biofilm growth in presence of NAC or colistin alone in comparison to control).
The presence or not of antibiofilm effect or antibiofilm synergism and paradoxical effect is in accordance with statistical analysis ($p \leq 0.05$). Δlog CFU/peg represents the CFU/peg log reduction and was calculated by the ratio between the median CFU/peg of the controls and the median CFU/peg detected for each drug alone or in combination after 24 hours of exposition. NAC-colistin combinations leading to biofilm eradication are shown with grey shading.

Table 7. Antibiofilm activity of NAC at 8,000 mg/L alone or in combination with colistin at 64 mg/L against *P. aeruginosa* Z154 and Z34 grown in the ASM biofilm model.

Strain	MIC		Drug concentrations tested		Antibiofilm activity					
					NAC		COL		NAC + COL	
	NAC (mg/L)	COL (mg/L)	NAC (mg/L)	COL (mg/L)	ΔLog CFU/mL		ΔLog CFU/mL		ΔLog CFU/mL	
Z154	16,000	2	8,000	64	0.09	–	2.90	+	6.00	+
Z34	64,000	2	8,000	64	0.10	–	2.21	+	4.32	+

MIC, minimum inhibitory concentration; NAC, *N*-acetylcysteine; COL, colistin; CFU, colony forming units; +, antibiofilm effect or antibiofilm synergism; –, no antibiofilm effect or antibiofilm synergism.
The presence or not of antibiofilm effect or antibiofilm synergism is in accordance with statistical analysis ($p \leq 0.05$). Δlog CFU/mL represents the CFU/peg log reduction and was calculated by the ratio between the median CFU/mL of the controls and the median CFU/mL detected for each drug alone or in combination after 24 hours of exposition.

2. Transcriptomic response to NAC exposure of a *Pseudomonas aeruginosa* strain from CF

RELATED PUBLICATION:

- Valzano F, Boncompagni SB, Micieli M, Di Maggio T, Di Pilato V, Colombini L, Santoro F, Pozzi G, Rossolini GM, Pallecchi L. Activity of *N*-Acetylcysteine Alone and in Combination with Colistin against *Pseudomonas aeruginosa* Biofilms and Transcriptomic Response to *N*-Acetylcysteine Exposure. *Microbiol Spectr.* 2022 10(4):e0100622.

The *in vitro* antibiofilm synergism of NAC-colistin combinations observed against *P. aeruginosa* (see part III, paragraph 1.3), highlight the potential efficacy of NAC alone and in combination with colistin in the treatment of respiratory tract infections caused by biofilm-associated Gram-negative pathogens. However, the mechanisms accounting for such a synergism as well as the potential antibiofilm activity of NAC alone are unknown. Advances in RNA-sequencing (RNA-seq) have enabled the analysis of transcriptional changes that occur in bacteria when grown *in vitro* in the presence of colistin or other antioxidants (Cianciulli Sesso *et al.*, 2021; Han *et al.*, 2019; Klare *et al.*, 2016), but not in the presence of NAC. For this reason, transcriptional response of *P. aeruginosa* planktonic cells exposed to NAC alone was assessed by RNA-seq. The choice of exploring such a response is related to the consideration of the complex and still largely unknown effects of NAC on microbial physiology and consequently the need to know the factors involved in the response to NAC treatment.

A colistin-susceptible mucoid strain isolated from CF (i.e., *P. aeruginosa* Z154) rather than a reference strain (i.e., PAO1) was selected to account for the phenotypic diversification of *in vivo* strains (Rossi *et al.*, 2021). Such a strain was also chosen according to biofilm susceptibility testing (i.e., Z154 biofilm cultures were eradicated by NAC at 8,000 mg/L plus colistin at 8 mg/L) (see part III, paragraph 1.3). Differentially expressed genes (DEGs) of *P. aeruginosa* Z154 planktonic cultures exposed to NAC at 8,000 mg/L compared to the control (i.e., the same cultures without NAC) were analyzed according to adjusted *p*-value of <0.05 and 99% confidence interval. Results were obtained from two independent experiments. A detailed RNA-seq workflow is reported in Figure 6.

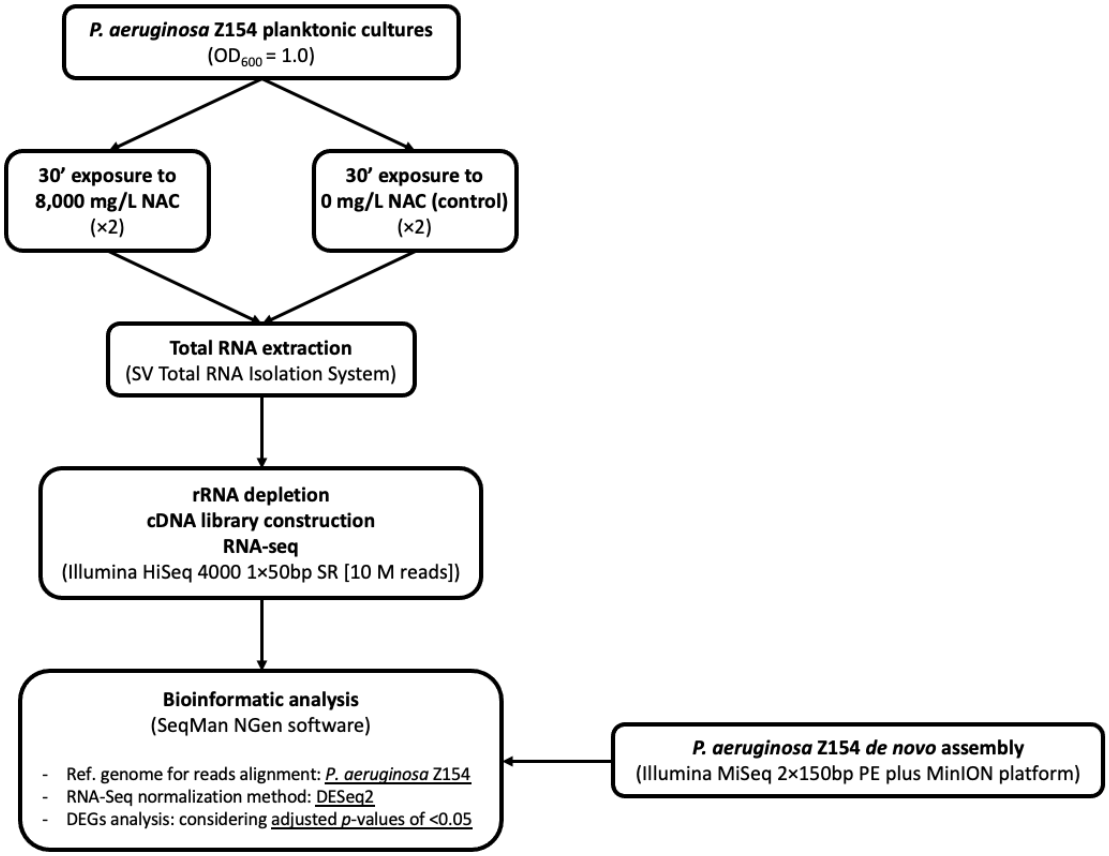

Figure 6. Schematic diagram illustrating the workflow of the study of the transcriptomic response of *P. aeruginosa* Z154 planktonic cultures exposed to *N*-acetylcysteine (NAC) at 8,000 mg/L.

Overall, DEGs analysis of the NAC-exposed cultures compared to the control indicate that NAC mainly might act through three mechanisms: i) by inducing a zinc starvation response, following to a probable Zn^{2+} chelating activity; ii) by affecting the anaerobic respiration through inhibition of the denitrification pathway; and iii) by affecting the flagellum-mediated motility. Tables 8 and 9 show the representative upregulated and downregulated DEGs discussed in this thesis work, respectively.

Table 8. Representative upregulated DEGs in *P. aeruginosa* Z154 planktonic cultures exposed to NAC at 8000 mg/L compared to control.

***P. aeruginosa locus* tag**		**Gene**	**Product**	**Protein function**	***zur* regulon**	**Adjusted *p*-value**	**Log_2 fold change**
Z154	**PAO1**						
IS492_19940	PA2437		HflC family modulator of membrane FtsH protease	Peptidase regulation	+	5.1E-06	0.8
IS492_19945	PA2438		HflC modulator of membrane FtsH protease	Peptidase regulation	+	7.0E-03	0.6
IS492_19950	PA2439	*hflK*	HflK family modulator of membrane FtsH protease	Peptidase regulation	+	6.5E-03	0.6
IS492_29825	PA4063		Zinc SBP	Zinc uptake	+	7.0E-41	2.0
IS492_29830	PA4064		Zinc ABC transporter, ATP-binding protein	Zinc uptake	+	4.2E-08	0.9
IS492_29835	PA4065		Zinc ABC transporter, permease	Zinc uptake	+	4.9E-13	1.2
IS492_29840	PA4066		Zinc SBP	Zinc uptake	+	8.5E-05	0.7
IS492_06220	PA4834	*cntI*	Pseudopaline transport plasma membrane protein CntI	Zinc uptake	+	6.1E-05	0.7
IS492_06215	PA4835	*cntM*	Pseudopaline biosynthesis dehydrogenase CntM	Zinc uptake	+	8.1E-26	1.7
IS492_06210	PA4836	*cntL*	Pseudopaline biosynthesis enzyme CntL	Zinc uptake	+	9.3E-39	2.0
IS492_06205	PA4837	*cntO*	Pseudopaline transport outer membrane protein CntO	Zinc uptake	+	0.0E+00	2.5
IS492_31595	PA5498	*znuA*	Zinc soluble binding protein ZnuA	Zinc uptake	+	9.0E-08	0.9
IS492_31600	PA5499	*zur*	Transcriptional regulator	Zinc homeostasis	+	5.3E-10	1.0
IS492_31605	PA5500	*znuC*	Zinc ABC transporter, ATP-binding protein ZnuC	Zinc uptake	+	1.2E-07	0.9
IS492_31610	PA5501	*znuB*	Zinc ABC transporter, ZnuB permease	Zinc uptake	+	1.9E-03	0.6
IS492_28280	PA3785		Copper chaperone PCu(A)C	Copper uptake		8.6E-07	0.9
IS492_28305	PA3790		TBDR copper receptor OprC	Copper uptake		1.0E-03	0.6

SBP, soluble binding protein; ABC, ATP-binding cassette; TBDR, TonB-dependent receptor.
Protein functions were inferred from the literature and PseudoCAP (https://www.Pseudomonas.com/pseudocap). DEGs were analyzed according to adjusted *p*-value of <0.05 and 99% confidence interval. In order to favor comparison with data present in the literature, genes have been also indicated as *P. aeruginosa* PAO1 *locus* tags.

Table 9. Representative downregulated DEGs in *P. aeruginosa* Z154 planktonic cultures exposed to NAC at 8000 mg/L compared to control.

***P. aeruginosa locus* tag**		**Gene**	**Product**	**Protein function**	***zur* regulon**	**Adjusted *p*-value**	**Log_2 fold change**
Z154	**PAO1**						
IS492_02660	PA0524	*norB*	Nitric-oxide reductase subunit NorB	Denitrification		3.9E-03	–0.6
IS492_12670	PA1101	*fliF*	Flagellar M-ring protein FliF	Motility		5.7E-05	–0.7
IS492_14625	PA1453	*flhF*	Flagellar biosynthesis protein FlhF	Motility		7.6E-03	–0.6
IS492_26340	PA3391	*nosR*	Regulatory protein NosR	Denitrification		3.2E-04	–0.6
IS492_26345	PA3392	*nosZ*	Nitrous-oxide reductase	Denitrification		4.1E-05	–0.8
IS492_27185	PA3574a	*copZ*	Copper chaperone CopZ	Copper efflux		9.1E-11	–1.0
IS492_28975	PA3920	*copA*	Copper-translocating P-type ATPase CopA	Copper efflux		1.2E-27	–1.2

Protein functions were inferred from the literature and PseudoCAP (https://www.Pseudomonas.com/pseudocap). DEGs were analyzed according to adjusted *p*-value of <0.05 and 99% confidence interval. In order to favor comparison with data present in the literature, genes have been also indicated as *P. aeruginosa* PAO1 *locus* tags.

2.1 NAC-induced zinc starvation response of *P. aeruginosa*

Results from transcriptomic analysis revealed that NAC was responsible of upregulation of 31 DEGs belonging to *zur* regulon, including zinc transporters (e.g., the PA4063-PA4064-PA4065-PA4066 operon, *cntOLMI* operon, and *znuABC* operon), and inhibitory proteins of virulence factors (i.e., HflC and HflK family modulators inhibiting FtsH proteases), known as genes required for adaptation to zinc starvation (Ducret *et al.*, 2021; Kamal *et al.*, 2019; Lhospice *et al.*, 2017; Pederick *et al.*, 2015) (Table 8). Other transcriptional changes related to such a response were upregulation and downregulation of genes encoding proteins involved in copper uptake and efflux, respectively (i.e., PA3785 and PA3790 involved in copper uptake; *copA* and *copZ* involved in copper efflux) (Quintana *et al.*, 2017; Lim *et al.*, 2013), in addition to downregulation of genes involved in the biosynthesis of flagellar apparatus (i.e., *fliF* and *flhF*, both virulence factors) (Tables 8 and 9), which lower expression seems to be modulated by zinc, as reported elsewhere (Mastropasqua *et al.*, 2018).

The compensatory strategies implemented by *P. aeruginosa* to grow in zinc-poor environments (i.e., upregulation of genes belonging to *zur* regulon) indicated that NAC may induce a zinc starvation, thus probably mitigating *P. aeruginosa* virulence.

2.2 NAC-induced inhibition of the *P. aeruginosa* denitrification pathway

Transcriptomic data showed that NAC was responsible of downregulation of three DEGs activated during denitrification (i.e., *norB*, *nosR* and *nosZ*) (Table 9), a strategy used by *P. aeruginosa* to grow under oxygen limitations (e.g., in biofilm layers in the CF mucus) (Line *et al.*, 2014). Such downregulation might inhibit anaerobic respiration via denitrification and in turn contribute to the observed NAC-colistin synergism in biofilms. In fact, since colistin is known to have higher activity in anoxic conditions, where *P. aeruginosa* has a decreased capacity to establish energy-dependent adaptive resistance mechanisms (e.g., LPS modifications, overexpression of efflux pumps) (Kolpen *et al.*, 2016), an impairment of anaerobic respiration mediate by NAC would further compromise the capacity of *P. aeruginosa* to protect from colistin toxicity, thus increasing colistin activity.

To confirm the role of NAC in the inhibition of the denitrification pathway, the consumption of NO_3^- and NO_2^- was estimated by the Griess colorimetric assay. The same strain used for transcriptomic analysis (i.e., *P. aeruginosa* Z154 strain) was assayed during anaerobic growth in culture media (i.e., CAMHB) supplemented with NO_3^- or NO_2^-, in the presence or absence of NAC at 8,000 mg/L. Experiments were carried out in triplicate, with one replicate per time point per condition.

Results displayed that the presence of NAC in anaerobic cultures of *P. aeruginosa* Z154 caused an accumulation of NO_2^- (i.e., the reduction product of NO_3^-) in culture media containing NO_3^- and NO_2^-, after 24 and 48 hours, respectively, in contrast to the same cultures in absence of NAC, which were able to metabolize NO_3^- and NO_2^- (Figure 7A and 7B), as expected (Kolpen *et al.*, 2015).

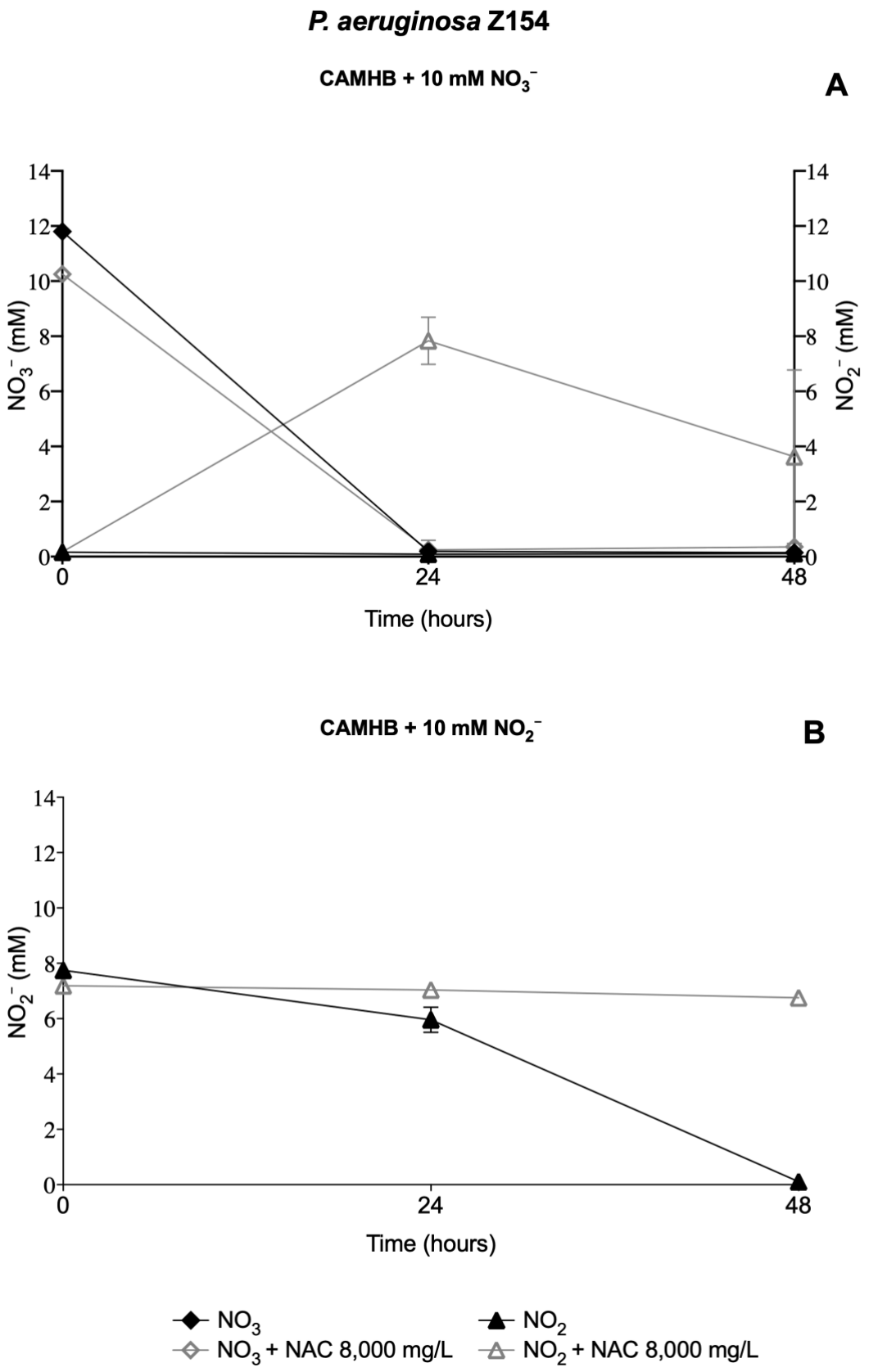

Figure 7. *N*-acetylcysteine (NAC)-mediated inhibition of *P. aeruginosa* Z154 denitrification pathway. (A) NO_3^- and NO_2^- concentrations in anaerobic CAMHB supplemented with 10 mM NO_3^-, with or without NAC at 8,000 mg/L; (B) NO_2^- concentration in anaerobic CAMHB supplemented with 10 mM NO_2^-, with or without NAC at 8,000 mg/L. Data are plotted as the mean values of NO_3^- and/or NO_2^- levels detected at each time point.

On the other hand, to prove the involvement of the NAC-mediated inhibition of denitrification on the observed antibiofilm synergism of NAC-colistin combinations, time-kill assays were performed under both anaerobic and aerobic conditions, according to CLSI guidelines (CLSI M026-A, 1999). *P. aeruginosa* Z154 (i.e., the same strain from transcriptomic analysis) was subjected to colistin at 0.25 mg/L (since higher colistin concentrations led to eradication of the planktonic cultures) alone and in combination with NAC at 8,000 mg/L. Data were obtained from at least four independent experiments, with two replicates per condition per experiment.

The killing curves showed that anaerobic cultures were more susceptible to killing by colistin than aerobic cultures, as previously demonstrated (Pompilio *et al.*, 2015; Brochmann *et al.*, 2014) (Figure 8A). Noteworthy, NAC potentiated the bactericidal activity of colistin only under anaerobic conditions, leading to eradication of planktonic cultures after 24 hours (Figure 8A). Conversely, such a combination did not show activity against the same cultures grown in the presence of oxygen, demonstrating the influence of the growth conditions on the susceptibility of *P. aeruginosa* to such a combination (Figure 8B).

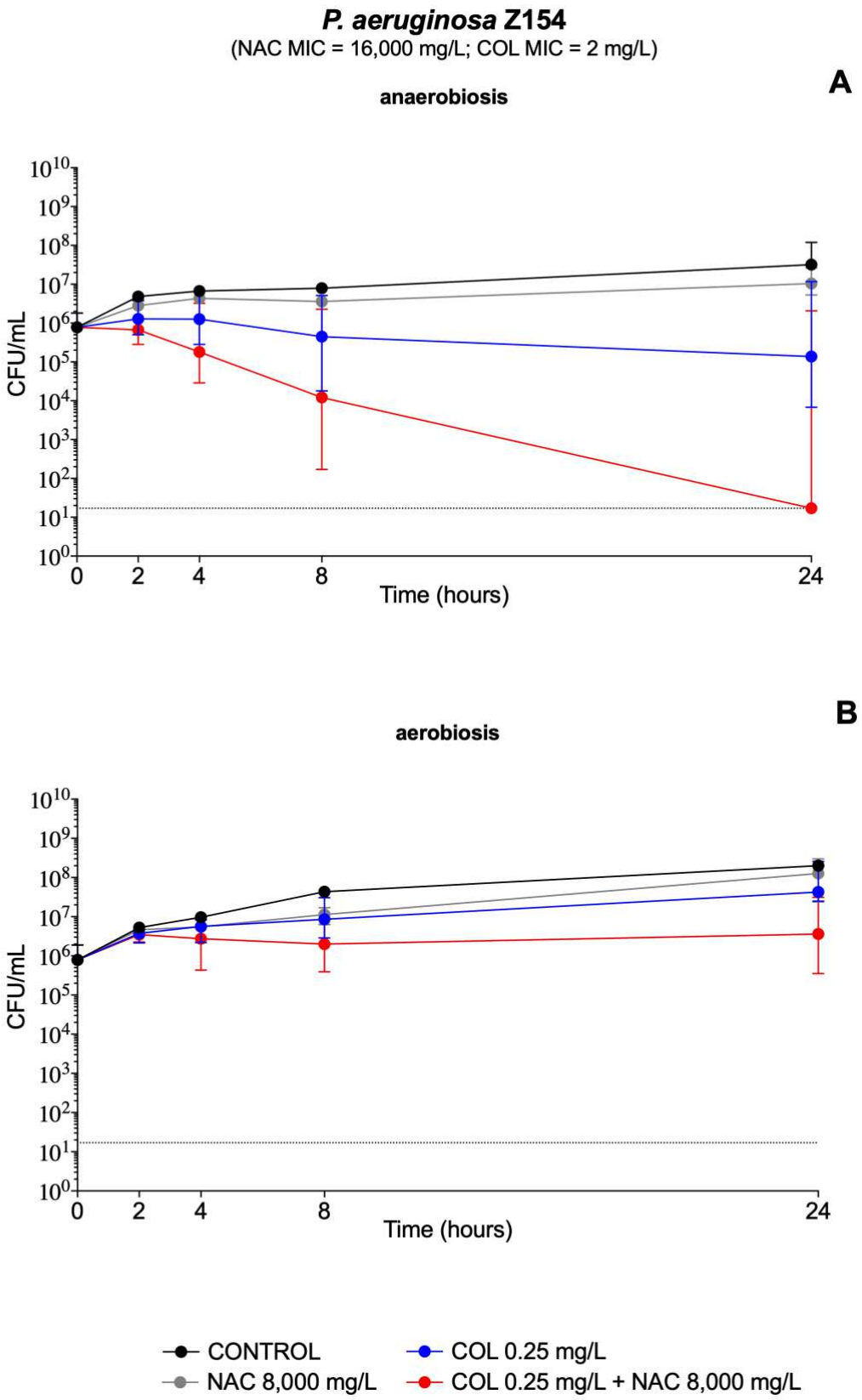

Figure 8. Time-kill curves of *P. aeruginosa* Z154 planktonic cultures exposed to *N*-acetylcysteine (NAC) at 8,000 mg/L, colistin (COL) at 0.25 mg/L, and the NAC-COL combination under anaerobic (A) and aerobic (B) conditions. Data are plotted as the median values of CFU/mL detected for each time point. Dotted lines indicate the detection limit (17 CFU/mL).

Taken together, such results clearly confirmed the transcriptomic data and demonstrated that NAC was able to inhibit the denitrification pathway in anaerobic environments (like those in the deeper biofilm layers and in CF mucus). Consequently, this feature might contribute to the observed antibiofilm synergism of NAC-colistin combinations, possibly preventing an adaptive response of *P. aeruginosa* to protect from colistin toxicity.

2.3 NAC-induced inhibition of the *P. aeruginosa* flagellum-mediated motility

Transcriptomic results also indicated that NAC downregulated two genes belonging to *P. aeruginosa* flagellar apparatus (i.e., *fliF* and *flhF*) (Table 9), which are necessary for the first step of flagellum assembly (Bouteiller *et al.*, 2021).

To confirm such transcriptional changes, swimming and swarming assay were carried out with the reference strain *P. aeruginosa* PAO1 and the CF strain *P. aeruginosa* Z154 (i.e., the strain used for transcriptomic analysis), in the presence or absence of NAC at 8,000 mg/L, following the protocol described by Rashid and Kornberg, with minor modifications (Rashid and Kornberg, 2000). The clinical isolate was resulted negative for the swarming motility without NAC, therefore only the effect of NAC on swimming motility could be tested with this strain. Assays were performed in at least three independent experiments, with three replicates per condition per experiment.

Overall, results showed a clear inhibition by NAC of both swimming and swarming motility (Figures 9 and 10), thus allowing to associate the downregulation of crucial genes of the flagellar apparatus biosynthesis to the observed impaired motility. Data from motility tests are consistent with previous studies that relate the reduced zinc availability with downregulation of virulence factors necessary for lung colonization (e.g., flagellar-dependent bacterial motility) (Mastropasqua *et al.*, 2018), further confirming the probable Zn^{2+} chelating activity of NAC and its involvement in the decrease of *P. aeruginosa* virulence.

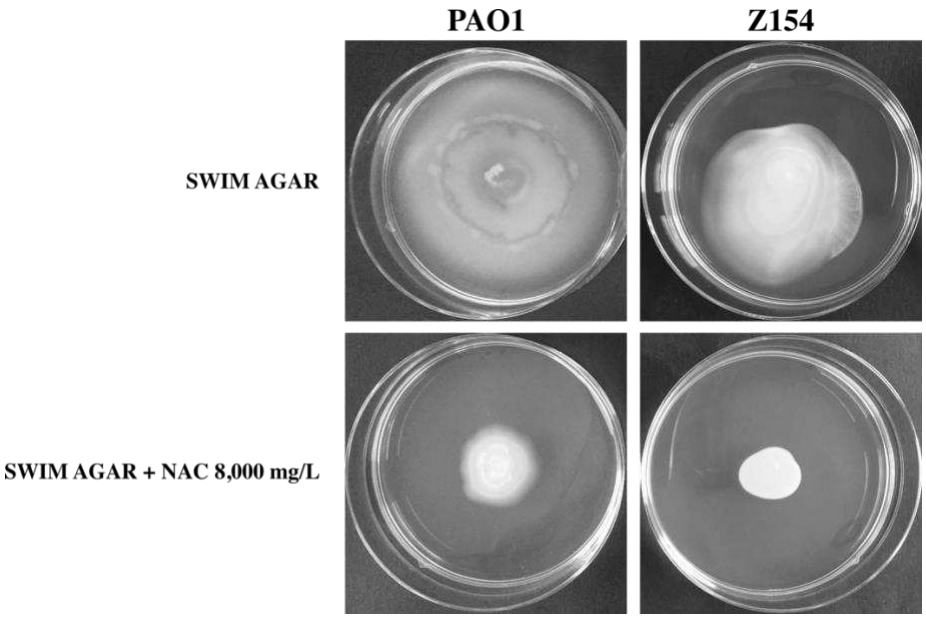

Figure 9. *N*-acetylcysteine (NAC)-mediated inhibition of *P. aeruginosa* PAO1 and Z154 swimming motility. Assays were performed in at least three independent experiments (with three replicates per condition per experiment), and representative data are shown.

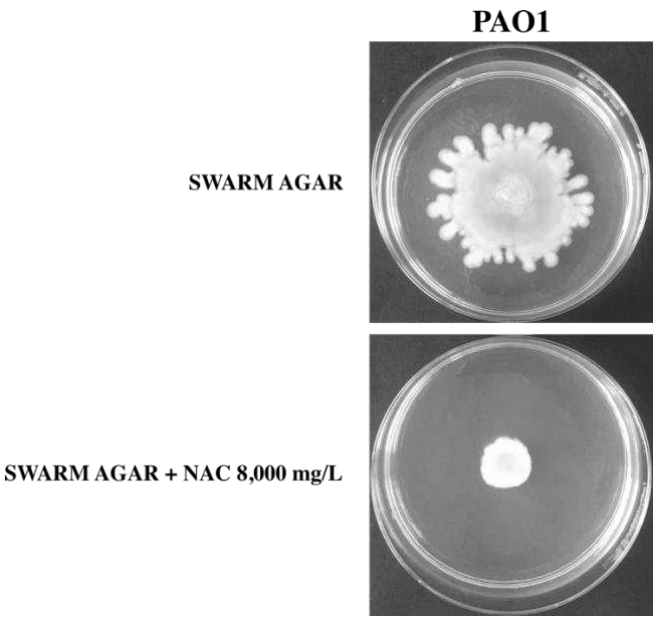

Figure 10. *N*-acetylcysteine (NAC)-mediated inhibition of *P. aeruginosa* PAO1 swarming motility. Assays were performed in at least three independent experiments (with three replicates per condition per experiment), and representative data are shown.

3. *In vitro* photokilling activity of light at 415 nm against *Pseudomonas aeruginosa* and *Staphylococcus aureus*

The potential photokilling activity of light at 415 nm (i.e., violet-blue light) was investigated against both planktonic and biofilm cultures of *P. aeruginosa* and *S. aureus* strains, including two reference strains (i.e., *P. aeruginosa* PAO1 and *S. aureus* USA300), and two strains isolated from CF patients (i.e., *P. aeruginosa* LESB65 and *S. aureus* CF-MRSA). The light source consisted of a light-emitting diode (LED) module emitting a light beam with 415 nm wavelength. Such a wavelength was chosen since the most effective in terms of photokilling action spectrum, according to the literature (Hamblin and Abrahamse, 2019; Wang *et al.*, 2017). Planktonic or biofilm cultures was irradiated from above at a distance of 15 cm from the LED illumination system, which was placed perpendicularly and centrally to them using a specific 3D printed holder (Figure 11A and 11B). The light dose (i.e., J/cm^2) received by the bacteria was calculated by multiplying the power output of LED light (i.e., W/cm^2) to which the sample was exposed by the exposure time (i.e., seconds). The power output was measured using a power meter positioned above the workbench where the bacterial cultures were placed, prior to *in vitro* testing.

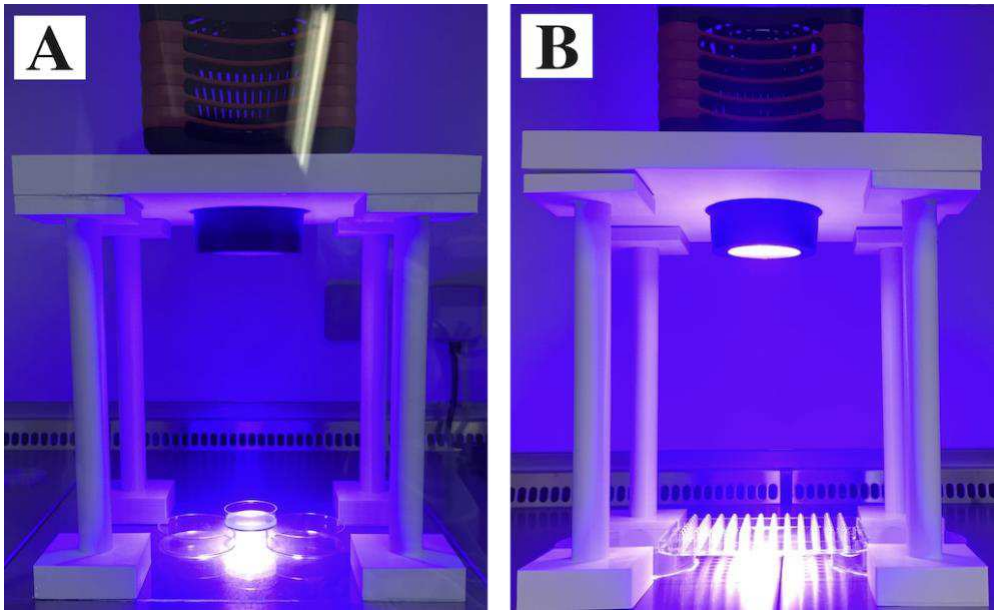

Figure 11. LED irradiation against planktonic (A) and biofilm (B) cultures.

3.1 Activity of light at 415 nm against planktonic cultures

To evaluate the potential antimicrobial activity of 415 nm LED light against planktonic cultures, all the four strains included in the study was tested following the protocol described by Biener *et al.* (Biener *et al.*, 2017), with some modifications. In particular, appropriate dilutions of bacterial cultures were plated onto agar plates (i.e., TSA) and immediately exposed to light at 415 nm. The same bacterial cultures plated and kept in the dark for the whole experiment duration represented the control. Such a protocol was chosen after preliminary experiments carried out with 96-wells plates using bacterial suspensions where was not observed photokilling effect for all strains (data not shown). The *P. aeruginosa* strains were exposed to 32, 63 and 95 J/cm^2 (i.e., doses potentially safe *in vivo*) corresponding to 5, 10 and 15 minutes of irradiation at 415 nm, respectively. The *S. aureus* strains were subjected only to 95 J/cm^2 since a scant effect was measured already with such a dose (see below). Data were obtained in at least three independent experiments, with one replicate per dose per experiment.

Results showed a dose-dependent effect of the light at 415 nm against both *P. aeruginosa* strains grown in planktonic phase, with a reduction of ≥2 log CFU/mL at the maximum dose tested (i.e., 95 J/cm^2) compared to the control (Figure 12A). On the contrary, a scant effect against *S. aureus* CF-MRSA (i.e., reduction <0.5 log CFU/mL), and no effect against *S. aureus* USA300 was observed (Figure 12B). For this reason, only *P. aeruginosa* strains were irradiated with other two lower doses (i.e., 32 and 63 J/cm^2) (Figure 12A). In absence of light (i.e., control plates) no killing was observed.

Overall, these results indicated that planktonic cells of *P. aeruginosa* had a higher susceptibility to the 415 nm LED light compared to *S. aureus* strains under the laboratory conditions used, demonstrating a probable species-dependent activity of the light at 415 nm. These data should be consolidated by investigating a wider panel of strains.

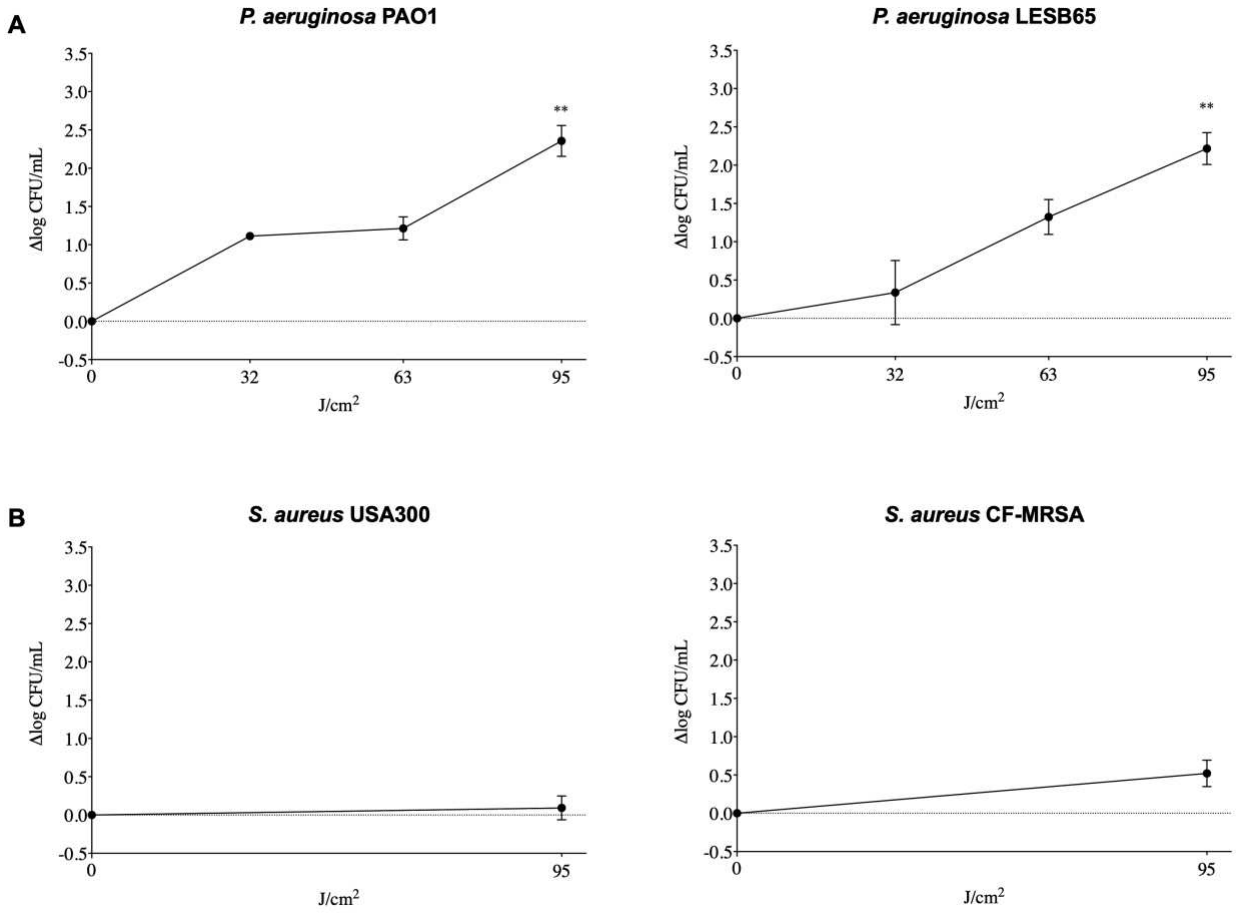

Figure 12. Antimicrobial activity of 415 nm wavelength against planktonic cultures of *P. aeruginosa* PAO1 and LESB65 (A), and *S. aureus* USA300 and CF-MRSA (B). The light doses used (i.e., 32, 63 and/or 95 J/cm^2) correspond to irradiation at 415 nm for 5, 10 and/or 15 minutes, respectively. Δlog CFU/mL represents the CFU/mL log reduction and was calculated by the ratio between the mean CFU/mL of the control and the mean CFU/mL detected for each dose. Filled dots represent the mean Δlog with standard deviation of the CFU/mL detected for each dose. Statistical analysis was performed using one-way ANOVA with Dunnett's correction by comparing the mean CFU/mL detected for each dose with the mean CFU/mL of the control (** p<0.01).

3.2 Activity of light at 415 nm in combination with potassium iodide against planktonic cultures

Data from paragraph 3.1 outlined the scant effect of 415 nm LED light against planktonic cultures of *S. aureus*. Recent findings have reported that the addition of inorganic salts, such as potassium iodide (KI), may potentiate the photokilling activity via photodynamic effect. In particular, the enhanced killing effect appears to involve the formation of extracellular free iodine and reactive iodine radicals which are able to kill bacteria when generated in solution (Hamblin, 2017). For this reason, a further investigation was conducted in order to assess the potentiation of the antimicrobial activity of light at 415 nm in the presence of KI against planktonic cultures. All the four strains included in the study were assayed. Bacterial suspensions were irradiated or not at 415 nm for 15 minutes (i.e., light dose of 95 J/cm^2), in the presence or absence of 100 mM KI, according to the protocol described by Huang *et al.* (Huang *et al.*, 2018) with some modifications. Bacterial cultures kept in the dark, with or without 100 mM KI, for the whole experiment duration represented the controls. The concentration of KI selected is the same reported in literature to be active against bacteria (Huang *et al.*, 2018; Vieira *et al.*, 2018; Wen *et al.*, 2017). Data were obtained in at least three independent experiments, with one replicate per dose per experiment.

Results showed that the exposure to 100 mM KI in combination with 415 nm LED light for 15 minutes (i.e., achieving a light dose of 95 J/cm^2) eradicated planktonic cultures of *P. aeruginosa* PAO1, while a bactericidal activity (i.e., reduction of >3 log CFU/mL compared to the control) was evident for *P. aeruginosa* LESB65 (Figure 13A). On the contrary, a slight effect (<1 log killing) was observed when both the *P. aeruginosa* strains were exposed to KI or 415 nm alone (Figure 13A). The photokilling activity (i.e., 415 nm alone) lower than reported in the paragraph 3.1 for the same strains was probably due to the different experimental approach used to evaluate the light effect in planktonic cultures (i.e., bacterial cells in suspension vs bacterial cells spread on a flat surface).

Interestingly, complete eradication of *S. aureus* planktonic cultures was achieved with the combination of 100 mM KI plus 415 nm LED light, while no antimicrobial effect was detected when the same cultures were exposed to KI or 415 nm alone (Figure 13B). In all cases, in absence of light (i.e., control plates) no killing was observed.

Overall, these data demonstrated that the addition of KI to *P. aeruginosa* and *S. aureus* planktonic cultures potentiated the photokilling activity of 415 nm LED light, thus probably confirming the involvement of KI in the bacterial cell death. Present findings are consistent with the previously observed KI-mediated potentiation of the antimicrobial activity of visible light against bacteria

(Huang *et al.*, 2018; Vieira *et al.*, 2018; Wen *et al.*, 2017). Further experiments with lower KI concentrations to find the minimum concentration allowing to observe the synergy *in vitro* are encouraged.

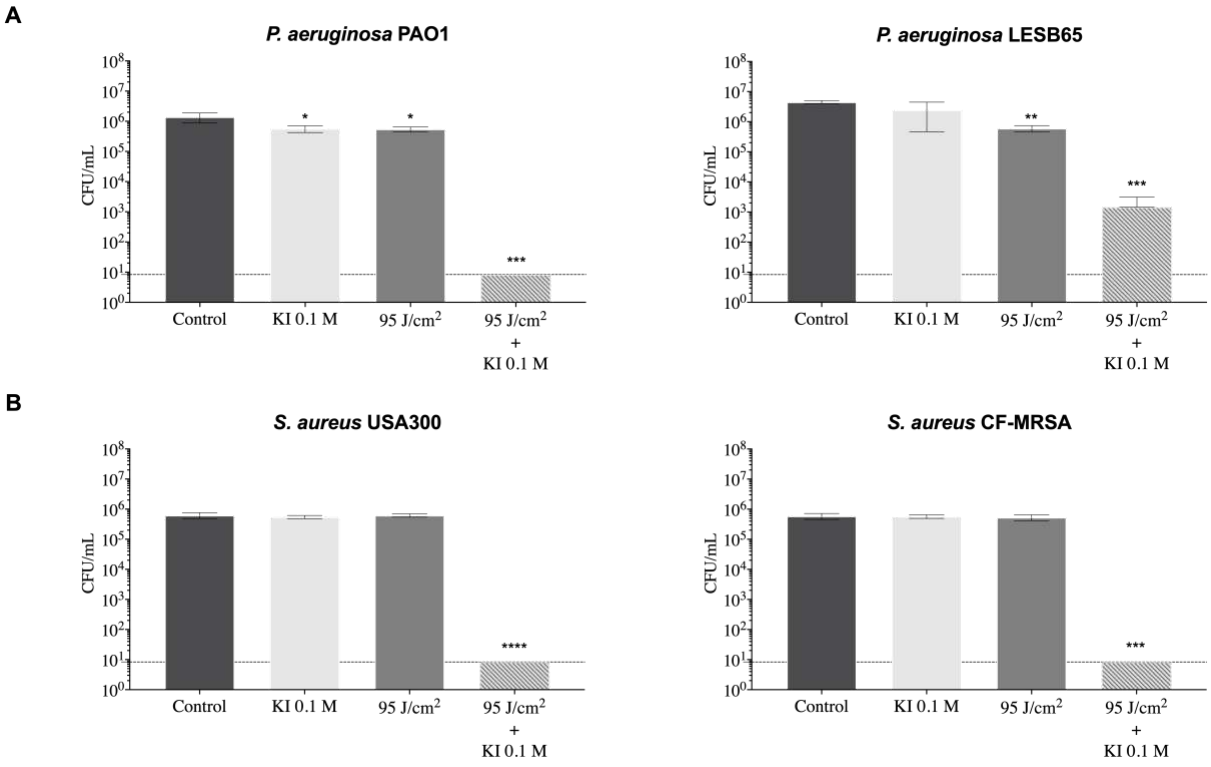

Figure 13. Antimicrobial activity of 415 nm wavelength alone and in combination with 100 mM potassium iodide (KI) against planktonic cultures of *P. aeruginosa* PAO1 and LESB65 (A), and *S. aureus* USA300 and CF-MRSA (B). The light dose used (i.e., 95 J/cm^2) correspond to irradiation at 415 nm for 15 minutes. Dotted lines indicate the detection limit (8.33 CFU/mL). Statistical analysis was performed using one-way ANOVA with Dunnett's correction by comparing the mean CFU/mL detected for each condition with the mean CFU/mL of the control (* p<0.05, ** p<0.01, *** p<0.001, **** p<0.0001).

3.3 Activity of light at 415 nm against preformed biofilms

To investigate the potential activity of 415 nm LED light against preformed biofilms, a standardized *in vitro* biofilm model (i.e., the same used for the experiments reported in part III, paragraphs 1.2 and 1.3) (Harrison *et al.*, 2010) was used. Four days-old biofilms (in the case of *P. aeruginosa* PAO1 and LESB65) and seven days-old biofilms (in the case of *S. aureus* USA300 and CF-MRSA) were exposed to light at 415 nm for 15 minutes. The dose was not uniform within all the plate (i.e., pegs lid) and was calculated to range from a minimum average of 8 J/cm^2 to a maximum average of 107 J/cm^2 (i.e., doses potentially safe *in vivo*). A twin pegs lid covered by a box wrapped in foil was placed close to the test area as unexposed control. After the irradiation, biofilm mass was evaluated by viable cell count (i.e., by disruption of biofilms by sonication, and determination of CFU/peg). Data were obtained in at least four independent experiments, with at least three replicate per dose per experiment.

Overall, a dose-dependent effect was observed against all the tested strains, with a reduction of ≥2 log CFU/peg at 60 J/cm^2 for three out of four tested strains (i.e., *P. aeruginosa* PAO1 and LESB65, and *S. aureus* CF-MRSA) (Figure 14A and 14B). *S. aureus* USA300 was the only one less affected by the light at 415 nm, with a reduction of <1.5 log CFU/peg at the maximum tested dose (i.e., 107 J/cm^2) (Figure 14B). *P. aeruginosa* LESB65 was also more susceptible to light than *P. aeruginosa* PAO1 at the lower doses tested (i.e., doses ranging from 20 to 40 J/cm^2), while at the maximum dose (i.e., 107 J/cm^2) the log reduction was similar for both strains (Figure 14A). However, the different biofilm susceptibility to the 415 nm LED light was more evident in the *S. aureus* strains, where a reduction >3 log CFU/peg was observed at 107 J/cm^2 against the CF-MRSA strain compared to that observed against the USA300 strain (i.e., a reduction of <1.5 log CFU/peg) at the same dose (Figure 14B). Moreover, *P. aeruginosa* LESB65 and *S. aureus* USA300 showed a plateau in the photokilling activity (i.e., approximately between 60 and 107 J/cm^2) (Figure 14A and 14B). The reason accounting for this phenomenon would deserve further investigation. In the absence of light (control plates) no killing was observed.

Taken together, these results showed a significant antimicrobial activity of the light at 415 nm against preformed biofilms of *P. aeruginosa* and *S. aureus*. Compared to results obtained with planktonic cells, a strain-dependent activity was detectable in biofilm cultures, demonstrating the existence of differences in the stress response between planktonic and biofilm cultures. Noteworthy, 415 nm LED light had more effect against biofilms of *P. aeruginosa* LESB65 and *S. aureus* CF-MRSA, both strains isolated from CF patients. This evidence would deserve further investigation due to the

potential clinical application of violet-blue light, especially in the management of biofilm-associated lung infections.

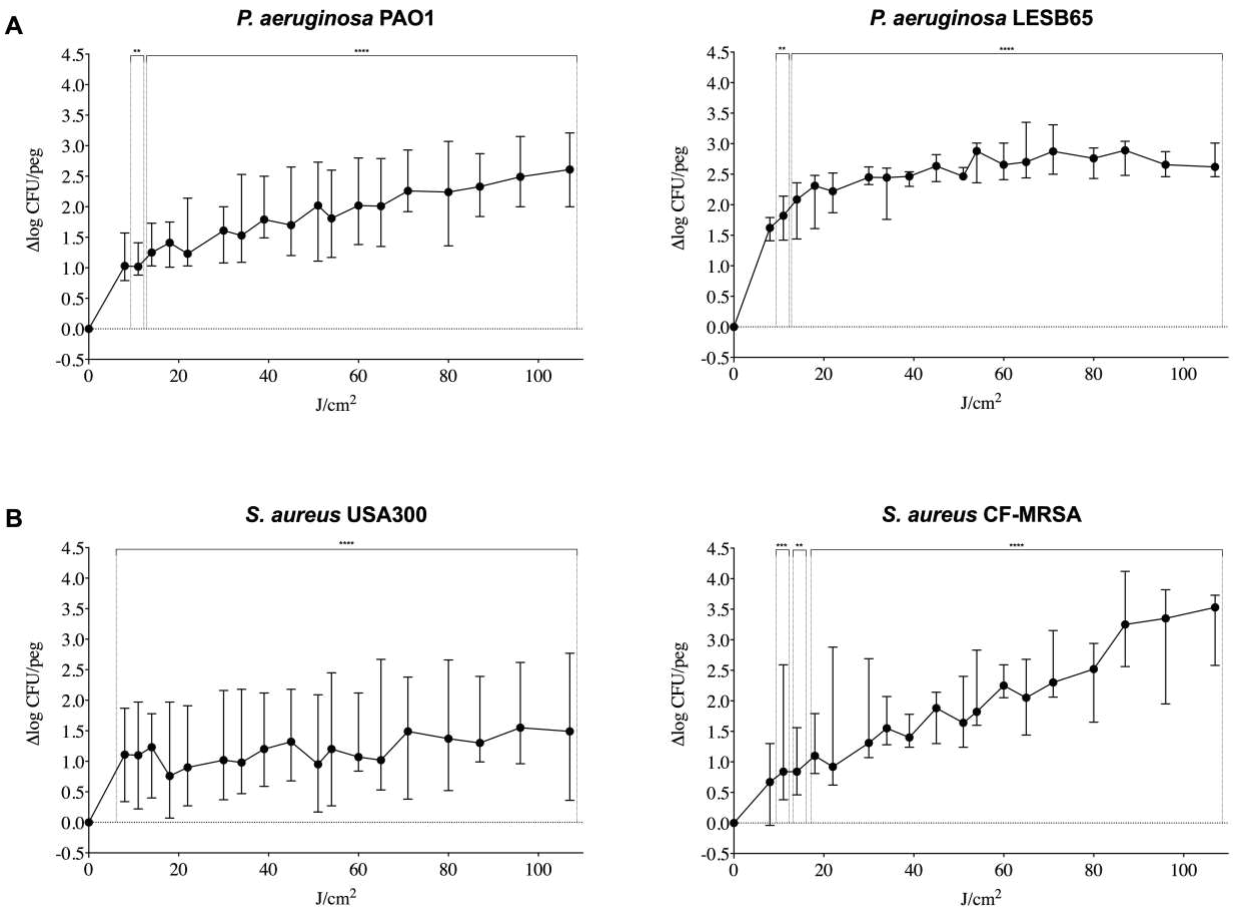

Figure 14. Antibiofilm activity of 415 nm wavelength against preformed biofilms of *P. aeruginosa* PAO1 and LESB65 (A), and *S. aureus* USA300 and CF-MRSA (B). Δlog CFU/peg represents the CFU/peg log reduction and was calculated by the ratio between the median CFU/peg of the controls and the median CFU/peg detected for each dose. Filled dots represent the median Δlog with error range of the CFU/peg detected for each dose. Statistical analysis was performed using Kruskal-Wallis test with Dunn's correction by comparing the mean CFU/mL detected for each dose with the mean CFU/mL of the control (** $p<0.01$, *** $p<0.001$, **** $p<0.0001$).

PART IV

CONCLUSIONS AND PERSPECTIVES

Pseudomonas aeruginosa, *Stenotrophomonas maltophilia* and *Staphylococcus aureus* are the major pathogens associated with respiratory tract infections, especially in patients affected by cystic fibrosis (CF) and other chronic lung diseases, such as chronic obstructive pulmonary disease and non-CF bronchiectasis. Due to intrinsic and acquired multidrug resistance mechanisms and the propensity to grow as biofilm, infections caused by such pathogens are difficult to treat, and the therapeutic options are very limited. Biofilms are responsible of chronic lung colonization since evade the host defences and express tolerance to antibiotic treatment, leading to therapeutic failure, airways chronic inflammation and worse clinical outcome. To overcome this issue, novel antibiofilm treatments are currently under study and the use of non-antibiotic therapies potentially administrable alone or in combination with antibiotics has been taken into consideration. Moreover, a renewed interest has been recently focused on topical routes of administration (e.g., inhalation, nebulization, and aerosolization), which allow the achievement of high drug concentrations in the lungs with limited systemic toxicity. *N*-acetylcysteine (NAC), a mucolytic agent with antioxidant activity, is commonly administered with antibiotics for the treatment of lower respiratory tract infections. Colistin, a last-resort antibiotic for the treatment of *P. aeruginosa* infections, it has been increasingly used in CF, especially by nebulization.

In this respect, a first study included in this thesis work involved the evaluation of the antimicrobial and antibiofilm activity of NAC alone in combination with colistin against a collection of *S. maltophilia* and *P. aeruginosa* strains, most of which isolated from CF patients and presenting different resistance phenotypes of clinical relevance.

NAC-colistin combinations were found to have an effective antimicrobial and antibiofilm activity against *S. maltophilia*, an emerging global difficult to treat opportunistic pathogen, with an important role also in CF. This effect was particularly evident for those isolates presenting very high colistin MICs, suggesting that NAC could affect the mechanisms of acquired colistin resistance, potentially restoring a susceptible phenotype.

Concerning *P. aeruginosa* strains, NAC potentiated colistin activity against *in vitro* biofilms, regardless phenotype and genotype. Interestingly, NAC-colistin were synergistic in the ASM biofilm model, which resemble the compositional environment present in the CF mucus, demonstrating the potential clinical applications of such a combination. These data also displayed that biofilm susceptibility to colistin was different regarding the *in vitro* model used, highlighting the influence exerted by the culture medium on *P. aeruginosa* biofilms responsiveness to antibiotics.

To assess as NAC might exert its antibiofilm activity in *P. aeruginosa*, a transcriptomic study in a mucoid CF strain exposed to NAC was also carried out. In particular, the obtained data represent the first evidence about transcriptional changes occurring in *P. aeruginosa* planktonic cultures in the presence of NAC *in vitro*. The study, followed by biological experiments, suggested that NAC inhibited *P. aeruginosa* anaerobic respiration, which could be relevant for the observed antibiofilm synergism with colistin. In addition, although NAC alone was not demonstrated to be effective against preformed *P. aeruginosa* biofilms, transcriptomic analysis of NAC-exposed planktonic cultures revealed that NAC could attenuate *P. aeruginosa* virulence, mainly by inducing a zinc starvation response, affecting anaerobic respiration, and inhibiting flagellum-mediated motility, the last two features confirmed experimentally.

An alternative and innovative way to overcome the antibiotic use could be found in the development of light-based approaches. A very promising approach is the antimicrobial photodynamic therapy, which is based on the generation of reactive oxygen species by the combined action of visible light, oxygen, and an endogenous photosensitiser, such as bacterial porphyrins.

In this respect, a further investigation was carried out as part of the Light4Lungs project, a four-year Horizon 2020 FET Open project, aimed at developing an alternative therapeutic scheme for the treatment of chronic lung diseases by the implementation of a novel inhalable photodynamic therapy. The potential antimicrobial activity of light at 415 nm, known to be active against different bacterial species, was investigated against *P. aeruginosa* and *S. aureus* strains, including clinical strains isolated from CF patients.

The results obtained showed a potential antimicrobial activity of the light at 415 nm against *P. aeruginosa* strains grown in planktonic phase, while *S. aureus* strains were irresponsive. However, the addition of potassium iodide (known to increase the light-mediated killing activity) to planktonic cultures allowed to observe a potentiation of the photokilling activity of 415 nm light, especially with *S. aureus* cultures which were eradicated. Conversely, an antibiofilm activity of the light at 415 nm was observed against both *P. aeruginosa* strains and *S. aureus* strains, underlining the differences of response to oxidative stress between diverse physiological states of growth. Interestingly, the major effects were more evident against the strains isolated from CF compared to the reference strains, underlining the potential clinical application of this approach.

In conclusion, NAC-colistin combinations at the high concentrations achievable by inhalation could represent an effective treatment against infections caused by biofilm-associated pathogens, such as *S. maltophilia* and *P. aeruginosa*, while potentially reducing the risk of *in vivo* selection of colistin

resistance. Moreover, based on transcriptomic data, NAC might have beneficial effects in the very first steps of lung infection, possibly preventing biofilm formation and the establishment of a chronic colonization. In this perspective, further studies should be performed because they could possibly help identifying critical targets in the complex biofilm environments, to be used for the implementation of new antibiofilm strategies.

The antimicrobial effect of light at 415 nm deserves further investigation with a wider collection of *P. aeruginosa* and *S. aureus* clinical isolates exhibiting different phenotypic and genotypic feature, for the potential applications as alternative antimicrobial treatment that such a light-based approach could represent, especially in biofilm-associated chronic infections. Further studies aimed at evaluating the potassium iodide-mediated potentiation of photokilling activity of antimicrobial light against *in vitro* biofilm models are also encouraged.

PART V

BIBLIOGRAPHY

Ahmed, M.N., Abdelsamad, A., Wassermann, T., Porse, A., Becker, J., Sommer, M.O.A., Høiby, N., Ciofu, O., 2020. The evolutionary trajectories of *P. aeruginosa* in biofilm and planktonic growth modes exposed to ciprofloxacin: beyond selection of antibiotic resistance. NPJ Biofilms Microbiomes 6, 28. https://doi.org/10.1038/s41522-020-00138-8

Aiyer, A., Manos, J., 2022. The Use of Artificial Sputum Media to Enhance Investigation and Subsequent Treatment of Cystic Fibrosis Bacterial Infections. Microorganisms 10, 1269. https://doi.org/10.3390/microorganisms10071269

Amin, R.M., Bhayana, B., Hamblin, M.R., Dai, T., 2016. Antimicrobial blue light inactivation of *Pseudomonas aeruginosa* by photo-excitation of endogenous porphyrins: In vitro and *in vivo* studies. Lasers Surg Med 48, 562–568. https://doi.org/10.1002/lsm.22474

Antonelli, A., D'Andrea, M.M., Galano, A., Borchi, B., Brenciani, A., Vaggelli, G., Cavallo, A., Bartoloni, A., Giovanetti, E., Rossolini, G.M., 2016. Linezolid-resistant cfr-positive MRSA, Italy. J Antimicrob Chemother 71, 2349–2351. https://doi.org/10.1093/jac/dkw108

Azeredo, J., Azevedo, N.F., Briandet, R., Cerca, N., Coenye, T., Costa, A.R., Desvaux, M., Di Bonaventura, G., Hébraud, M., Jaglic, Z., Kačániová, M., Knøchel, S., Lourenço, A., Mergulhão, F., Meyer, R.L., Nychas, G., Simões, M., Tresse, O., Sternberg, C., 2017. Critical review on biofilm methods. Crit Rev Microbiol 43, 313–351. https://doi.org/10.1080/1040841X.2016.1208146

Beasley, V., Joshi, P.V., Singanayagam, A., Molyneaux, P.L., Johnston, S.L., Mallia, P., 2012. Lung microbiology and exacerbations in COPD. Int J Chron Obstruct Pulmon Dis 7, 555–569. https://doi.org/10.2147/COPD.S28286

Biener, G., Masson-Meyers, D.S., Bumah, V.V., Hussey, G., Stoneman, M.R., Enwemeka, C.S., Raicu, V., 2017. Blue/violet laser inactivates methicillin-resistant *Staphylococcus aureus* by altering its transmembrane potential. J Photochem Photobiol B 170, 118–124. https://doi.org/10.1016/j.jphotobiol.2017.04.002

Bjarnsholt, T., 2013. The role of bacterial biofilms in chronic infections. APMIS Suppl 1–51. https://doi.org/10.1111/apm.12099

Blasi, F., Page, C., Rossolini, G.M., Pallecchi, L., Matera, M.G., Rogliani, P., Cazzola, M., 2016. The effect of N-acetylcysteine on biofilms: Implications for the treatment of respiratory tract infections. Respir Med 117, 190–197. https://doi.org/10.1016/j.rmed.2016.06.015

Boisson, M., Grégoire, N., Cormier, M., Gobin, P., Marchand, S., Couet, W., Mimoz, O., 2017. Pharmacokinetics of nebulized colistin methanesulfonate in critically ill patients. J Antimicrob Chemother 72, 2607–2612. https://doi.org/10.1093/jac/dkx167

Bonapace, C.R., Bosso, J.A., Friedrich, L.V., White, R.L., 2002. Comparison of methods of interpretation of checkerboard synergy testing. Diagn Microbiol Infect Dis 44, 363–366. https://doi.org/10.1016/s0732-8893(02)00473-x

Boudet, A., Jay, A., Dunyach-Remy, C., Chiron, R., Lavigne, J.-P., Marchandin, H., 2021. In-Host Emergence of Linezolid Resistance in a Complex Pattern of Toxic Shock Syndrome Toxin-1-Positive Methicillin-Resistant *Staphylococcus aureus* Colonization in Siblings with Cystic Fibrosis. Toxins (Basel) 13, 317. https://doi.org/10.3390/toxins13050317

Bouteiller, M., Dupont, C., Bourigault, Y., Latour, X., Barbey, C., Konto-Ghiorghi, Y., Merieau, A., 2021. *Pseudomonas* Flagella: Generalities and Specificities. Int J Mol Sci 22, 3337. https://doi.org/10.3390/ijms22073337

Brochmann, R.P., Toft, A., Ciofu, O., Briales, A., Kolpen, M., Hempel, C., Bjarnsholt, T., Høiby, N., Jensen, P.Ø., 2014. Bactericidal effect of colistin on planktonic *Pseudomonas aeruginosa* is independent of hydroxyl radical formation. Int J Antimicrob Agents 43, 140–147. https://doi.org/10.1016/j.ijantimicag.2013.10.015

Brooke, J.S., 2012. *Stenotrophomonas maltophilia*: an emerging global opportunistic pathogen. Clin Microbiol Rev 25, 2–41. https://doi.org/10.1128/CMR.00019-11

Ceri, H., Olson, M.E., Stremick, C., Read, R.R., Morck, D., Buret, A., 1999. The Calgary Biofilm Device: new technology for rapid determination of antibiotic susceptibilities of bacterial biofilms. J Clin Microbiol 37, 1771–1776. https://doi.org/10.1128/JCM.37.6.1771-1776.1999

CFF, 2019. 2019 Patient Registry Annual Data Report 92.

Chalmers, J.D., Hill, A.T., 2013. Mechanisms of immune dysfunction and bacterial persistence in non-cystic fibrosis bronchiectasis. Mol Immunol 55, 27–34. https://doi.org/10.1016/j.molimm.2012.09.011

Chen, H., Mai, H., Lopes, B., Wen, F., Patil, S., 2022. Novel *Pseudomonas aeruginosa* Strains Co-Harbouring *bla*$_{NDM-1}$ Metallo β-Lactamase and *mcr-1* Isolated from Immunocompromised Paediatric Patients. Infect Drug Resist 15, 2929–2936. https://doi.org/10.2147/IDR.S368566

Cianciulli Sesso, A., Lilić, B., Amman, F., Wolfinger, M.T., Sonnleitner, E., Bläsi, U., 2021. Gene Expression Profiling of *Pseudomonas aeruginosa* Upon Exposure to Colistin and Tobramycin. Front Microbiol 12, 626715. https://doi.org/10.3389/fmicb.2021.626715

Ciofu, O., Moser, C., Jensen, P.Ø., Høiby, N., 2022. Tolerance and resistance of microbial biofilms. Nat Rev Microbiol. https://doi.org/10.1038/s41579-022-00682-4

Ciofu, O., Tolker-Nielsen, T., Jensen, P.Ø., Wang, H., Høiby, N., 2015. Antimicrobial resistance, respiratory tract infections and role of biofilms in lung infections in cystic fibrosis patients. Adv Drug Deliv Rev 85, 7–23. https://doi.org/10.1016/j.addr.2014.11.017

CLSI M026-A, 1999. Methods for determining bactericidal activity of antimicrobial agents: approved guideline. National Committee for Clinical Laboratory Standards, Wayne, PA.

Davies, D., 2003. Understanding biofilm resistance to antibacterial agents. Nat Rev Drug Discov 2, 114–122. https://doi.org/10.1038/nrd1008

Ducret, V., Abdou, M., Goncalves Milho, C., Leoni, S., Martin--Pelaud, O., Sandoz, A., Segovia Campos, I., Tercier-Waeber, M.-L., Valentini, M., Perron, K., 2021. Global Analysis of the Zinc Homeostasis Network in *Pseudomonas* aeruginosa and Its Gene Expression Dynamics. Front Microbiol 12, 2694. https://doi.org/10.3389/fmicb.2021.739988

Fernández-Barat, L., Torres, A., 2016. Biofilms in ventilator-associated pneumonia. Future Microbiol 11, 1599–1610. https://doi.org/10.2217/fmb-2016-0040

Ferrer-Espada, R., Wang, Y., Goh, X.S., Dai, T., 2020. Antimicrobial Blue Light Inactivation of Microbial Isolates in Biofilms. Lasers Surg Med 52, 472–478. https://doi.org/10.1002/lsm.23159

Flume, P.A., Chalmers, J.D., Olivier, K.N., 2018. Advances in bronchiectasis: endotyping, genetics, microbiome, and disease heterogeneity. Lancet 392, 880–890. https://doi.org/10.1016/S0140-6736(18)31767-7

Fothergill, J.L., Neill, D.R., Loman, N., Winstanley, C., Kadioglu, A., 2014. *Pseudomonas aeruginosa* adaptation in the nasopharyngeal reservoir leads to migration and persistence in the lungs. Nat Commun 5, 4780. https://doi.org/10.1038/ncomms5780

Frimodt-Møller, J., Rossi, E., Haagensen, J.A.J., Falcone, M., Molin, S., Johansen, H.K., 2018. Mutations causing low level antibiotic resistance ensure bacterial survival in antibiotic-treated hosts. Sci Rep 8, 12512. https://doi.org/10.1038/s41598-018-30972-y

Gil-Perotin, S., Ramirez, P., Marti, V., Sahuquillo, J.M., Gonzalez, E., Calleja, I., Menendez, R., Bonastre, J., 2012. Implications of endotracheal tube biofilm in ventilator-associated pneumonia response: a state of concept. Crit Care 16, R93. https://doi.org/10.1186/cc11357

Guerini, M., Condrò, G., Friuli, V., Maggi, L., Perugini, P., 2022. N-acetylcysteine (NAC) and Its Role in Clinical Practice Management of Cystic Fibrosis (CF): A Review. Pharmaceuticals (Basel) 15, 217. https://doi.org/10.3390/ph15020217

Guerini, M., Perugini, P., Grisoli, P., 2020. Evaluation of the Effectiveness of N-Acetylcysteine (NAC) and N-acetylcysteine-cyclodextrins Multi-Composite in *Pseudomonas aeruginosa* Biofilm Formation. Applied Sciences 10, 3466. https://doi.org/10.3390/app10103466

Guo, Y., Song, G., Sun, M., Wang, J., Wang, Y., 2020. Prevalence and Therapies of Antibiotic-Resistance in *Staphylococcus aureus*. Front Cell Infect Microbiol 10, 107. https://doi.org/10.3389/fcimb.2020.00107

Halstead, F.D., Thwaite, J.E., Burt, R., Laws, T.R., Raguse, M., Moeller, R., Webber, M.A., Oppenheim, B.A., 2016. Antibacterial Activity of Blue Light against Nosocomial Wound Pathogens Growing Planktonically and as Mature Biofilms. Appl Environ Microbiol 82, 4006–4016. https://doi.org/10.1128/AEM.00756-16

Hamblin, M.R., 2017. Potentiation of antimicrobial photodynamic inactivation by inorganic salts. Expert Rev Anti Infect Ther 15, 1059–1069. https://doi.org/10.1080/14787210.2017.1397512

Hamblin, M.R., Abrahamse, H., 2019. Can light-based approaches overcome antimicrobial resistance? Drug Dev Res 80, 48–67. https://doi.org/10.1002/ddr.21453

Han, M.-L., Zhu, Y., Creek, D.J., Lin, Y.-W., Gutu, A.D., Hertzog, P., Purcell, T., Shen, H.-H., Moskowitz, S.M., Velkov, T., Li, J., 2019. Comparative Metabolomics and Transcriptomics Reveal Multiple Pathways Associated with Polymyxin Killing in *Pseudomonas aeruginosa*. mSystems 4, e00149-18. https://doi.org/10.1128/mSystems.00149-18

Harrison, J.J., Stremick, C.A., Turner, R.J., Allan, N.D., Olson, M.E., Ceri, H., 2010. Microtiter susceptibility testing of microbes growing on peg lids: a miniaturized biofilm model for high-throughput screening. Nat Protoc 5, 1236–1254. https://doi.org/10.1038/nprot.2010.71

Hassett, D.J., Borchers, M.T., Panos, R.J., 2014. Chronic obstructive pulmonary disease (COPD): evaluation from clinical, immunological and bacterial pathogenesis perspectives. J Microbiol 52, 211–226. https://doi.org/10.1007/s12275-014-4068-2

Hennequin, C., Aumeran, C., Robin, F., Traore, O., Forestier, C., 2012. Antibiotic resistance and plasmid transfer capacity in biofilm formed with a CTX-M-15-producing *Klebsiella pneumoniae* isolate. J Antimicrob Chemother 67, 2123–2130. https://doi.org/10.1093/jac/dks169

Høiby, N., Bjarnsholt, T., Moser, C., Jensen, P.Ø., Kolpen, M., Qvist, T., Aanaes, K., Pressler, T., Skov, M., Ciofu, O., 2017. Diagnosis of biofilm infections in cystic fibrosis patients. APMIS 125, 339–343. https://doi.org/10.1111/apm.12689

Huang, J.X., Blaskovich, M.A.T., Pelingon, R., Ramu, S., Kavanagh, A., Elliott, A.G., Butler, M.S., Montgomery, A.B., Cooper, M.A., 2015. Mucin Binding Reduces Colistin Antimicrobial Activity. Antimicrob Agents Chemother 59, 5925–5931. https://doi.org/10.1128/AAC.00808-15

Huang, L., El-Hussein, A., Xuan, W., Hamblin, M.R., 2018. Potentiation by potassium iodide reveals that the anionic porphyrin TPPS4 is a surprisingly effective photosensitizer for antimicrobial photodynamic inactivation. J Photochem Photobiol B 178, 277–286. https://doi.org/10.1016/j.jphotobiol.2017.10.036

Jaiyesimi, O.A., McAvoy, A.C., Fogg, D.N., Garg, N., 2021. Metabolomic profiling of *Burkholderia cenocepacia* in synthetic cystic fibrosis sputum medium reveals nutrient environment-specific production of virulence factors. Sci Rep 11, 21419. https://doi.org/10.1038/s41598-021-00421-4

Kamal, S.M., Rybtke, M.L., Nimtz, M., Sperlein, S., Giske, C., Trček, J., Deschamps, J., Briandet, R., Dini, L., Jänsch, L., Tolker-Nielsen, T., Lee, C., Römling, U., 2019. Two FtsH Proteases Contribute to Fitness and Adaptation of *Pseudomonas aeruginosa* Clone C Strains. Front Microbiol 10, 1372. https://doi.org/10.3389/fmicb.2019.01372

Karaiskos, I., Souli, M., Galani, I., Giamarellou, H., 2017. Colistin: still a lifesaver for the 21st century? Expert Opin Drug Metab Toxicol 13, 59–71. https://doi.org/10.1080/17425255.2017.1230200

Klare, W., Das, T., Ibugo, A., Buckle, E., Manefield, M., Manos, J., 2016. Glutathione-Disrupted Biofilms of Clinical *Pseudomonas aeruginosa* Strains Exhibit an Enhanced Antibiotic Effect and a Novel Biofilm Transcriptome. Antimicrob Agents Chemother 60, 4539–4551. https://doi.org/10.1128/AAC.02919-15

Kolpen, M., Appeldorff, C.F., Brandt, S., Mousavi, N., Kragh, K.N., Aydogan, S., Uppal, H.A., Bjarnsholt, T., Ciofu, O., Høiby, N., Jensen, P.Ø., 2016. Increased bactericidal activity of colistin on *Pseudomonas aeruginosa* biofilms in anaerobic conditions. Pathog Dis 74, ftv086. https://doi.org/10.1093/femspd/ftv086

Kolpen, M., Kragh, K.N., Bjarnsholt, T., Line, L., Hansen, C.R., Dalbøge, C.S., Hansen, N., Kühl, M., Høiby, N., Jensen, P.Ø., 2015. Denitrification by cystic fibrosis pathogens - *Stenotrophomonas maltophilia* is dormant in sputum. Int J Med Microbiol 305, 1–10. https://doi.org/10.1016/j.ijmm.2014.07.002

Koo, H., Allan, R.N., Howlin, R.P., Stoodley, P., Hall-Stoodley, L., 2017. Targeting microbial biofilms: current and prospective therapeutic strategies. Nat Rev Microbiol 15, 740–755. https://doi.org/10.1038/nrmicro.2017.99

Lakhundi, S., Zhang, K., 2018. Methicillin-Resistant *Staphylococcus aureus*: Molecular Characterization, Evolution, and Epidemiology. Clin Microbiol Rev 31, e00020-18. https://doi.org/10.1128/CMR.00020-18

Landini, G., Di Maggio, T., Sergio, F., Docquier, J.-D., Rossolini, G.M., Pallecchi, L., 2016. Effect of High N-Acetylcysteine Concentrations on Antibiotic Activity against a Large Collection of Respiratory Pathogens. Antimicrob Agents Chemother 60, 7513–7517. https://doi.org/10.1128/AAC.01334-16

Lebeaux, D., Ghigo, J.-M., Beloin, C., 2014. Biofilm-related infections: bridging the gap between clinical management and fundamental aspects of recalcitrance toward antibiotics. Microbiol Mol Biol Rev 78, 510–543. https://doi.org/10.1128/MMBR.00013-14

Lee, J.-Y., Park, Y.K., Chung, E.S., Na, I.Y., Ko, K.S., 2016. Evolved resistance to colistin and its loss due to genetic reversion in *Pseudomonas aeruginosa*. Sci Rep 6, 25543. https://doi.org/10.1038/srep25543

Lhospice, S., Gomez, N.O., Ouerdane, L., Brutesco, C., Ghssein, G., Hajjar, C., Liratni, A., Wang, S., Richaud, P., Bleves, S., Ball, G., Borezée-Durant, E., Lobinski, R., Pignol, D., Arnoux, P., Voulhoux, R., 2017. *Pseudomonas aeruginosa* zinc uptake in chelating environment is primarily mediated by the metallophore pseudopaline. Sci Rep 7, 17132. https://doi.org/10.1038/s41598-017-16765-9

Lim, C.K., Hassan, K.A., Penesyan, A., Loper, J.E., Paulsen, I.T., 2013. The effect of zinc limitation on the transcriptome of *Pseudomonas* protegens Pf-5. Environ Microbiol 15, 702–715. https://doi.org/10.1111/j.1462-2920.2012.02849.x

Line, L., Alhede, M., Kolpen, M., Kühl, M., Ciofu, O., Bjarnsholt, T., Moser, C., Toyofuku, M., Nomura, N., Høiby, N., Jensen, P.Ø., 2014. Physiological levels of nitrate support anoxic growth by denitrification of *Pseudomonas aeruginosa* at growth rates reported in cystic fibrosis lungs and sputum. Front Microbiol 5, 554. https://doi.org/10.3389/fmicb.2014.00554

Long, S.W., Olsen, R.J., Mehta, S.C., Palzkill, T., Cernoch, P.L., Perez, K.K., Musick, W.L., Rosato, A.E., Musser, J.M., 2014. PBP2a mutations causing high-level Ceftaroline resistance in clinical methicillin-resistant *Staphylococcus aureus* isolates. Antimicrob Agents Chemother 58, 6668–6674. https://doi.org/10.1128/AAC.03622-14

Malhotra, S., Hayes, D., Wozniak, D.J., 2019. Cystic Fibrosis and *Pseudomonas aeruginosa*: the Host-Microbe Interface. Clin Microbiol Rev 32, e00138-18. https://doi.org/10.1128/CMR.00138-18

Mammen, M.J., Sethi, S., 2016. COPD and the microbiome. Respirology 21, 590–599. https://doi.org/10.1111/resp.12732

Manos, J., 2021. Current and Emerging Therapies to Combat Cystic Fibrosis Lung Infections. Microorganisms 9, 1874. https://doi.org/10.3390/microorganisms9091874

Marsh, R.L., Binks, M.J., Smith-Vaughan, H.C., Janka, M., Clark, S., Richmond, P., Chang, A.B., Thornton, R.B., 2022. Prevalence and subtyping of biofilms present in bronchoalveolar lavage from children with protracted bacterial bronchitis or non-cystic fibrosis bronchiectasis: a cross-sectional study. Lancet Microbe 3, e215–e223. https://doi.org/10.1016/S2666-5247(21)00300-1

Martegani, E., Bolognese, F., Trivellin, N., Orlandi, V.T., 2020. Effect of blue light at 410 and 455 nm on *Pseudomonas aeruginosa* biofilm. J Photochem Photobiol B 204, 111790. https://doi.org/10.1016/j.jphotobiol.2020.111790

Mastropasqua, M.C., Lamont, I., Martin, L.W., Reid, D.W., D'Orazio, M., Battistoni, A., 2018. Efficient zinc uptake is critical for the ability of *Pseudomonas aeruginosa* to express virulence traits and colonize the human lung. J Trace Elem Med Biol 48, 74–80. https://doi.org/10.1016/j.jtemb.2018.03.009

McCarron, A., Parsons, D., Donnelley, M., 2021. Animal and Cell Culture Models for Cystic Fibrosis: Which Model Is Right for Your Application? Am J Pathol 191, 228–242. https://doi.org/10.1016/j.ajpath.2020.10.017

Mitchelmore, P., Wilson, C., Hettle, D., 2018. Risk of Bacterial Transmission in Bronchiectasis Outpatient Clinics. Curr Pulmonol Rep 7, 72–78. https://doi.org/10.1007/s13665-018-0203-6

Mojica, M.F., Humphries, R., Lipuma, J.J., Mathers, A.J., Rao, G.G., Shelburne, S.A., Fouts, D.E., Van Duin, D., Bonomo, R.A., 2022. Clinical challenges treating *Stenotrophomonas maltophilia* infections: an update. JAC Antimicrob Resist 4, dlac040. https://doi.org/10.1093/jacamr/dlac040

Moskowitz, S.M., Brannon, M.K., Dasgupta, N., Pier, M., Sgambati, N., Miller, A.K., Selgrade, S.E., Miller, S.I., Denton, M., Conway, S.P., Johansen, H.K., Høiby, N., 2012. PmrB mutations promote polymyxin resistance of *Pseudomonas aeruginosa* isolated from colistin-treated cystic fibrosis patients. Antimicrob Agents Chemother 56, 1019–1030. https://doi.org/10.1128/AAC.05829-11

Neve, R.L., Carrillo, B.D., Phelan, V.V., 2021. Impact of Artificial Sputum Medium Formulation on *Pseudomonas aeruginosa* Secondary Metabolite Production. J Bacteriol 203, e0025021. https://doi.org/10.1128/JB.00250-21

O'Toole, G.A., Kolter, R., 1998. Initiation of biofilm formation in *Pseudomonas* fluorescens WCS365 proceeds via multiple, convergent signalling pathways: a genetic analysis. Mol Microbiol 28, 449–461. https://doi.org/10.1046/j.1365-2958.1998.00797.x

Pang, Z., Raudonis, R., Glick, B.R., Lin, T.-J., Cheng, Z., 2019. Antibiotic resistance in *Pseudomonas aeruginosa*: mechanisms and alternative therapeutic strategies. Biotechnol Adv 37, 177–192. https://doi.org/10.1016/j.biotechadv.2018.11.013

Papazian, L., Klompas, M., Luyt, C.-E., 2020. Ventilator-associated pneumonia in adults: a narrative review. Intensive Care Med 46, 888–906. https://doi.org/10.1007/s00134-020-05980-0

Pederick, V.G., Eijkelkamp, B.A., Begg, S.L., Ween, M.P., McAllister, L.J., Paton, J.C., McDevitt, C.A., 2015. ZnuA and zinc homeostasis in *Pseudomonas aeruginosa*. Sci Rep 5, 13139. https://doi.org/10.1038/srep13139

Pollini, S., Boncompagni, S., Di Maggio, T., Di Pilato, V., Spanu, T., Fiori, B., Blasi, F., Aliberti, S., Sergio, F., Rossolini, G.M., Pallecchi, L., 2018a. In vitro synergism of colistin in combination with N-acetylcysteine against *Acinetobacter baumannii* grown in planktonic phase and in biofilms. J Antimicrob Chemother 73, 2388–2395. https://doi.org/10.1093/jac/dky185

Pollini, S., Di Pilato, V., Landini, G., Di Maggio, T., Cannatelli, A., Sottotetti, S., Cariani, L., Aliberti, S., Blasi, F., Sergio, F., Rossolini, G.M., Pallecchi, L., 2018b. In vitro activity of N-acetylcysteine against *Stenotrophomonas maltophilia* and *Burkholderia cepacia* complex grown in planktonic phase and biofilm. PLoS One 13, e0203941. https://doi.org/10.1371/journal.pone.0203941

Pompilio, A., Crocetta, V., Pomponio, S., Fiscarelli, E., Di Bonaventura, G., 2015. In vitro activity of colistin against biofilm by *Pseudomonas aeruginosa* is significantly improved under "cystic fibrosis-like" physicochemical conditions. Diagn Microbiol Infect Dis 82, 318–325. https://doi.org/10.1016/j.diagmicrobio.2015.01.006

Quintana, J., Novoa-Aponte, L., Argüello, J.M., 2017. Copper homeostasis networks in the bacterium *Pseudomonas aeruginosa*. J Biol Chem 292, 15691–15704. https://doi.org/10.1074/jbc.M117.804492

Rashid, M.H., Kornberg, A., 2000. Inorganic polyphosphate is needed for swimming, swarming, and twitching motilities of *Pseudomonas aeruginosa*. Proc Natl Acad Sci U S A 97, 4885–4890. https://doi.org/10.1073/pnas.060030097

Rodríguez-Beltrán, J., Cabot, G., Valencia, E.Y., Costas, C., Bou, G., Oliver, A., Blázquez, J., 2015. N-acetylcysteine selectively antagonizes the activity of imipenem in *Pseudomonas aeruginosa* by an OprD-mediated mechanism. Antimicrob Agents Chemother 59, 3246–3251. https://doi.org/10.1128/AAC.00017-15

Rossi, E., La Rosa, R., Bartell, J.A., Marvig, R.L., Haagensen, J.A.J., Sommer, L.M., Molin, S., Johansen, H.K., 2021. *Pseudomonas aeruginosa* adaptation and evolution in patients with cystic fibrosis. Nat Rev Microbiol 19, 331–342. https://doi.org/10.1038/s41579-020-00477-5

Rumpf, C., Lange, J., Schwartbeck, B., Kahl, B.C., 2021. *Staphylococcus aureus* and Cystic Fibrosis-A Close Relationship. What Can We Learn from Sequencing Studies? Pathogens 10, 1177. https://doi.org/10.3390/pathogens10091177

Rupel, K., Zupin, L., Ottaviani, G., Bertani, I., Martinelli, V., Porrelli, D., Vodret, S., Vuerich, R., Passos da Silva, D., Bussani, R., Crovella, S., Parsek, M., Venturi, V., Di Lenarda, R., Biasotto, M., Zacchigna, S., 2019. Blue laser light inhibits biofilm formation *in vitro* and *in vivo* by inducing oxidative stress. NPJ Biofilms Microbiomes 5, 29. https://doi.org/10.1038/s41522-019-0102-9

Savage, V.J., Chopra, I., O'Neill, A.J., 2013. *Staphylococcus aureus* Biofilms Promote Horizontal Transfer of Antibiotic Resistance. Antimicrob Agents Chemother 57, 1968–1970. https://doi.org/10.1128/AAC.02008-12

Shen, Y., Li, P., Chen, X., Zou, Y., Li, H., Yuan, G., Hu, H., 2020. Activity of Sodium Lauryl Sulfate, Rhamnolipids, and N-Acetylcysteine Against Biofilms of Five Common Pathogens. Microb Drug Resist 26, 290–299. https://doi.org/10.1089/mdr.2018.0385

Taccetti, G., Francalanci, M., Pizzamiglio, G., Messore, B., Carnovale, V., Cimino, G., Cipolli, M., 2021. Cystic Fibrosis: Recent Insights into Inhaled Antibiotic Treatment and Future Perspectives. Antibiotics (Basel) 10, 338. https://doi.org/10.3390/antibiotics10030338

Tenover, F.C., Nicolau, D.P., Gill, C.M., 2022. Carbapenemase-producing *Pseudomonas aeruginosa* -an emerging challenge. Emerg Microbes Infect 11, 811–814. https://doi.org/10.1080/22221751.2022.2048972

Vardakas, K.Z., Voulgaris, G.L., Samonis, G., Falagas, M.E., 2018. Inhaled colistin monotherapy for respiratory tract infections in adults without cystic fibrosis: a systematic review and meta-analysis. Int J Antimicrob Agents 51, 1–9. https://doi.org/10.1016/j.ijantimicag.2017.05.016

Verderosa, A.D., Totsika, M., Fairfull-Smith, K.E., 2019. Bacterial Biofilm Eradication Agents: A Current Review. Front Chem 7, 824. https://doi.org/10.3389/fchem.2019.00824

Vieira, C., Gomes, A.T.P.C., Mesquita, M.Q., Moura, N.M.M., Neves, M.G.P.M.S., Faustino, M.A.F., Almeida, A., 2018. An Insight Into the Potentiation Effect of Potassium Iodide on aPDT Efficacy. Front Microbiol 9, 2665. https://doi.org/10.3389/fmicb.2018.02665

Wainwright, M., Maisch, T., Nonell, S., Plaetzer, K., Almeida, A., Tegos, G.P., Hamblin, M.R., 2017. Photoantimicrobials-are we afraid of the light? Lancet Infect Dis 17, e49–e55. https://doi.org/10.1016/S1473-3099(16)30268-7

Wang, Y., Wu, X., Chen, J., Amin, R., Lu, M., Bhayana, B., Zhao, J., Murray, C.K., Hamblin, M.R., Hooper, D.C., Dai, T., 2016. Antimicrobial Blue Light Inactivation of Gram-Negative Pathogens in Biofilms: *In Vitro* and *In Vivo* Studies. J Infect Dis 213, 1380–1387. https://doi.org/10.1093/infdis/jiw070

Wang, Yucheng, Wang, Ying, Wang, Yuguang, Murray, C.K., Hamblin, M.R., Hooper, D.C., Dai, T., 2017. Antimicrobial blue light inactivation of pathogenic microbes: State of the art. Drug Resist Updat 33–35, 1–22. https://doi.org/10.1016/j.drup.2017.10.002

Wen, X., Zhang, X., Szewczyk, G., El-Hussein, A., Huang, Y.-Y., Sarna, T., Hamblin, M.R., 2017. Potassium Iodide Potentiates Antimicrobial Photodynamic Inactivation Mediated by Rose Bengal in *In Vitro* and *In Vivo* Studies. Antimicrob Agents Chemother 61, e00467-17. https://doi.org/10.1128/AAC.00467-17

Wijers, C.D.M., Vagedes, R., Weingart, C., 2016. A novel method for investigating *Burkholderia cenocepacia* infections in patients with cystic fibrosis and other chronic diseases of the airways. BMC Microbiol 16, 200. https://doi.org/10.1186/s12866-016-0811-7

Willsey, G.G., Eckstrom, K., LaBauve, A.E., Hinkel, L.A., Schutz, K., Meagher, R.J., LiPuma, J.J., Wargo, M.J., 2019. *Stenotrophomonas maltophilia* Differential Gene Expression in Synthetic Cystic Fibrosis Sputum Reveals Shared and Cystic Fibrosis Strain-Specific Responses to the Sputum Environment. J Bacteriol 201, e00074-19. https://doi.org/10.1128/JB.00074-19

Zhang, Y., Zhu, Y., Gupta, A., Huang, Y., Murray, C.K., Vrahas, M.S., Sherwood, M.E., Baer, D.G., Hamblin, M.R., Dai, T., 2014. Antimicrobial blue light therapy for multidrug-resistant *Acinetobacter baumannii* infection in a mouse burn model: implications for prophylaxis and treatment of combat-related wound infections. J Infect Dis 209, 1963–1971. https://doi.org/10.1093/infdis/jit842

Zhao, T., Liu, Y., 2010. N-acetylcysteine inhibit biofilms produced by *Pseudomonas aeruginosa*. BMC Microbiol 10, 140. https://doi.org/10.1186/1471-2180-10-140

PART VI

MY PhD ACTIVITIES

My PhD activities were carried out in the Laboratory of Physiology and Biotechnology of Microorganisms, at the University of Siena, Department of Medical Biotechnologies, under the supervision of Professor Lucia Pallecchi.

The main activities were focused on a project, supported by a research grant from Zambon S.p.A., regarding the evaluation of the potential antibiofilm activity of *N*-acetylcysteine (NAC) in combination with colistin against relevant respiratory pathogens. Based on preliminary data obtained in the same laboratory, my research activities were conducted on two important pathogens in cystic fibrosis (CF), such as *Stenotrophomonas maltophilia* and *Pseudomonas aeruginosa*.

A first study involved the isolation and identification of clinical isolates, with a special focus on strains isolated from cystic fibrosis, and those exhibiting multidrug resistance phenotypes. The determination of the antimicrobial resistance profile was used as selection criterion, in order to obtain a representative strains collection showing different resistance phenotypes, with regard to colistin and/or NAC susceptibility. Whole genome sequencing of the selected strains followed by processing of the sequencing data using bioinformatic tools was also carried out to fully characterize such strains in terms of genotyping.

Afterwards, the synergism of NAC and colistin was investigated using all the strains included in the study grown both in planktonic cultures and biofilms. In both cases, standardized protocols were used, albeit with some modifications.

Finally, the transcriptomic analysis of planktonic cultures of a representative *P. aeruginosa* strain exposed to NAC was performed with the aim to obtain new insights about the gene expression triggered by such an antimicrobial against *P. aeruginosa* bacterial cultures *in vitro*. For this purpose, appropriate bioinformatic tools were used to manage RNA-seq reads and to analyze the differentially expressed genes. Such investigation was followed by biological experiments aimed at confirming the transcriptomic data.

The secondary PhD activities were part of the follow-up activities of the European project "Light4Lungs" (L4L), a four-year Horizon 2020 FET Open project, aimed at developing an alternative therapeutic scheme for the treatment of chronic lung diseases by the implementation of a novel inhalable photodynamic therapy.

The research activities involved me were in collaboration with a research group of Applied Physics of the University of Florence, and were included in several work packages, such as: i) the selection and development of models, and ii) the action spectrum determination. The former was aimed at

defining the *in vitro* models (bacterial strains) and relative methods for irradiation. The strains included in the study were kindly provided by the group of Bacterial Pathogenesis and Immunity of the Institute of Infection & Global Health of the University of Liverpool, as a further participant in this European project. The second work package was aimed at identifying the best light emission spectrum by determining the *in vitro* bacterial photokilling efficiency. For this purpose, the potential *in vitro* activity of violet-blue light, using a 415 nm LED light, was investigated against planktonic and biofilm cultures of clinical and reference strains of *P. aeruginosa* and *Staphylococcus aureus*.

Concerning this European project, I attended different meetings during which I reported on activities and results obtained in front of the whole L4L consortium. The meetings I attended were held both remotely (due to Pandemic) and face-to-face, including the kick-off-meeting in Barcelona (on 17th-19th December 2019), and the general assembly meetings in Florence (on 14th and 15th June 2022) and in Barcelona (on 7th and 8th November 2022).

The research work carried out during the main PhD activities led to the writing of two research articles published in international scientific journals and attached below.

PART VII

ANNEXES

antibiotics

MDPI

Article

In Vitro Synergism of Colistin and N-acetylcysteine against *Stenotrophomonas maltophilia*

Nagaia Ciacci [1], Selene Boncompagni [1], Felice Valzano [1], Lisa Cariani [2], Stefano Aliberti [3,4], Francesco Blasi [3,4], Simona Pollini [5,6], Gian Maria Rossolini [5,6] and Lucia Pallecchi [1,*]

1 Department of Medical Biotechnologies, University of Siena, 53100 Siena, Italy
2 Fondazione IRCCS Ca' Granda Ospedale Maggiore Policlinico, Cystic Fibrosis Microbiology Laboratory, 20122 Milan, Italy
3 Department of Pathophysiology and Transplantation, University of Milan, 20122 Milan, Italy
4 Fondazione IRCCS Ca' Granda Ospedale Maggiore Policlinico, Internal Medicine Department, Respiratory unit and Adult Cystic Fibrosis Center, 20122 Milan, Italy
5 Department of Experimental and Clinical Medicine, University of Florence, 50134 Florence, Italy
6 Microbiology and Virology Unit, Florence Careggi University Hospital, 50134 Florence, Italy
* Correspondence: lucia.pallecchi@unisi.it

Received: 5 July 2019; Accepted: 23 July 2019; Published: 25 July 2019

Abstract: *Stenotrophomonas maltophilia* is an emerging global opportunistic pathogen, responsible for a wide range of human infections, including respiratory tract infections. Intrinsic multidrug resistance and propensity to form biofilms make *S. maltophilia* infections recalcitrant to treatment. Colistin is among the second-line options in case of difficult-to-treat *S. maltophilia* infections, with the advantage of being also administrable by nebulization. We investigated the potential synergism of colistin in combination with N-acetylcysteine (NAC) (a mucolytic agent with antioxidant and anti-inflammatory properties) against *S. maltophilia* grown in planktonic phase and biofilm. Eighteen *S. maltophilia* clinical isolates (comprising three isolates from cystic fibrosis (CF) and two trimethoprim-sulfamethoxazole (SXT)-resistant strains) were included. Checkerboard assays showed a synergism of colistin/NAC combinations against the strains with colistin Minimum Inhibitory Concentration (MIC) >2 μg/mL (n = 13), suggesting that NAC could antagonize the mechanisms involved in colistin resistance. Nonetheless, time–kill assays revealed that NAC might potentiate colistin activity also in case of lower colistin MICs. A dose-dependent potentiation of colistin activity by NAC was also clearly observed against *S. maltophilia* biofilms, also at sub-MIC concentrations. Colistin/NAC combinations, at concentrations likely achievable by topical administration, might represent a valid option for the treatment of *S. maltophilia* respiratory infections and should be examined further.

Keywords: colistin; N-acetylcysteine; *Stenotrophomonas maltophilia*; biofilm

1. Introduction

Stenotrophomonas maltophilia is an emerging global opportunistic pathogen, responsible for a wide range of human infections, including chronic lung colonization and acute exacerbations in patients affected by chronic respiratory diseases, such as cystic fibrosis (CF), chronic obstructive pulmonary disease (COPD), and bronchiectasis [1]. As reported by the Italian Cystic Fibrosis Registry, *S. maltophilia* is the second most common non-fermenting Gram-negative respiratory pathogen, following *Pseudomonas aeruginosa*, in patients affected by CF, with a prevalence of chronic lung colonization of 4.6% and 4.7% in adult and pediatric patients, respectively [2]. Despite the precise clinical relevance of *S. maltophilia* in CF remains undetermined [3,4], chronic pulmonary colonization by *S. maltophilia* has been recently associated with an increased risk of pulmonary exacerbations

requiring intravenous antibiotics, lung transplantation, and death [5–7]. Due to intrinsic and acquired multidrug resistance mechanisms and the propensity to grow as biofilm, *S. maltophilia* infections are difficult-to-treat and the therapeutic options are very limited [1,5,8–11]. Clinical breakpoints for the interpretation of susceptibility testing are available only for trimethoprim-sulfamethoxazole (SXT) (i.e., the first-line treatment option) and few other compounds, namely levofloxacin, some beta-lactams (i.e., ticarcillin-clavulanate and ceftazidime), minocycline, and chloramphenicol [12,13].

In order to find new drugs and their combinations to improve outcomes of difficult-to-treat respiratory tract infections, a renewed interest has been recently focused on topical routes of administration (e.g., inhalation, nebulization, and aerosolization), which allow the achievement of high drug concentrations in the lungs with limited systemic toxicity [14,15].

N-acetylcysteine (NAC) is a mucolytic agent commonly administered together with antibiotics for the management of lower respiratory tract infections, especially in patients with chronic respiratory diseases characterized by abundant and/or thick mucus production (i.e., CF, COPD, and bronchiectasis) [16]. In addition, an increasing amount of data points to an intrinsic antimicrobial and antibiofilm activity of NAC against some pathogens, including relevant CF pathogens such as *P. aeruginosa*, *S. maltophilia,* and *Burkholderia cepacia* complex (BCC) [16,17]. Colistin is among the last-resort agents for the treatment of infections caused by multidrug-resistant Gram-negative bacteria, and inhaled colistin (alone or in combination with intravenous colistin) has been increasingly used for the treatment of difficult-to-treat respiratory tract infections, especially in CF [15,18–20]. Nonetheless, apart from intrinsic resistance of BCC, colistin is not recommended as first-line treatment option for other relevant CF pathogens (e.g., *S. maltophilia* and *Achromobacter xylosoxidans*), due to lack of clinical breakpoints and high rates of organisms with high Minimum Inhibitory Concentration (MIC) values [21]. Recently, it has been shown that colistin/NAC combinations exert a relevant antimicrobial and antibiofilm synergistic activity against *Acinetobacter baumannii* [22]. In particular, high NAC concentrations (potentially achievable by topical administration) can revert the colistin resistance phenotype in this pathogen [22].

The aim of this study was to investigate the potential synergism of colistin in combination with NAC against *S. maltophilia* strains grown in planktonic phase and in vitro biofilm models, at drugs concentrations likely achievable by topical administration.

2. Results

2.1. Colistin Susceptibility of S. maltophilia Strains Included in the Study

The study was performed with 18 *S. maltophilia* clinical isolates (including isolates from CF and SXT-resistant strains), which had been previously investigated for NAC susceptibility [17]. Among the strains tested, 13 showed colistin MIC >2 μg/mL (MIC range 4–>256 μg/mL), and for the purposes of this study were categorized as "colistin-resistant" (according to the colistin clinical breakpoints for *P. aeruginosa*) (Table 1) [12,13]. The remaining 5 isolates showed colistin MIC <2 μg/mL (MIC range 0.125–1 μg/mL) and were therefore categorized as "colistin-susceptible" (Table 1). Overall, colistin susceptibility patterns of strains included in this study were consistent with those recently reported in other studies on *S. maltophilia* antibiotic susceptibility [8,23].

Table 1. Main features of the 18 *S. maltophilia* clinical isolates investigated in this study.

Strain	MLST	Origin	Antibiotics MIC (μg/mL)				
			COL	SXT	CAZ	LVX	MIN
Z63	NA	BSI	>256	0.5	2	≤0.25	0.125
Z64	NA	BSI	64	2	64	2	2
Z119	NA	LRTI	32	0.5	32	2	0.5
Z128	NA	LRTI	32	≤0.25	4	1	0.25
Z117	NA	LRTI	16	0.5	64	0.5	0.25
Z129	NA	LRTI	16	≤0.25	4	1	0.25
Z65	NA	IAI	8	1	64	2	1
Z118	ST162	LRTI	8	0.5	8	2	0.25
Z130	NA	IAI	8	0.5	16	16	2
Z131	NA	BSI	8	>8	64	32	1
Z132	NA	LRTI	8	1	2	16	1
Z157	NA	CF	8	0.5	4	2	1
Z155	ST335	CF	4	>8	32	4	2
Z116	NA	LRTI	1	0.5	16	2	0.25
Z156	NA	CF	0.25	1	16	2	0.25
Z120	ST334	LRTI	0.25	0.5	32	1	0.5
Z66	NA	LRTI	0.25	0.5	≤1	1	0.25
Z133	NA	LRTI	0.125	1	2	1	0.25

MLST, multi locus sequence type; NA, not available; BSI, bloodstream infection; LRTI, lower respiratory tract infection; IAI, intra-abdominal infection; CF, cystic fibrosis; COL, colistin (breakpoint not available); SXT, trimethoprim-sulfamethoxazole (S ≤2/38, R ≥4/76 μg/mL); CAZ, ceftazidime (S ≤8, I = 16, R ≥16 μg/mL); LVX, levofloxacin (S ≤2, I = 4, R ≥8 μg/mL); MIN, minocycline (S ≤4, I = 8, R ≥16 μg/mL). S, susceptible; I, intermediate; R, resistant [13].

2.2. In Vitro Synergism of Colistin/NAC Combinations against S. maltophilia Strains Grown in Planktonic Phase

Checkerboard assays showed a notable synergistic activity of colistin/NAC combinations against the 13 colistin-resistant strains (i.e., fractional inhibitory concentration index (FICI) ≤0.5) (Table 2). In particular, a decrease of colistin MICs to ≤2 μg/mL (i.e., the susceptibility breakpoint for *P. aeruginosa*) was observed with 12 strains in the presence of NAC 4 mg/mL and with all strains in the presence of NAC >4 mg/mL (Table 2). The 5 colistin-susceptible strains showed no synergistic effect, although a trend toward colistin MIC decrease was observed in the presence of increasing NAC concentrations (Table 2).

Table 2. Colistin MICs (μg/mL) and corresponding fractional inhibitory concentration indices (FICIs) in the presence of increasing N-acetylcysteine (NAC) concentrations for the 18 *S. maltophilia* clinical isolates investigated in this study. MIC and FICI values corresponding to synergism are shown with grey shading.

Strain	MIC		NAC Concentrations (mg/mL)													
	NAC (mg/mL)	COL (μg/mL)	0.5		1		2		4		8		16		32	
			COL (μg/mL)	FICI	COL (μg/mL)	FICI	COL (μg/mL)	FICI	COL (μg/mL)	FICI	COL (μg/mL)	FICI	COL (μg/mL)	FICI	COL (μg/mL)	FICI
1-17 Z63	32	>256	32	0.14	16	0.09	2	0.07	1	0.13	0.5	0.25	≤0.25	0.50	≤0.25	1.00
Z64	32	64	64	0.02	32	0.53	16	0.31	1	0.14	1	0.27	0.5	0.51	0.25	1.00
Z119	32	32	32	1.02	16	0.53	8	0.31	4	0.25	1	0.28	1	0.53	≤0.25	1.01
Z128	16	32	32	1.03	32	1.06	16	0.63	2	0.31	1	0.53	≤0.25	1.01	≤0.25	2.01
Z117	32	16	32	2.02	32	2.03	16	1.06	1	0.19	1	0.31	≤0.25	0.52	≤0.25	1.02
Z129	32	16	32	2.02	16	1.03	16	1.06	2	0.25	1	0.31	0.5	0.53	≤0.25	1.02
Z65	32	8	16	2.02	8	1.03	4	0.56	1	0.25	≤0.25	0.28	≤0.25	0.53	≤0.25	1.03
Z118	16	8	2	0.28	2	0.31	2	0.38	1	0.38	≤0.25	0.53	≤0.25	1.03	≤0.25	2.03
Z130	32	8	16	2.02	8	1.03	2	0.31	1	0.25	1	0.38	0.5	0.56	≤0.25	1.03
Z131	32	8	16	2.02	8	1.03	4	0.56	2	0.38	1	0.38	0.5	0.56	≤0.25	1.03
Z132	32	8	16	2.02	8	1.03	2	0.31	1	0.25	1	0.38	0.5	0.56	≤0.25	1.03
Z157	32	8	32	4.02	32	4.03	8	1.06	2	0.38	1	0.38	1	0.63	≤0.25	1.03
Z155	16	4	4	1.03	4	1.06	2	0.63	1	0.50	1	0.75	≤0.25	1.06	≤0.25	2.06
Z116	32	1	1	1.02	1	1.03	1	1.06	1	1.13	0.5	0.75	0.25	0.75	≤0.003	1.00
Z156	16	0.25	0.5	2.03	0.5	2.06	0.25	1.13	0.25	1.25	0.06	0.75	≤0.003	1.02	≤0.003	2.02
Z120	16	0.25	0.5	2.03	0.5	2.06	0.25	1.13	0.25	1.25	0.06	0.75	≤0.003	1.02	≤0.003	2.02
Z66	16	0.25	0.25	1.03	0.25	1.06	0.25	1.13	0.125	0.75	0.125	1.00	≤0.003	1.02	≤0.003	2.02
Z133	32	0.125	0.25	2.03	0.25	2.06	0.125	1.13	0.125	1.25	0.125	1.50	≤0.003	1.03	≤0.003	2.03

2.3. Time-Kill Assays of Colistin/NAC Combinations against Three Selected S. Maltophilia Strains Grown in Planktonic Phase

Time–kill assays were performed with three selected *S. maltophilia* strains, namely Z131 (from bloodstream infection; resistant to SXT, ceftazidime and levofloxacin; colistin MIC = 8 μg/mL), Z157 (from CF; colistin MIC = 8 μg/mL), and Z66 (from lower respiratory tract infection; colistin MIC = 0.25 μg/mL). Colistin and NAC concentrations potentially achievable by topical administration were tested. Results showed a relevant dose-dependent potentiation of colistin activity by NAC, with the three strains investigated (Figure 1a,b). Overall, these data were in accordance with those obtained in checkerboard assays, supporting the notion of synergism of colistin/NAC combinations, and of a possible role of NAC in reverting colistin resistance in *S. maltophilia*.

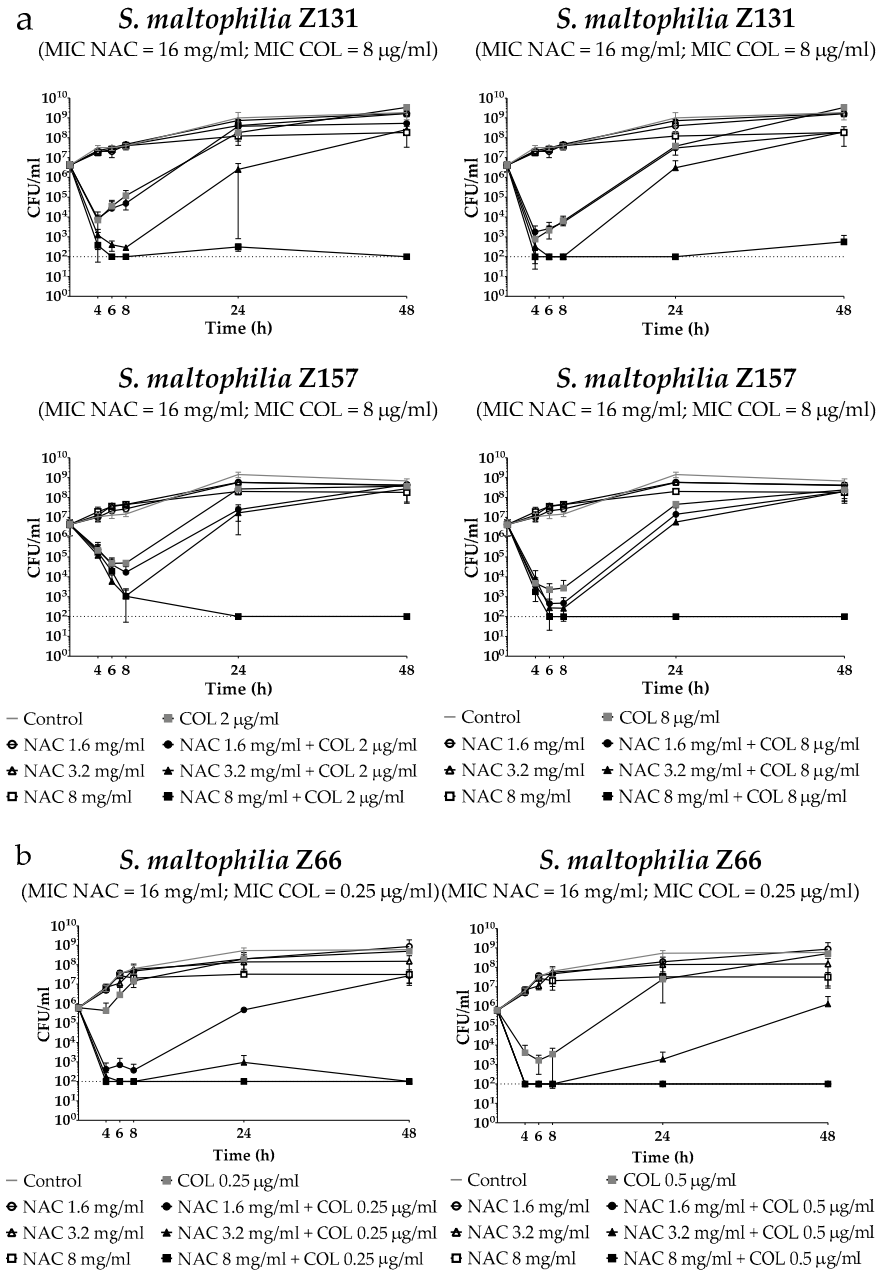

Figure 1. Time–kill assays of colistin/NAC combinations against (**a**) colistin-resistant and (**b**) colistin-susceptible *S. maltophilia* strains. Dotted lines indicate the detection limit (100 CFU/mL). CFU: Colony-forming units.

2.4. In Vitro Activity of Colistin/NAC Combinations against S. maltophilia Biofilms

The antibiofilm activity of colistin/NAC combinations was tested against all the 18 *S. maltophilia* strains, using a standardized in vitro biofilm model [24]. Preformed *S. maltophilia* biofilms were exposed to nine different colistin/NAC combinations, and the antibiofilm activity was evaluated by determining the number of viable cells in biofilms treated with colistin/NAC combinations compared to colistin alone. Colistin and NAC concentrations potentially achievable by topical administration were tested. In the in vitro biofilm model adopted, *S. maltophilia* biofilms ranged from 2.5 ± 1.7 × 10^5 to 1.3 ± 0.4 × 10^7 colony-forming units (CFU)/peg after 24 h of growth. Overall, a synergism of colistin/NAC combinations was observed with all the colistin-resistant strains, except for strain Z155 (colistin MIC = 4 μg/mL) (Figures 2–4). In particular, the combination colistin 8 μg/mL plus NAC 16 mg/mL was synergistic against the majority of colistin-resistant strains (i.e., 7 out of 13 strains) (Figures 2–4). *S. maltophilia* Z155 (the only colistin-resistant strain with which no synergism was observed) was extremely susceptible to NAC 16 mg/mL, which alone achieved complete eradication of the in vitro biofilm model (Figure 4). In addition, with two strains (i.e., Z119 and Z131), a paradoxical effect of the combination colistin 128 μg/mL plus NAC 1.6 mg/mL was observed, which will deserve further attention (Figures 2 and 3).

A statistically significant potentiation of colistin activity by NAC was also observed with one of the five colistin-susceptible strains (i.e., Z156) (Figure 4). For the remaining four colistin-susceptible strains, a trend suggesting a potentiation of colistin activity by NAC was observed, even though the results did not reach a statistical significance, likely due to not optimal colistin concentrations tested. In order to partially address this point, strain Z133 was selected and tested also with a lower range of colistin concentrations. Results showed a clear synergism of colistin/NAC combinations also against this strain (Figure 5).

Taken together, these results indicated a NAC-mediated dose-dependent potentiation of the antibiofilm activity of colistin against *S. maltophilia* strains. Biofilm susceptibility to colistin/NAC combinations was anyway strain-dependent and not directly correlated to colistin or NAC MICs.

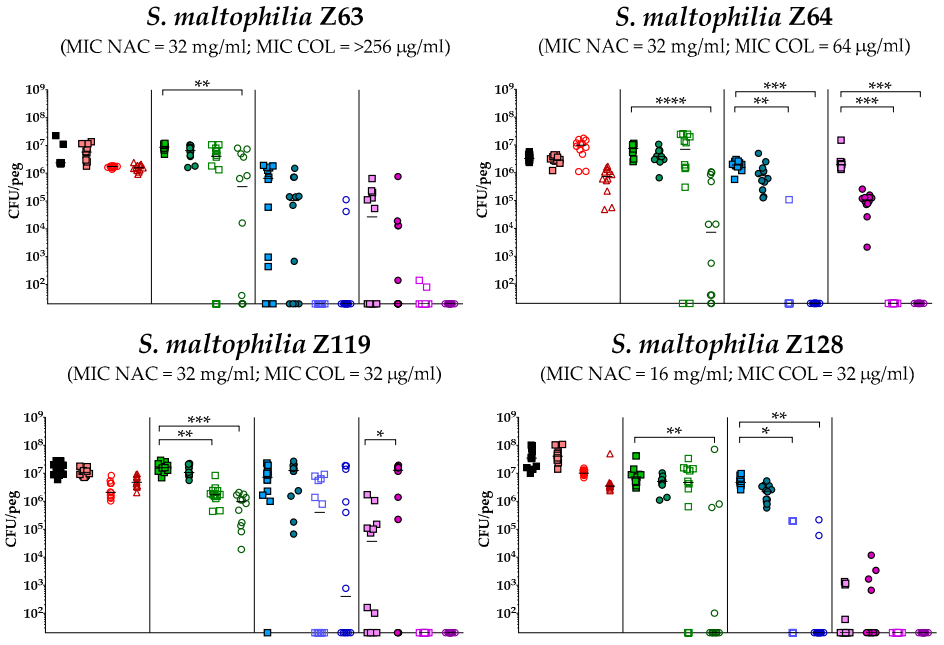

Figure 2. *Cont.*

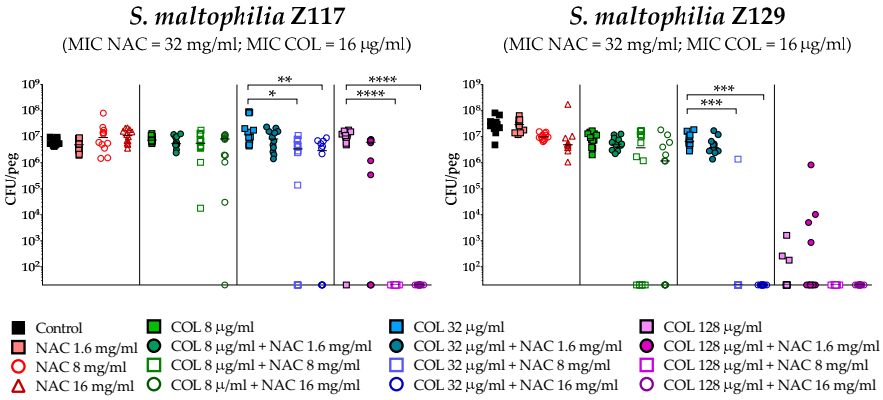

Figure 2. Antibiofilm activity of colistin/NAC combinations against *S. maltophilia* strains with colistin MIC range 16–>256 μg/mL. The x-axis is set at the limit of detection (20 CFU/peg). CFU: Colony-forming units. Each data point represents a replicate, for a total of 12 replicates per condition.

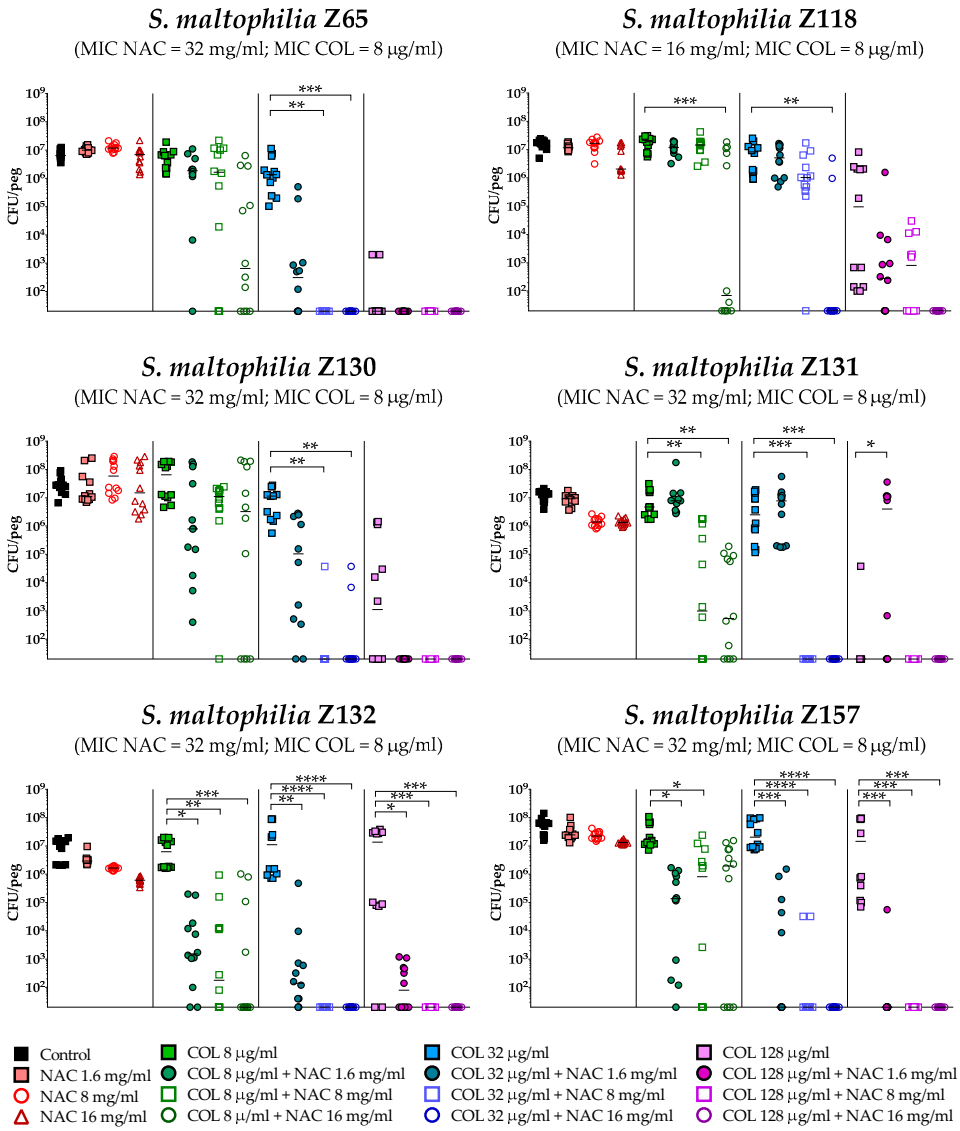

Figure 3. Antibiofilm activity of colistin/NAC combinations against *S. maltophilia* strains with colistin MIC = 8 μg/mL. The x-axis is set at the limit of detection (20 CFU/peg). CFU: Colony-forming units. Each data point represents a replicate, for a total of 12 replicates per condition.

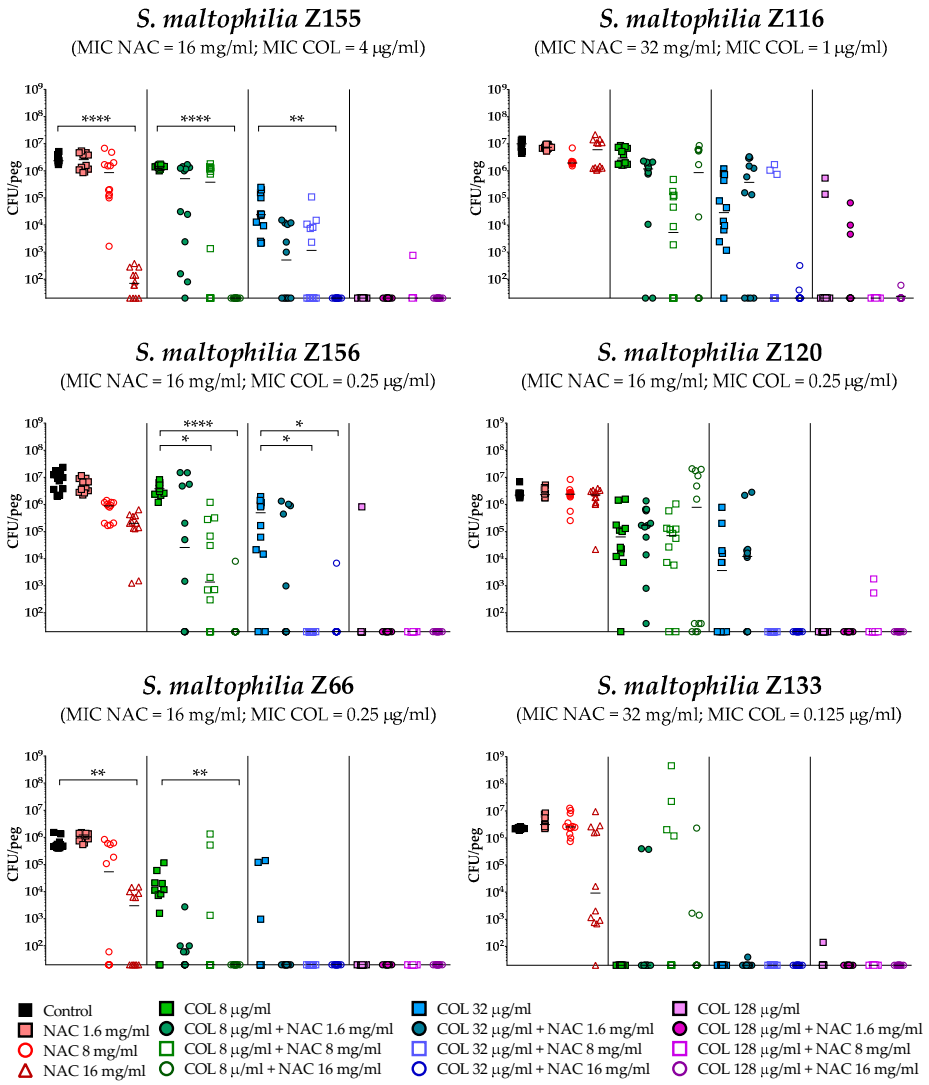

Figure 4. Antibiofilm activity of colistin/NAC combinations against *S. maltophilia* strains with colistin MIC 0.125–4 μg/mL. The x-axis is set at the limit of detection (20 CFU/peg). CFU: Colony-forming units. Each data point represents a replicate, for a total of 12 replicates per condition.

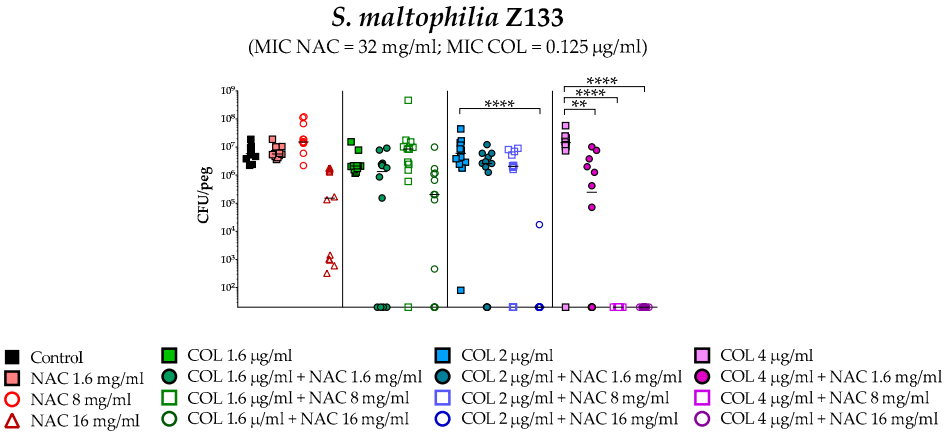

Figure 5. Antibiofilm activity of colistin/NAC combinations against *S. maltophilia* Z133. The x-axis is set at the limit of detection (20 CFU/peg). CFU: Colony-forming units. Each data point represents a replicate, for a total of 12 replicates per condition.

3. Discussion

Colistin/NAC combinations, at the high concentrations potentially achievable by topical administration, have been recently found to exert a relevant synergistic activity against *A. baumannii* grown in planktonic and biofilm phase [22]. In particular, NAC was demonstrated to revert the colistin resistance phenotype in this pathogen and to significantly potentiate colistin antibiofilm activity [22].

Our study demonstrated that the antimicrobial and antibiofilm synergism of colistin/NAC combinations is also exerted against *S. maltophilia*, an emerging global difficult-to-treat opportunistic pathogen, with a relevant role in respiratory tract infections, especially in CF.

Inhaled colistin has been increasingly used since late 1980s, especially for the treatment of individuals with CF, health care-associated pneumonia, and ventilator-associated pneumonia [15,25–27]. Very high colistin concentrations (up to 1137 µg/mL) have been reported in the epithelial lining fluid (ELF) of critically ill patients, after aerosol delivery of 2 million IU (MIU) of colistin methanesulfonate [19,20]. In addition, even higher ELF concentrations are expected to be achieved by using colistin dry powder formulations, which have recently been approved [15,26,28].

Despite inhaled NAC has been used safely for decades as a mucus-dissolving treatment in respiratory diseases associated to abundant and/or thick mucus production (e.g., CF, COPD, bronchiectasis), the actual NAC concentrations achievable in the ELF after topical administration have never been determined. Nonetheless, considering the multiple-dosage regimes of nebulized administration (e.g., 1–10 mL of 200 mg/mL solution every 6–8 h), the higher performance of last-generation nebulizers, and the possibility of direct instillation, topical NAC could reach the ELF concentrations needed for exerting the antimicrobial and antibiofilm potentiation of colistin activity [16,29]. In addition, NAC dry powder formulations have recently been implemented, with the aim of potentiating the penetration through the respiratory mucus of inhaled antibiotics (i.e., clarithromycin and fluoroquinolones) [30,31].

Colistin has gained a renewed interest only in the last years as salvage therapy for the treatment of infections caused by multidrug-resistant Gram-negative pathogens, and many aspects concerning the molecular mechanisms of colistin bactericidal activity and acquired resistance remain still scarcely known [32,33]. Apart from the well described primary mechanism of action (i.e., interaction with lipid A of lipopolysaccharide followed by bacterial membranes derangement), alternative secondary antibacterial mechanisms have been proposed, including inhibition of NDH-2 respiratory chain enzymes (i.e., type II NADH-quinone oxidoreductases) located in the plasma membrane [33–35]. In support to the existence of alternative secondary mechanisms of colistin, plasma membrane disruption and oxidative damage have been demonstrated to have a role in colistin bactericidal activity against some Gram-positive bacteria, which lack the primary colistin molecular target (i.e., lipid A of lipopolysaccharide) [36].

Similarly, no solid data are available on the molecular mechanisms accounting for the intrinsic antimicrobial and antibiofilm activity of NAC, which most likely is multifactorial [16]. NAC has been hypothesized to exert its intrinsic antimicrobial activity by competitive inhibition of cysteine utilization, reaction of the NAC sulfhydryl group with bacterial proteins, and perturbation of the intracellular redox equilibrium with potential indirect effects on cell metabolism and intracellular signal transduction pathways [16]. The antibiofilm activity of NAC could be related either to perturbation of microbial physiology (e.g., responsible for inhibition of biofilm formation and/or induction of biofilm disruption), or to a direct destabilization of biofilm matrix architecture (e.g., by chelation of calcium and magnesium or interaction with crucial components in the matrix) [16].

The reasons accounting for the antimicrobial and antibiofilm synergism of colistin/NAC combinations are not easy to be hypothesized due to the relevant knowledge gaps on the mechanisms of action of both compounds. In this perspective, understanding the mechanisms of such a synergism would be relevant not only for optimization of clinical applications but also for drug discovery purposes (e.g., new molecular targets for antibiotic drugs, new compounds able to potentiate colistin activity).

Based on the in vitro evidence of potentiation of colistin antimicrobial and antibiofilm activity by NAC, in vivo animal models to evaluate the potential clinical relevance of topical colistin/NAC combinations are warranted.

4. Materials and Methods

4.1. Bacterial Strains Tested

A total of 18 *S. maltophilia* clinical isolates were investigated, including isolates from CF and SXT-resistant strains (Table 1). The strains were the same as in a previous study, aimed at investigating the antimicrobial and antibiofilm activity of NAC against *S. maltophilia* [17]. Colistin (Applichem, Darmstadt, Germany) MICs were determined using the reference broth microdilution method [37]. For the purposes of this study, *S. maltophilia* strains were categorized as susceptible or resistant to colistin based on clinical breakpoints available for *P. aeruginosa* (MIC <2 μg/mL, susceptible; MIC >2 μg/mL resistant) [12,13].

4.2. Preparation of NAC-Containing Medium

NAC stock solutions (100 mg/mL) were prepared immediately before use. NAC powder (Zambon, Bresso, Italy) was dissolved in sterile double-distilled water, pH was adjusted at 6.5–6.8 with NaOH, and the solution was filtered through a 0.22-μm membrane filter. All experiments were performed in cation-adjusted Mueller-Hinton broth (CAMHB; Becton Dickinson, Milan, Italy), starting from an appropriately concentrated medium in order to avoid broth dilution when testing high NAC concentrations.

4.3. Checkerboard Assays

The potential synergism of colistin/NAC combinations was investigated by checkerboard assay as described previously [38]. The ranges of colistin concentrations tested were 0.003–4 μg/mL and 0.25–256 μg/mL for colistin-susceptible and colistin-resistant strains, respectively. Considering the high drug concentrations potentially achievable by topical administration, the range of NAC concentrations tested was 0.5–32 mg/mL for all strains [16,19]. FICIs values were interpreted as follows: ≤0.5, synergy; >0.5–≤1, partial synergism; >1–4.0, no interaction; >4.0, antagonism.

4.4. Time–Kill Assays of Colistin/NAC Combinations Against Planktonic Cultures

Time–Kill assays were performed according to CLSI guidelines [39], with three selected *S. maltophilia* strains: Z131 (from bloodstream infection; resistant to SXT, ceftazidime and levofloxacin; colistin MIC = 8 μg/mL), Z157 (from CF; colistin MIC = 8 μg/mL), and Z66 (from lower respiratory tract infection; colistin MIC = 0.25 μg/mL) (Table 1). Two colistin concentrations (i.e., 2 and 8 μg/mL for colistin-resistant strains; 0.25 and 0.5 μg/mL for colistin-susceptible strains) and three NAC concentrations (i.e., 1.6, 3.2, and 8 mg/mL, corresponding to 0.1× MIC, 0.2× MIC, and 0.5× MIC, respectively, for the selected strains) were tested alone and in combination. Viable cell counts were performed at the beginning of the experiment and after 2, 4, 6, 8, 24, and 48 h of exposure (detection limit, 100 CFU/mL). Data were obtained from at least two independent experiments, with two replicates per condition per experiment.

4.5. In Vitro Biofilm Susceptibility Testing

The potential antibiofilm synergism of colistin/NAC combinations was investigated using the Nunc-TSP lid system (Thermo Fisher Scientific, Waltham, MA, USA), as described previously [24]. Briefly, biofilms were grown for 24 h in CAMHB at 35 °C, static conditions. Preformed biofilms were then exposed to three concentrations of colistin (i.e., 8, 32, and 128 μg/mL) and NAC (i.e., 1.6, 8. and 16 mg/mL), alone or in combination. After 24 h of exposure (i.e., 35 °C, static conditions), loosely attached bacteria were removed by two 1-minute washes with 200 μL of phosphate-buffered saline (PBS)

(Sigma Aldrich, Milan, Italy). Biofilms were then subjected to 30-minutes sonication (Elma Transsonic T 460, Singen, Germany) in 200 µL of tryptic soy broth (TSB) (Oxoid, Milan, Italy) supplemented with 0.1% Tween 20 (Sigma Aldrich) (i.e., the recovery medium) to remove sessile cells. Mean viable cell counts per peg (CFU/peg) were determined by plating 10 µL of appropriate dilutions of the recovery medium onto tryptic soy agar (TSA) (Oxoid) plates and incubating for 24 h at 35 °C (detection limit, 20 CFU/peg). Colony count was also repeated after 48 h of incubation. Data were obtained in at least two independent experiments, with at least six replicates per condition per experiment.

4.6. Statistical Analysis

Statistical analysis was performed using GraphPad Prism version 6.0 (San Diego, CA, USA). D'Agostino-Pearson and Shapiro-Wilk normality tests were applied. Multiple comparison tests were performed by Kruskal-Wallis test with Dunn's correction.

5. Conclusions

In conclusion, we demonstrated a relevant in vitro antimicrobial and antibiofilm activity of colistin/NAC combinations (at the high concentrations likely achievable by topical administration) against *S. maltophilia*, an emerging global difficult-to-treat opportunistic pathogen, with an important role also in CF.

Further studies are needed to understand the molecular bases of such a synergism and to evaluate the potential clinical relevance of colistin/NAC topical formulations.

6. Patents

International patent application No. WO2018/154091.

Author Contributions: Conceptualization, L.C., S.A., F.B., G.M.R., S.P. and L.P.; methodology, L.C., S.A., F.B., G.M.R., S.P. and L.P.; software, N.C. and L.P.; formal analysis, N.C., S.P., and L.P.; investigation, N.C., S.B., F.V., S.P. and L.P.; resources, G.M.R. and L.P.; data curation, N.C., S.P. and L.P.; writing—original draft preparation, N.C., S.P. and L.P.; writing—review and editing, L.C., S.A., F.B., G.M.R., S.P. and L.P.; supervision, L.C., S.A., F.B., G.M.R., S.P. and L.P.; project administration, G.M.R., S.P. and L.P.; funding acquisition, G.M.R. and L.P.

Funding: This research was funded by a research grant from Zambon S.p.A.

Conflicts of Interest: S.A., F.B., G.M.R., and L.P. are Advisory Board members for Zambon S.p.A. The remaining authors have none to declare. The funders had no role in the design of the study; in the collection, analyses, or interpretation of data; in the writing of the manuscript, or in the decision to publish the results.

References

1. Brooke, J.S. *Stenotrophomonas maltophilia*: An emerging global opportunistic pathogen. *Clin. Microbiol. Rev.* **2012**, *25*, 2–41. [CrossRef] [PubMed]
2. Giordani, B.; Amato, A.; Majo, F.; Ferrari, G.; Quattrucci, S.; Minicucci, L.; Padoan, R.; Floridia, G.; Puppo Fornaro, G.; Taruscio, D.; et al. Italian Cystic Fibrosis Registry. Report 2011–2014. *Epidemiol. Prev.* **2018**, *42*, 1–32. [CrossRef] [PubMed]
3. Amin, R.; Waters, V. Antibiotic treatment for *Stenotrophomonas maltophilia* in people with cystic fibrosis. *Cochrane. Database. Syst. Rev.* **2016**, *7*. [CrossRef] [PubMed]
4. O'Sullivan, B.P.; Freedman, S.D. Cystic fibrosis. *Lancet* **2009**, *373*, 1891–1904. [CrossRef]
5. Esposito, A.; Pompilio, A.; Bettua, C.; Crocetta, V.; Giacobazzi, E.; Fiscarelli, E.; Jousson, O.; Di Bonaventura, G. Evolution of *Stenotrophomonas maltophilia* in cystic fibrosis lung over chronic infection: A genomic and phenotypic population study. *Front. Microbiol.* **2017**, *8*, 1590. [CrossRef] [PubMed]
6. Barsky, E.E.; Williams, K.A.; Priebe, G.P.; Sawicki, G.S. Incident *Stenotrophomonas maltophilia* infection and lung function decline in cystic fibrosis. *Pediatr. Pulmonol.* **2017**, *52*, 1276–1282. [CrossRef] [PubMed]
7. Waters, V.; Atenafu, E.G.; Lu, A.; Yau, Y.; Tullis, E.; Ratjen, F. Chronic *Stenotrophomonas maltophilia* infection and mortality or lung transplantation in cystic fibrosis patients. *J. Cyst. Fibros.* **2013**, *12*, 482–486. [CrossRef] [PubMed]

8. Díez-Aguilar, M.; Ekkelenkamp, M.; Morosini, M.I.; Merino, I.; de Dios Caballero, J.; Jones, M.; van Westreenen, M.; Tunney, M.M.; Cantón, R.; Fluit, A.C. Antimicrobial susceptibility of non-fermenting Gram-negative pathogens isolated from cystic fibrosis patients. *Int. J. Antimicrob. Agents.* **2019**, *53*, 84–88. [CrossRef] [PubMed]
9. Adegoke, A.A.; Stenström, T.A.; Okoh, A.I. *Stenotrophomonas maltophilia* as an emerging ubiquitous pathogen: Looking beyond contemporary antibiotic therapy. *Front. Microbiol.* **2017**, *8*, 2276. [CrossRef] [PubMed]
10. Ciofu, O.; Tolker-Nielsen, T.; Jensen, P.Ø.; Wang, H.; Høiby, N. Antimicrobial resistance, respiratory tract infections and role of biofilms in lung infections in cystic fibrosis patients. *Adv. Drug. Deliv. Rev.* **2015**, *85*, 7–23. [CrossRef]
11. Chang, Y.T.; Lin, C.Y.; Chen, Y.H.; Hsueh, P.R. Update on infections caused by *Stenotrophomonas maltophilia* with particular attention to resistance mechanisms and therapeutic options. *Front. Microbiol.* **2015**, *6*, 893. [CrossRef] [PubMed]
12. The European Committee on Antimicrobial Susceptibility Testing. Breakpoint tables for interpretation of MICs and zone diameters. Version 9.0. 2019. Available online: http://www.eucast.org (accessed on 18 February 2019).
13. Clinical and Laboratory Standards Institute. *Performance Standards for Antimicrobial Susceptibility Testing*, 29th ed.; M100; Clinical and Laboratory Standards Institute: Wayne, PA, USA, 2019.
14. Maselli, D.J.; Keyt, H.; Restrepo, M.I. Inhaled antibiotic therapy in chronic respiratory diseases. *Int. J. Mol. Sci.* **2017**, *18*. [CrossRef] [PubMed]
15. Fiel, S.B. Aerosolized antibiotics in cystic fibrosis: An update. *Expert. Rev. Respir. Med.* **2014**, *8*, 305–314. [CrossRef] [PubMed]
16. Blasi, F.; Page, C.; Rossolini, G.M.; Pallecchi, L.; Matera, M.G.; Rogliani, P.; Cazzola, M. The effect of N-acetylcysteine on biofilms: Implications for the treatment of respiratory tract infections. *Respir. Med.* **2016**, *117*, 190–197. [CrossRef] [PubMed]
17. Pollini, S.; Di Pilato, V.; Landini, G.; Di Maggio, T.; Cannatelli, A.; Sottotetti, S.; Cariani, L.; Aliberti, S.; Blasi, F.; Sergio, F.; et al. *In vitro* activity of N-acetylcysteine against *Stenotrophomonas maltophilia* and *Burkholderia cepacia* complex grown in planktonic phase and biofilm. *PloS. One.* **2018**, *13*, e0203941. [CrossRef] [PubMed]
18. Vardakas, K.Z.; Voulgaris, G.L.; Samonis, G.; Falagas, M.E. Inhaled colistin monotherapy for respiratory tract infections in adults without cystic fibrosis: A systematic review andmeta-analysis. *Int. J. Antimicrob. Agents.* **2018**, *51*, 1–9. [CrossRef] [PubMed]
19. Boisson, M.; Grégoire, N.; Cormier, M.; Gobin, P.; Marchand, S.; Couet, W.; Mimoz, O. Pharmacokinetics of nebulized colistin methanesulfonate in critically ill patients. *J. Antimicrob. Chemother.* **2017**, *72*, 2607–2612. [CrossRef]
20. Boisson, M.; Jacobs, M.; Grégoire, N.; Gobin, P.; Marchand, S.; Couet, W.; Mimoz, O. Comparison of intrapulmonary and systemic pharmacokinetics of colistin methanesulfonate (CMS) and colistin after aerosol delivery and intravenous administration of CMS in critically ill patients. *Antimicrob. Agents. Chemother.* **2014**, *58*, 7331–7339. [CrossRef]
21. Abbott, I.J.; Peleg, A.Y. *Stenotrophomonas*, *Achromobacter*, and nonmelioid *Burkholderia* species: Antimicrobial resistance and therapeutic strategies. *Semin. Respir. Crit. Care. Med.* **2015**, *36*, 99–110. [CrossRef]
22. Pollini, S.; Boncompagni, S.; Di Maggio, T.; Di Pilato, V.; Spanu, T.; Fiori, B.; Blasi, F.; Aliberti, S.; Sergio, F.; Rossolini, G.M.; et al. *In vitro* synergism of colistin in combination with N-acetylcysteine against *Acinetobacter baumannii* grown in planktonic phase and in biofilms. *J. Antimicrob. Chemother.* **2018**, *73*, 2388–2395. [CrossRef]
23. Martínez-Servat, S.; Yero, D.; Huedo, P.; Marquez, R.; Molina, G.; Daura, X.; Gibert, I. Heterogeneous colistin-resistance phenotypes coexisting in *Stenotrophomonas maltophilia* isolates influence colistin susceptibility testing. *Front. Microbiol.* **2018**, *9*, 2871. [CrossRef] [PubMed]
24. Harrison, J.J.; Stremick, C.A.; Turner, R.J.; Allan, N.D.; Olson, M.E.; Ceri, H. Microtiter susceptibility testing of microbes growing on peg lids: A miniaturized biofilm model for high-throughput screening. *Nat. Protoc.* **2010**, *5*, 1236–1254. [CrossRef] [PubMed]

25. Tsuji, B.T.; Pogue, J.M.; Zavascki, A.P.; Paul, M.; Daikos, G.L.; Forrest, A.; Giacobbe, D.R.; Viscoli, C.; Giamarellou, H.; Karaiskos, I.; et al. International Consensus Guidelines for the Optimal Use of the Polymyxins: Endorsed by the American College of Clinical Pharmacy (ACCP), European Society of Clinical Microbiology and Infectious Diseases (ESCMID), Infectious Diseases Society of America (IDSA), International Society for Anti-infective Pharmacology (ISAP), Society of Critical Care Medicine (SCCM), and Society of Infectious Diseases Pharmacists (SIDP). *Pharmacotherapy* **2019**, *39*, 10–39. [CrossRef] [PubMed]
26. Kukut Hatipoglu, M.; Hickey, A.J.; Garcia–Contreras, L. Pharmacokinetics and pharmacodynamics of high doses of inhaled dry powder drugs. *Int. J. Pharm.* **2018**, *549*, 306–316. [CrossRef] [PubMed]
27. Müller, L.; Murgia, X.; Siebenbürger, L.; Börger, C.; Schwarzkopf, K.; Sewald, K.; Häussler, S.; Braun, A.; Lehr, C.M.; Hittinger, M.; et al. Human airway mucus alters susceptibility of *Pseudomonas aeruginosa* biofilms to tobramycin, but not colistin. *J. Antimicrob. Chemother.* **2018**, *73*, 2762–2769. [CrossRef] [PubMed]
28. Conole, D.; Keating, G.M. Colistimethate sodium dry powder for inhalation: A review of its use in the treatment of chronic *Pseudomonas aeruginosa* infection in patients with cystic fibrosis. *Drugs* **2014**, *74*, 377–387. [CrossRef] [PubMed]
29. Mata, A.F.; Sarnaik, A.A. Bronchoscopy with N–acetylcysteine lavage in severe respiratory failure from pertussis infection. *Pediatrics* **2013**, *132*, e1418–e1423. [CrossRef] [PubMed]
30. Akdag Cayli, Y.; Sahin, S.; Buttini, F.; Balducci, A.G.; Montanari, S.; Vural, I.; Oner, L. Dry powders for the inhalation of ciprofloxacin or levofloxacin combined with a mucolytic agent for cystic fibrosis patients. *Drug. Dev. Ind. Pharm.* **2017**, *43*, 1378–1389. [CrossRef]
31. Manniello, M.D.; Del Gaudio, P.; Aquino, R.P.; Russo, P. Clarithromycin and N-acetylcysteine co-spray-dried powders for pulmonary drug delivery: A focus on drug solubility. *Int. J. Pharm.* **2017**, *533*, 463–469. [CrossRef] [PubMed]
32. Poirel, L.; Jayol, A.; Nordmann, P. Polymyxins: Antibacterial Activity, Susceptibility Testing, and Resistance Mechanisms Encoded by Plasmids or Chromosomes. *Clin. Microbiol. Rev.* **2017**, *30*, 557–596. [CrossRef] [PubMed]
33. Zhu, Y.; Zhao, J.; Maifiah, M.H.M.; Velkov, T.; Schreiber, F.; Li, J. Metabolic Responses to Polymyxin Treatment in *Acinetobacter baumannii* ATCC 19606: Integrating Transcriptomics and Metabolomics with Genome-Scale Metabolic Modeling. *mSystems* **2019**, *4*, e00157-18. [CrossRef] [PubMed]
34. Deris, Z.Z.; Akter, J.; Sivanesan, S.; Roberts, K.D.; Thompson, P.E.; Nation, R.L.; Li, J.; Velkov, T. A secondary mode of action of polymyxins against Gram-negative bacteria involves the inhibition of NADH-quinone oxidoreductase activity. *J. Antibiot.* **2014**, *67*, 147–151. [CrossRef] [PubMed]
35. Sampson, T.R.; Liu, X.; Schroeder, M.R.; Kraft, C.S.; Burd, E.M.; Weiss, D.S. Rapid killing of *Acinetobacter baumannii* by polymyxins is mediated by a hydroxyl radical death pathway. *Antimicrob. Agents. Chemother.* **2012**, *56*, 5642–5649. [CrossRef] [PubMed]
36. Yu, Z.; Zhu, Y.; Fu, J.; Qiu, J.; Yin, J. Enhanced NADH Metabolism Involves Colistin-Induced Killing of *Bacillus subtilis* and *Paenibacillus polymyxa*. *Molecules* **2019**, *24*, 387. [CrossRef] [PubMed]
37. Clinical and Laboratory Standards Institute. *Methods for Dilution Antimicrobial Susceptibility Tests for Bacteria That Grow Aerobically*, 11th ed.; M07; Clinical and Laboratory Standards Institute: Wayne, PA, USA, 2018.
38. Bonapace, C.R.; Bosso, J.A.; Friedrich, L.V.; White, R.L. Comparison of methods of interpretation of checkerboard synergy testing. *Diagn. Microbiol. Infect. Dis.* **2002**, *44*, 363–366. [CrossRef]
39. Clinical and Laboratory Standards Institute. *Methods for Determining Bactericidal Activity of Antimicrobial Agents: Approved Guideline*, 1st ed.; M026-A; Clinical and Laboratory Standards Institute: Wayne, PA, USA, 1999.

AMERICAN SOCIETY FOR MICROBIOLOGY | Microbiology Spectrum

RESEARCH ARTICLE

Activity of *N*-Acetylcysteine Alone and in Combination with Colistin against *Pseudomonas aeruginosa* Biofilms and Transcriptomic Response to *N*-Acetylcysteine Exposure

Felice Valzano,[a] Selene Rebecca Boncompagni,[a] Maria Micieli,[b] Tiziana Di Maggio,[a] Vincenzo Di Pilato,[c] Lorenzo Colombini,[d] Francesco Santoro,[d] Gianni Pozzi,[d] Gian Maria Rossolini,[b,e] Lucia Pallecchi[a]

[a]Department of Medical Biotechnologies, University of Siena, Siena, Italy
[b]Department of Experimental and Clinical Medicine, University of Florence, Florence, Italy
[c]Department of Surgical Sciences and Integrated Diagnostics, University of Genoa, Genoa, Italy
[d]Laboratory of Molecular Microbiology and Biotechnology, Department of Medical Biotechnologies, University of Siena, Siena, Italy
[e]Clinical Microbiology and Virology Unit, Careggi University Hospital, Florence, Italy

ABSTRACT Chronic colonization by *Pseudomonas aeruginosa* is critical in cystic fibrosis (CF) and other chronic lung diseases, contributing to disease progression. Biofilm growth and a propensity to evolve multidrug resistance phenotypes drastically limit the available therapeutic options. In this perspective, there has been growing interest in evaluating combination therapies, especially for drugs that can be administered by nebulization, which allows high drug concentrations to be reached at the site of infections while limiting systemic toxicity. Here, we investigated the potential antibiofilm activity of *N*-acetylcysteine (NAC) alone and in combination with colistin against a panel of *P. aeruginosa* strains (most of which are from CF patients) and the transcriptomic response of a *P. aeruginosa* CF strain to NAC exposure. NAC alone (8,000 mg/L) showed a limited and strain-dependent antibiofilm activity. Nonetheless, a relevant antibiofilm synergism of NAC-colistin combinations (NAC at 8,000 mg/L plus colistin at 2 to 32 mg/L) was observed with all strains. Synergism was also confirmed with the artificial sputum medium model. RNA sequencing of NAC-exposed planktonic cultures revealed that NAC (8,000 mg/L) mainly induced (i) a Zn^{2+} starvation response (known to induce attenuation of *P. aeruginosa* virulence), (ii) downregulation of genes of the denitrification apparatus, and (iii) downregulation of flagellar biosynthesis pathway. NAC-mediated inhibition of *P. aeruginosa* denitrification pathway and flagellum-mediated motility were confirmed experimentally. These findings suggested that NAC-colistin combinations might contribute to the management of biofilm-associated *P. aeruginosa* lung infections. NAC might also have a role in reducing *P. aeruginosa* virulence, which could be relevant in the very early stages of lung colonization.

IMPORTANCE *Pseudomonas aeruginosa* biofilm-related chronic lung colonization contributes to cystic fibrosis (CF) disease progression. Colistin is often a last-resort antibiotic for the treatment of such *P. aeruginosa* infections, and it has been increasingly used in CF, especially by nebulization. *N*-acetylcysteine (NAC) is a mucolytic agent with antioxidant activity, commonly administered with antibiotics for the treatment of lower respiratory tract infections. Here, we show that NAC potentiated colistin activity against *in vitro* biofilms models of *P. aeruginosa* strains, with both drugs tested at the high concentrations achievable after nebulization. In addition, we report the first transcriptomic data on the *P. aeruginosa* response to NAC exposure.

KEYWORDS *N*-acetylcysteine, *Pseudomonas aeruginosa*, biofilms, colistin, cystic fibrosis, synergism, transcriptomic response

Editor Cezar M. Khursigara, University of Guelph

Address correspondence to Lucia Pallecchi, lucia.pallecchi@unisi.it.

The authors declare a conflict of interest. G.M.R. and L.P. have been Advisory Board members for Zambon S.p.A. and have participated to scientific events financed by Zambon.

Received 18 March 2022
Accepted 3 June 2022
Published 23 June 2022

Pseudomonas aeruginosa is a leading pathogen infecting the airways of patients affected by cystic fibrosis (CF) and other chronic lung diseases (e.g., chronic obstructive pulmonary disease and non-CF bronchiectasis) (1). Once established in the CF airways, *P. aeruginosa* develops into chronic infections and generally persists indefinitely, contributing to frequent exacerbations, decline of pulmonary function, and higher rates of mortality (1, 2). Chronic infections by *P. aeruginosa* in CF lungs are associated with adaptive changes of the pathogen, such as conversion to a mucoid phenotype, switching to the biofilm mode of growth, and acquisition of antibiotic resistance (3). Cumulative exposure to antibiotics during treatment causes dissemination of multidrug-resistant (MDR) *P. aeruginosa* strains, leading to the ineffectiveness of the antibiotic therapy and consequently worse clinical outcomes (3).

Colistin is among the last-resort agents for the treatment of *P. aeruginosa* infections caused by MDR strains, with the advantage of being also administrable by nebulization, which allows the achieving of high lung concentrations while reducing systemic toxicity (4). In this perspective, inhaled colistin has been increasingly used for the treatment of difficult-to-treat respiratory tract infections, especially those related to biofilm formation (5).

N-acetylcysteine (NAC) is a mucolytic agent commonly administered with antibiotics for the treatment of lower respiratory tract infections, which has been demonstrated to exert also antimicrobial and antibiofilm activity against relevant respiratory pathogens (6–8). Recently, a potent *in vitro* antibiofilm synergism of NAC-colistin combinations was demonstrated against colistin-susceptible and colistin-resistant *Acinetobacter baumannii* and *Stenotrophomonas maltophilia* strains (9, 10).

NAC has been demonstrated to exert several heterogeneous biological activities (whose molecular bases have not always been clearly elucidated) and has recently been under extensive investigation for potential clinical applications beyond the approved therapeutic usage as an antidote in acetaminophen (paracetamol) overdose and as a mucolytic (11). Overall, NAC can act as a direct or indirect antioxidant, due to the ability of the free thiol group to react with reactive oxygen and nitrogen species and by constituting a precursor of intracellular glutathione (11). In addition, NAC can bind transition and heavy metal ions and act as a reducing agent of protein sulfhydryl groups involved in intracellular redox homeostasis (11). Despite several studies that have addressed the biological effects of NAC on planktonic and biofilm bacterial cultures (8), to the best of our knowledge, no data on bacterial transcriptomic response to NAC exposure have been reported so far.

In this study, we investigated the *in vitro* antibiofilm activities of NAC alone and in combination with colistin (at the high concentrations achievable by the inhalation route of administration) (8, 12) against a panel of *P. aeruginosa* strains (most of which are from CF patients) representative of different phenotypes (in terms of mucoidy, antimicrobial susceptibility pattern, and O type) and multilocus sequence type (MLST) genotypes. In addition, we provided original data on the transcriptomic response of *P. aeruginosa* planktonic cultures to NAC exposure.

RESULTS AND DISCUSSION

Activity of NAC alone against preformed biofilm. The antibiofilm activity of NAC alone was tested with 17 *P. aeruginosa* strains (Table 1), of which 15 were from CF patients, using the Nunc-TSP lid system.

NAC at 8,000 mg/L (i.e., a high concentration achievable after inhalation) showed limited and strain-dependent activity (Fig. 1 to 4). In particular, major effects were observed with *P. aeruginosa* Z154 (i.e., decrease of $>$1 log CFU/peg compared to the control) (Fig. 1) and *P. aeruginosa* PAO1 (i.e., increase of $>$1 log CFU/peg compared to the control) (Fig. 2). With an additional 7 strains, a very slight but statistically significant activity was observed (i.e., $<$0.5 log CFU/peg compared to the control), resulting in biofilm reduction in six cases (i.e., *P. aeruginosa* Z33, Z35, Z152, M13, M19, and M25) and biofilm increase in the remaining one (i.e., *P. aeruginosa* M42) (Fig. 2 and 3).

Overall, these results indicated that inhaled NAC alone might not have major effects on

TABLE 1 Features of the 17 *P. aeruginosa* strains included in this study

Strain	yr of isolation	Phenotype	Origin[a]	ST[b]	O type	Resistance pattern[c]	MIC (mg/L)[d]	
							CST	NAC
PAO1	1954	Nonmucoid	Wound	ST549	O5	Wild type	2	64,000
Z33	2005	Nonmucoid	CF	ST235	O11	CP^r, FQ^r, AG^r	1	16,000
Z34	2006	Nonmucoid	CF	ST17	O1	CB^r, CP^r, FQ^r, AG^r	2	64,000
Z35	2006	Nonmucoid	CF	ST235	O11		1	16,000
Z152	2013	Mucoid	CF	ST155	O6	CB^r, FQ^r, AG^r	2	8,000
Z154	2016	Mucoid	CF	ST412	O6	CP^r, FQ^r, AG^r	2	16,000
M1	2002	Mucoid	CF	ST155	O6	CB^r, CP^r, FQ^r, AG^r	2	16,000
M4	2005	Mucoid	CF	ST155	O6	CB^r, CP^r, FQ^r, AG^r	2	32,000
M7	2005	Mucoid	CF	ST253	O10	AG^r	2	64,000
M13	2000	Mucoid	CF	ST274	O3	CB^r, CP^r, AG^r	1	32,000
M19	2006	Mucoid	CF	ST3509	O7		1	64,000
M25	2002	Mucoid	CF	ST235	O11		2	16,000
M32	2006	Mucoid	CF	ST235	O11		2	16,000
M42	2007	Mucoid	CF	ST2437	O6	CB^r, CP^r, FQ^r, AG^r	2	32,000
FC237	2007	Nonmucoid	CF	ST365	O3	CB^r, FQ^r, AG^r, CST^r	512	64,000
FC238	2007	Nonmucoid	CF	ST910	O6	CB^r, CST^r	8	64,000
FZ99	2018	Nonmucoid	RTI_{ICU}	ST111	O12	CB^r, CP^r, FQ^r, AG^r, CST^r	4	64,000

[a]CF, cystic fibrosis; RTI_{ICU}, respiratory tract infection in intensive care unit.
[b]According to the MLST Pasteur scheme.
[c]CB^r, resistance to carbapenems (imipenem and meropenem); CP^r, resistance to cephems (ceftazidime and cefepime); FQ^r, resistance to fluoroquinolones (ciprofloxacin); AG^r, resistance to aminoglycosides (amikacin and gentamicin); CST^r, resistance to colistin.
[d]CST, colistin; NAC, *N*-acetylcysteine.

P. aeruginosa biofilms already established in the lung and that the response to NAC was not related to phenotypic or genotypic features. The few previous studies that have addressed the activity of NAC against preformed *P. aeruginosa* biofilms have reported similar results (i.e., usually limited and strain-dependent effects), although a direct comparison of data is not straightforward due to different methodological approaches (e.g., different biofilm models and different NAC concentrations tested) and the low number of strains often tested in such studies (i.e., usually reference strains) (8, 13, 14). This study provided a wider picture on this topic by investigating a panel of characterized *P. aeruginosa* strains using a standardized *in vitro* biofilm model and *in vivo* achievable NAC concentrations. Interestingly, NAC alone (at the concentration used in this study and the same biofilm

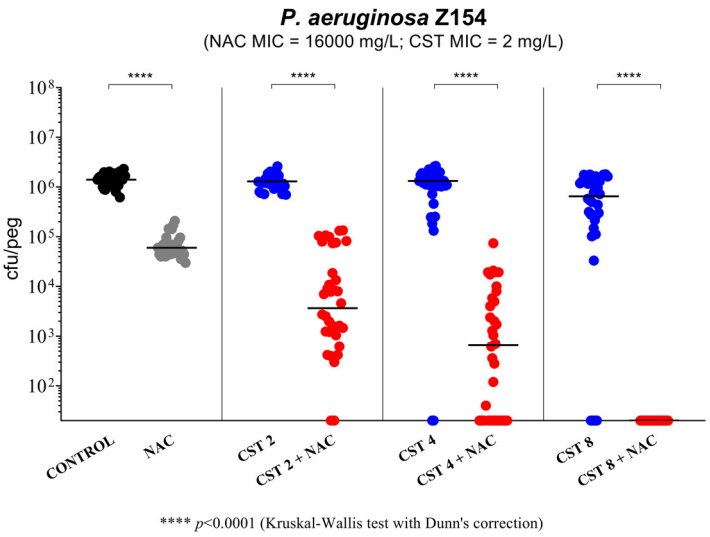

FIG 1 Antibiofilm activity of *N*-acetylcysteine (NAC) at 8,000 mg/L, colistin (CST), and NAC-CST combinations against *P. aeruginosa* Z154 in the Nunc-TSP lid system. A relevant potentiation of colistin antibiofilm activity was observed with all NAC-CST combinations tested. CST 2, colistin at 2 mg/L; CST 4, colistin at 4 mg/L; CST 8, colistin at 8 mg/L. Biofilms not exposed to NAC or CST represent the control. Black lines indicate median values. The *x* axis is set at the limit of detection (20 CFU/peg).

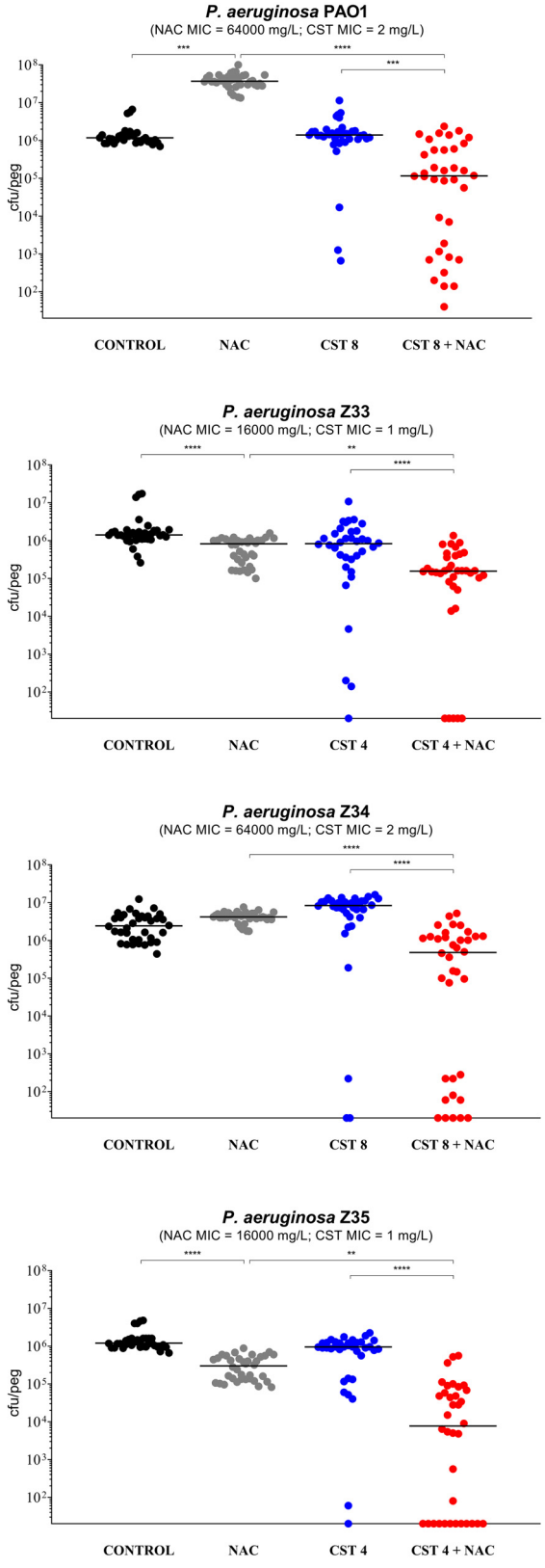

** $p<0.01$, *** $p<0.001$, **** $p<0.0001$ (Kruskal-Wallis test with Dunn's correction)

FIG 2 Antibiofilm activity of *N*-acetylcysteine (NAC) at 8,000 mg/L, colistin (CST), and NAC-CST combinations against *P. aeruginosa* PAO1 and three colistin-susceptible nonmucoid strains in the

(Continued on next page)

model) was recently shown to exert relevant activity against preformed biofilms of two relevant CF pathogens, namely, *S. maltophilia* and *Burkholderia cepacia* complex (BCC) (7). The reasons for such a diverse response of *P. aeruginosa* compared to *S. maltophilia* and BCC should deserve further attention, because they could possibly help identifying critical targets in the complex biofilm environments, to be used for the implementation of new antibiofilm strategies.

Activity of NAC-colistin combinations against preformed biofilms. *P. aeruginosa* Z154 (a mucoid, MDR, colistin-susceptible CF strain) was first used to test the potential antibiofilm synergism of NAC at 8,000 mg/L plus diverse colistin concentrations. As shown in Fig. 1, a relevant synergism was observed already with colistin at 2 mg/L (i.e., the colistin MIC for the tested strain), with a dose-dependent effect at increasing colistin concentrations, and complete biofilm eradication was achieved with the combination of NAC at 8,000 mg/L plus colistin at 8 mg/L (Fig. 1).

The remaining 16 strains were initially tested with the combination of NAC at 8,000 mg/L plus colistin at 8 mg/L. In order to detect a potential synergism, the concentration of colistin was then modified for strains forming biofilms highly susceptible to colistin ($n = 7$) or particularly resistant ($n = 2$) (Fig. 2 to 4). Overall, a relevant synergism of NAC-colistin combinations was observed with all tested strains (including the three colistin-resistant ones), although in two cases (i.e., *P. aeruginosa* M4 and M32), statistical significance was not achieved (Fig. 2 to 4). These latter strains were also tested with lower colistin concentrations (i.e., 2 and 4 mg/L, respectively), but synergism was not observed (data not shown). Concerning the synergism observed with the three colistin-resistant strains (Fig. 4), it is interesting to note that with strain FC237 (nonmucoid, MDR), an important decrease in viable biofilm cells was observed with a combination including a colistin concentration much lower than the colistin MIC for this strain (i.e., 1/64 MIC) (Fig. 4).

Overall, these data demonstrated that NAC could potentiate colistin activity against preformed biofilms of colistin-susceptible and colistin-resistant *P. aeruginosa* strains, regardless of the mucoid/nonmucoid phenotype, the resistance pattern, and the ST and O type. Present findings are consistent with the previously observed antibiofilm synergism of NAC-colistin combinations against colistin-susceptible and colistin-resistant strains of *A. baumannii* and *S. maltophilia* (9, 10). Further studies with a higher number of *P. aeruginosa* clinical isolates, especially with a colistin-resistant phenotype, are encouraged.

Activity of NAC-colistin combinations in the ASM biofilm model. Two *P. aeruginosa* CF strains exhibiting different phenotypes were selected for susceptibility assays with the artificial sputum medium (ASM) biofilm model: *P. aeruginosa* Z34 (nonmucoid, MDR, ST17, O1) and *P. aeruginosa* Z154 (mucoid, MDR, ST412, O6). Biofilms were grown in ASM, in order to mimic the *P. aeruginosa* biofilm environmental conditions experienced in the CF mucus. Preformed biofilms were then challenged in the same medium with NAC-colistin combinations.

As shown in Fig. 5, a clear synergism of NAC at 8,000 mg/L in combination with colistin at 64 mg/L was observed with both strains (Fig. 5). Compared to the experiments performed with the Nunc-TSP lid system, the concentration of colistin that allowed observation of a synergism was much higher (i.e., 32× the MIC), possibly due to colistin strong ionic interactions with ASM components (e.g., extracellular DNA and mucin) (15). Indeed, preliminary experiments carried out with lower colistin concentrations did not show either colistin antibiofilm activity or synergism with NAC (data not shown). In addition, the antibiofilm activity of NAC alone observed against *P. aeruginosa* Z154 in the Nunc-TSP lid system was not observed in the ASM model (Fig. 5), confirming that

FIG 2 Legend (Continued)
Nunc-TSP lid system. A potentiation by NAC of colistin antibiofilm activity was observed with all tested strains. CST 4, colistin 4 mg/L; CST 8, colistin 8 mg/L. Biofilms not exposed to NAC or CST represented the control. Black lines indicate median values. The *x* axis is set at the limit of detection (20 CFU/peg).

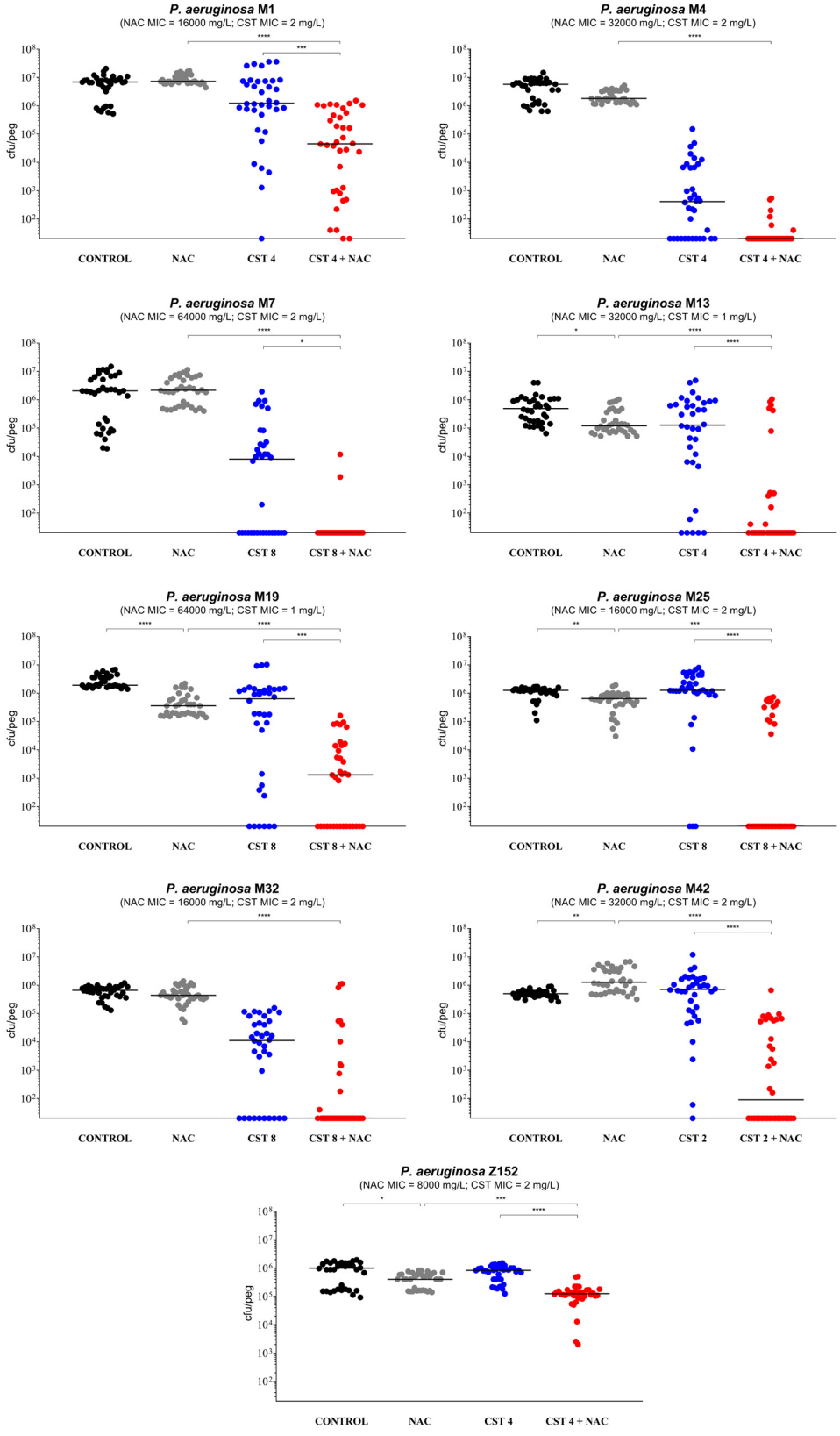

* $p<0.05$, ** $p<0.01$, *** $p<0.001$, **** $p<0.0001$ (Kruskal-Wallis test with Dunn's correction)

FIG 3 Antibiofilm activity of *N*-acetylcysteine (NAC) at 8,000 mg/L, colistin (CST), and NAC-CST combinations against nine colistin-susceptible mucoid *P. aeruginosa* strains in the Nunc-TSP lid system. A potentiation by

(Continued on next page)

the efficacy of NAC alone against preformed *P. aeruginosa* biofilms could be limited *in vivo*.

Overall, these data demonstrated that the antibiofilm synergism of NAC-colistin combinations against *P. aeruginosa* strains is preserved also under the environmental conditions mimicking the CF mucus, which is promising for clinical applications. Furthermore, the lower susceptibility to colistin of *P. aeruginosa* biofilms in the ASM model compared to biofilm susceptibility in standard media observed in this study is consistent with what was previously reported with *P. aeruginosa* (16).

Transcriptomic response of *P. aeruginosa* Z154 to NAC exposure. *P. aeruginosa* Z154 (i.e., colistin-susceptible CF strain, mucoid, MDR, ST412, O6) was selected for investigating the transcriptome response of planktonic cultures to NAC exposure (i.e., NAC at 8,000 mg/L). A total of 66 differentially expressed genes (DEGs) were identified (adjusted *P* value of <0.05 with 99% confidence interval [CI]), of which 46 were upregulated and 20 downregulated compared to the control (Table 2).

Analysis of DEGs revealed that NAC mainly acted as Zn^{2+} chelator, inducing a strong Zn^{2+} starvation response. DEGs associated with such response were consistent with data reported in previous studies addressing zinc homeostasis in *P. aeruginosa* and other bacteria (Table 2) (17–22). In particular, 31 of the 46 upregulated DEGs belonged to the *zur* regulon and are known to be activated in response to Zn^{2+} starvation (Table 2) (17–22). Such genes mainly included operons involved in zinc uptake (e.g., the PA4063-PA4064-PA4065-PA4066 operon, *cntOLMI* operon, and *znuABC* operon) and genes encoding zinc-independent paralogs of cellular proteins (i.e., type B 50S ribosomal proteins L31 and L36, RNA polymerase-binding protein DksA2, adn GTP-cyclohydrolase FolE2) (Table 2) (17–23). Upregulated DEGs belonging to the *zur* regulon also included genes encoding an *N*-acetylmuramoyl-L-alanine amidase (AmiA, involved in splitting of septal peptidoglycan during cell division), a γ-carbonic anhydrase (Cam, involved in reversible hydration of carbon dioxide and important for growth under low-CO_2 conditions), and three modulators of the membrane FtsH protease (i.e., HflC and HflK family modulators) (Table 2). The membrane FtsH zinc-dependent protease is required for the expression of diverse unrelated phenotypes (e.g., swimming and twitching motility, biofilm formation, autolysis, production of secondary metabolites, maintenance of plasma membrane integrity by degrading misfolded proteins), and it has been recently demonstrated to represent an important virulence factor in *P. aeruginosa* clone C (23). HflC and HflK family modulators interact with FtsH at the level of the plasma membrane, usually with an inhibitory effect (23). The NAC-mediated effects on the phenotypes related to FtsH would deserve further attention.

The remaining 15 upregulated DEGs included genes encoding a recently described transcriptional regulator, PA2100 (also named MdrR2) (24), an AhpC-like alkyl hydroperoxide reductase (involved in protection from oxidative stress) (25), and proteins possibly involved in copper and iron uptake (Table 2).

MdrR2, together with MdrR1, has been demonstrated to repress the *mexAB-oprM* operon (independently from the MexR repressor), activate the EmrAB efflux pump, and indirectly inhibit biofilm formation (Table 2) (24). The effect of NAC on the MdrR1-MdrR2 dual-regulation system should be further investigated. Nonetheless, a previous study aimed at investigating the potential antagonism of high NAC concentrations (i.e., as those tested in this study) on the activity of the major classes of antibiotics used in the clinical practice, did not show major effects (with the exception of carbapenems, due to a chemical instability of carbapenems in the presence of NAC) (26), suggesting that the activation of the EmrAB efflux could not be relevant or circumvented by compensatory mechanisms.

Analysis of downregulated DEGs identified genes involved in denitrification, in particular *norB* (encoding the nitric oxide reductase subunit NorB), *nosR* (encoding the

FIG 3 Legend (Continued)
NAC of colistin antibiofilm activity was observed with all tested strains, although in two cases, statistical significance was not achieved (i.e., strains M4 and M32). CST 2, colistin at 2 mg/L; CST 4, colistin at 4 mg/L; CST 8, colistin at 8 mg/L. Biofilms not exposed to NAC or CST represent the control. Black lines indicate median values. The *x* axis is set at the limit of detection (20 CFU/peg).

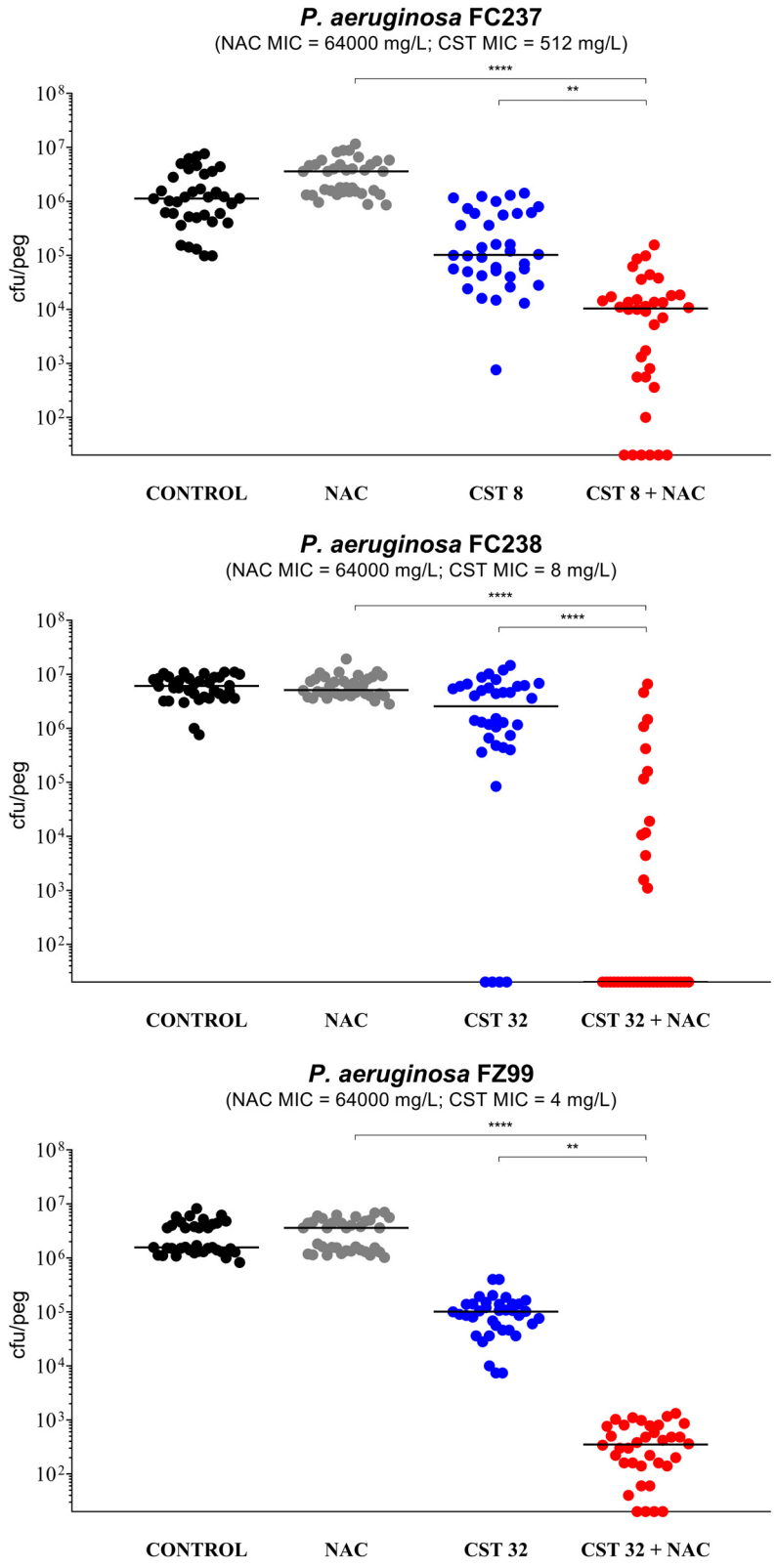

** $p<0.01$, **** $p<0.0001$ (Kruskal-Wallis test with Dunn's correction)

FIG 4 Antibiofilm activity of *N*-acetylcysteine (NAC) at 8,000 mg/L, colistin (CST), and NAC-CST combinations against three colistin-resistant nonmucoid *P. aeruginosa* strains in the Nunc-TSP lid

(Continued on next page)

regulatory protein NosR), and *nosZ* (encoding the nitrous oxide reductase NosZ) (Table 2). These data suggested that NAC might affect *P. aeruginosa* anaerobic respiration (which is crucial in the deeper biofilm layers and in the CF mucus) (27), because the nitric oxide reductase NorBC and the regulatory protein NosR have been recently demonstrated to constitute the nucleus of the denitrification protein network (28). NAC-mediated inhibition of the *P. aeruginosa* denitrification pathway might be implicated in the observed antibiofilm synergism of the NAC-colistin combination. Indeed, colistin has been demonstrated to exert increased antibiofilm activity against *P. aeruginosa* under anaerobic conditions, possibly due to a lower ability to implement the tolerance mechanism (e.g., lipopolysaccharide [LPS] modification) because of the low metabolism accompanying anaerobic growth (29). In this perspective, the inhibition of anaerobic respiration by NAC would further inhibit a *P. aeruginosa* adaptive response to colistin toxicity. This could be particularly relevant in *P. aeruginosa* biofilm in the CF mucus, where the anoxic conditions of biofilm cells are related not only to the position of the bacteria within the biofilm (i.e., anoxic conditions in the deeper layers), but also to the intense O_2 depletion caused by polymorphonuclear leukocytes (PMNs), determining entire biofilm growth without aerobic respiration (29).

Downregulated DEGs also included the following: (i) two genes involved in flagellar biosynthesis (i.e., *fliF*, encoding the flagellar M-ring protein FliF, and *flhF*, encoding the flagellar biosynthesis protein FlhF); (ii) a NAD(P)H-quinone oxidoreductase protecting against ROS-induced oxidative stress, which was recently demonstrated to be part of the core biofilm transcriptome (PA1137) (30); and (iii) *nalD*, encoding a second repressor of the *mexAB-oprM* operon (31). Finally, consistent with previous studies on *Pseudomonas* response to zinc starvation, downregulation of *copA* and *copZ*, involved in copper efflux, was observed, suggesting interplay between zinc and copper homeostasis (Table 2) (32).

NAC-mediated inhibition of *P. aeruginosa* denitrification pathway. The role of NAC in the inhibition of the denitrification pathway was confirmed by measuring NO_3^- and NO_2^- concentrations during anaerobic growth of the *P. aeruginosa* Z154 strain (i.e., the strain used for transcriptomic analysis) in culture media supplemented with 10 mM $NaNO_3$ or KNO_2, in the presence or absence of NAC at 8,000 mg/L.

As expected from previous studies (33), in $NaNO_3$-containing medium, the levels of NO_3^- and its reduction product, NO_2^-, fell below the detection limit after 24 h, in the absence of NAC (Fig. 6A). However, in the presence of NAC at 8,000 mg/L, the depletion of NO_3^- was followed by an accumulation of NO_2^- (evident at both 24 and 48 h), indicating that further reduction of NO_2^- was inhibited in the presence of NAC (Fig. 6A). In order to consolidate these data, the experiments were repeated using a medium supplemented with KNO_2. In the absence on NAC, complete reduction of NO_2 was observed after 48 h (Fig. 6B), as expected (33). On the contrary, in the presence of NAC at 8,000 mg/L, NO_2 levels did not decrease (Fig. 6B).

These results were consistent with the transcriptomic data and showed that NAC was able to inhibit the denitrification pathway in anaerobic environments, such as those encountered in endobronchial CF mucus. This feature might contribute to the observed antibiofilm synergism of NAC-colistin combinations, as previously discussed.

Time-kill assays of the NAC-colistin combination against planktonic cultures grown under anaerobic and aerobic conditions. Transcriptomic and biological data from this study suggested a role of NAC in inhibiting the *P. aeruginosa* denitrification apparatus, which could contribute to the observed antibiofilm synergy of NAC-colistin combinations. In order to further investigate this issue, time-kill assays of the NAC-colistin combination were performed with *P. aeruginosa* Z154 (i.e., the strain used for transcriptomic analysis) planktonic cultures, under both anaerobic and aerobic conditions.

FIG 4 Legend (Continued)
system. A potentiation by NAC of colistin antibiofilm activity was observed with all tested strains. CST 8, colistin at 8 mg/L; CST 32, colistin at 32 mg/L. Biofilms not exposed to NAC or CST represent the control. Black lines indicate median values. The *x* axis is set at the limit of detection (20 CFU/peg).

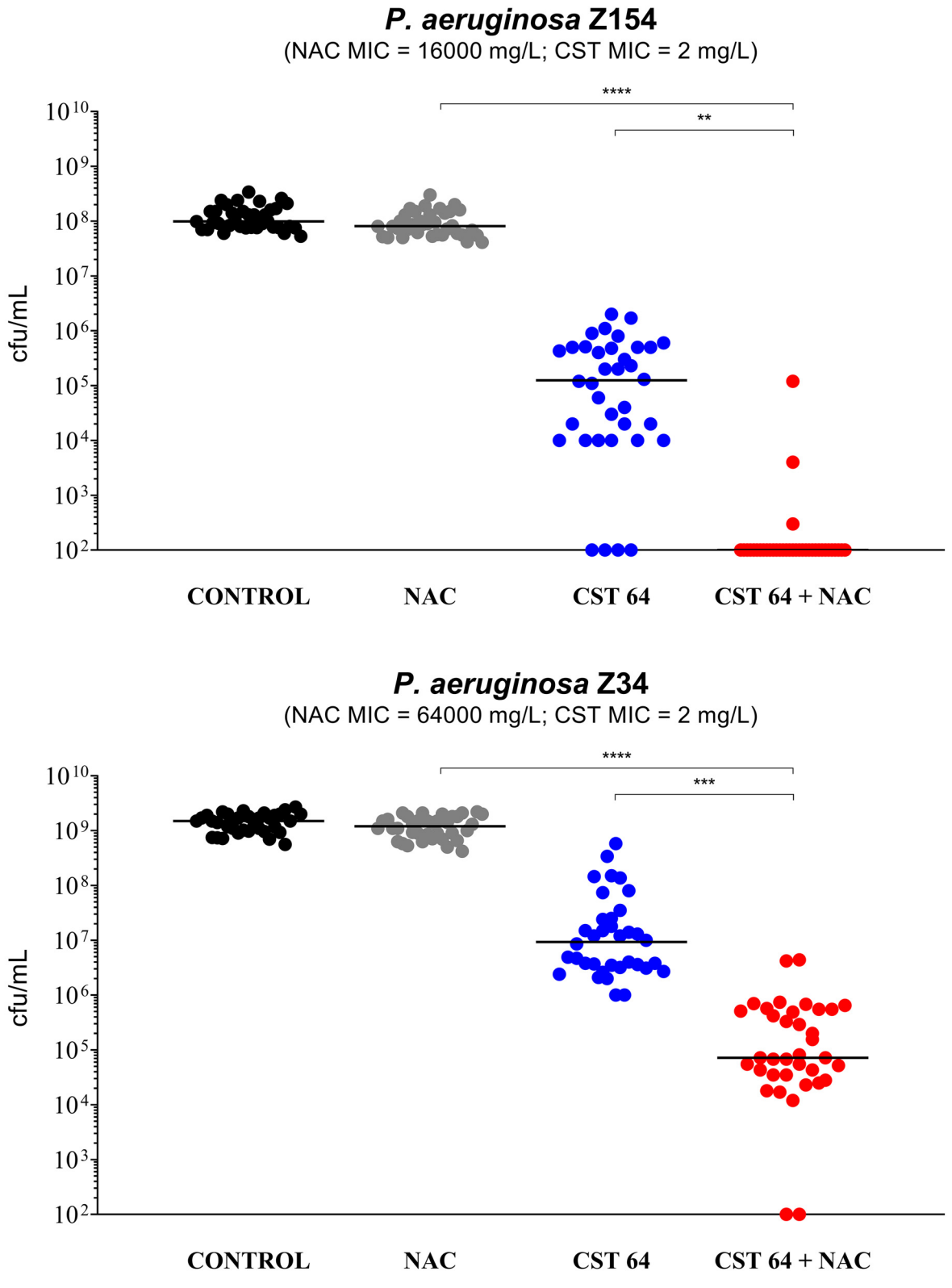

** $p<0.01$, *** $p<0.001$, **** $p<0.0001$ (Kruskal-Wallis test with Dunn's correction)

FIG 5 Antibiofilm activity of *N*-acetylcysteine (NAC) at 8,000 mg/L, colistin at 64 mg/L (CST 64), and the NAC-CST combination against *P. aeruginosa* Z154 and *P. aeruginosa* Z34 in the ASM biofilm model. A potentiation by NAC of colistin antibiofilm activity was observed with both strains. Biofilms not exposed to NAC or CST represent the control. Black lines indicate median values. The *x* axis is set at the limit of detection (100 CFU/mL).

TABLE 2 DEGs in *P. aeruginosa* Z154 planktonic cultures exposed to 8,000 mg/L NAC compared to control

DEG	Locus tag in *P. aeruginosa* strain			Gene	Product (function)[a]	Zur regulon	Adjusted *P* value	Log_2 fold change
	Z154	PAO1	UCBPP-PA14					
Upregulated	IS492_10415	PA0781	PA14_54180	*znuD*	TBDR ZnuD (zinc uptake)	+	4.6E−36	1.9
	IS492_17070	PA1922	PA14_39650	*cirA*	TBDR CirA (iron and zinc uptake)	+	0.0E+00	2.4
	IS492_17075	PA1923	PA14_39640		Cobaltochelatase subunit CobN-like (cobalamin biosynthesis)	+	7.9E−36	1.9
	IS492_17080	PA1924	PA14_39630	*exbD*	ExbD proton channel family protein (energy support for TBDR, cotranscribed with PA1922)	+	1.7E−03	0.6
	IS492_17085	PA1925	PA14_39620		Hypothetical protein (unknown function, DUF2149 domain-containing protein)	+	7.5E−06	0.8
	IS492_19940	PA2437	PA14_33110		HflC family modulator of membrane FtsH protease	+	5.1E−06	0.8
	IS492_19945	PA2438	PA14_33080		HflC modulator of membrane FtsH protease	+	7.0E−03	0.6
	IS492_19950	PA2439	PA14_33070	*hflK*	HflK family modulator of membrane FtsH protease	+	6.5E−03	0.6
	IS492_23615	PA2911	PA14_26420		TBDR (possibly involved in zinc uptake)	+	7.6E−03	0.6
	IS492_27310	PA3600	PA14_17710	*rpmJ2*	Zinc-independent paralog type B 50S ribosomal protein L36	+	2.0E−16	1.3
	IS492_27315	PA3601	PA14_17700	*rpmE2*	Zinc-independent paralog type B 50S ribosomal protein L31	+	1.2E−04	0.7
	IS492_29825	PA4063	PA14_11320		Zinc SBP (zinc uptake)	+	7.0E−41	2.0
	IS492_29830	PA4064	PA14_11310		Zinc ABC transporter, ATP-binding protein (zinc uptake)	+	4.2E−08	0.9
	IS492_29835	PA4065	PA14_11290		Zinc ABC transporter, permease (zinc uptake)	+	4.9E−13	1.2
	IS492_29840	PA4066	PA14_11280		Zinc SBP (zinc uptake)	+	8.5E−05	0.7
	IS492_06220	PA4834	PA14_63910	*cntI*	Pseudopaline transport plasma membrane protein CntI (zinc uptake)	+	6.1E−05	0.7
	IS492_06215	PA4835	PA14_63920	*cntM*	Pseudopaline biosynthesis dehydrogenase CntM (zinc uptake)	+	8.1E−26	1.7
	IS492_06210	PA4836	PA14_63940	*cntL*	Pseudopaline biosynthesis enzyme CntL (zinc uptake)	+	9.3E−39	2.0
	IS492_06205	PA4837	PA14_63960	*cntO*	Pseudopaline transport outer membrane protein CntO (zinc uptake)	+	0.0E+00	2.5
	IS492_06200	PA4838	PA14_63970		Hypothetical membrane protein	+	8.0E−04	0.7
	IS492_31595	PA5498	PA14_72550	*znuA*	Zinc soluble binding protein ZnuA (zinc uptake)	+	9.0E−08	0.9
	IS492_31600	PA5499	PA14_72560	*zur*	Transcriptional regulator for zinc homeostasis	+	5.3E−10	1.0
	IS492_31605	PA5500	PA14_72580	*znuC*	Zinc ABC transporter, ATP-binding protein ZnuC (zinc uptake)	+	1.2E−07	0.9
	IS492_31610	PA5501	PA14_72590	*znuB*	Zinc ABC transporter, ZnuB permease (zinc uptake)	+	1.9E−03	0.6
	IS492_31780	PA5534	PA14_73000		Hypothetical protein (unknown function, DUF1826 domain-containing protein)	+	9.8E−23	1.5
	IS492_31785	PA5535	PA14_73010	*zigA*	Zinc metallochaperone GTPase ZigA	+	5.9E−42	2.1
	IS492_31790	PA5536	PA14_73020	*dksA2*	Zinc-independent paralog of RNA polymerase-binding protein DksA	+	2.4E−23	1.5
	IS492_31800	PA5538	PA14_73040	*amiA*	*N*-acetylmuramoyl-L-alanine amidase (splitting of septal peptidoglycan during cell division)	+	1.3E−08	1.0
	IS492_31805	PA5539	PA14_73050	*folE2*	Zinc-independent paralog of GTP-cyclohydrolase FolE (folate biosynthesis)	+	4.5E−28	1.7
	IS492_31810	PA5540	PA14_73060	*cam*	γ-Carbonic anhydrase (reversible hydration of carbon dioxide)	+	1.5E−24	1.6
	IS492_31815	PA5541	PA14_73070	*pyrC2*	Zinc-independent paralog of dihydroorotase PyrC (pyrimidine biosynthesis)	+	3.1E−09	1.0
	IS492_02205	PA0433	PA14_05630		Hypothetical protein (unknown function, DUF2946 domain-containing protein)		1.3E−03	0.7
	IS492_02210	PA0434	PA14_05640		TBDR for which the siderophore has not been identified		1.5E−28	1.7
	IS492_02430	PA0478	PA14_06250	*fiuC*	GNAT family *N*-acetyltransferase (release of iron from desferrichrome in the cytoplasm)		3.9E−06	0.8
	IS492_10765	PA0848	PA14_53300	*ahpB*	AhpC-like alkylhydroperoxide reductase (oxidative stress response and cell redox homeostasis)		3.9E−16	1.3
	IS492_17945	PA2100	ND[b]	*mdrR2*	Transcriptional regulator, regulatory partner of MdrR1 (regulator of efflux systems)		6.3E−05	0.7
	IS492_17950	PA2101	ND		Conserved hypothetical protein (EamA-like transporter family)		1.7E−26	1.7
	IS492_17955	PA2102	ND		Hypothetical protein (unknown function, Mov34/MPN/PAD-1 family protein)		5.7E−13	1.2
	IS492_17960	PA2103	ND	*moeB*	Probable molybdopterin biosynthesis protein MoeB (ubiquitin-like modifier-activating activity)		7.5E−06	0.8
	IS492_25770	PA3287	PA14_21530		Ankyrin repeat domain-containing protein (unknown function)		1.9E−04	0.7
	IS492_27305	PA3599	PA14_17720		Probable transcriptional regulator		5.2E−12	1.1
	IS492_28275	PA3784	PA14_15130		Hypothetical protein (unknown function)		1.4E−05	0.8
	IS492_28280	PA3785	PA14_15120		Copper chaperone PCu(A)C		8.6E−07	0.9
	IS492_28305	PA3790	PA14_15070		TBDR copper receptor OprC (copper uptake)		1.0E−03	0.6
	IS492_06715	PA4739	PA14_62690		Hypothetical protein (unknown function, BON domain-containing protein)		9.8E−03	0.6

(Continued on next page)

TABLE 2 (Continued)

DEG	Locus tag in *P. aeruginosa* strain			Gene	Product (function)[a]	Zur regulon	Adjusted *P* value	Log_2 fold change
	Z154	PAO1	UCBPP-PA14					
	IS492_31510	PA5481	PA14_72360		Hypothetical periplasmic protein (inhibitor of vertebrate lysozyme)		3.9E−04	0.7
Downregulated	IS492_00850	PA0164	PA14_02050		γ-Glutamyltransferase family protein		8.0E−04	−0.6
	IS492_02660	PA0524	PA14_06830	*norB*	Nitric oxide reductase subunit NorB (denitrification)		3.9E−03	−0.6
	IS492_02685	PA0529	PA14_06890		Hypothetical protein (unknown function, MOSC domain-containing protein)		2.0E−05	−0.7
	IS492_02690	PA0530	PA14_06900		Probable class III pyridoxal phosphate-dependent aminotransferase (diverse metabolic pathways)		5.7E−05	−0.8
	IS492_02695	PA0531	PA14_06920		Aspartate aminotransferase family protein		4.7E−03	−0.6
	IS492_12670	PA1101	PA14_50140	*fliF*	Flagellar M-ring protein FliF (motility)		5.7E−05	−0.7
	IS492_12855	PA1136	PA14_49700		Probable transcriptional regulator		1.5E−12	−1.1
	IS492_12860	PA1137	PA14_49690		Oxidoreductase zinc-binding dehydrogenase family protein (protection from oxidative stress)		0.0E+00	−2.3
	IS492_14625	PA1453	PA14_45660	*flhF*	Flagellar biosynthesis protein FlhF (motility)		7.6E−03	−0.6
	IS492_19230	PA2298	PA14_34900		Probable oxidoreductase		4.9E−05	−0.7
	IS492_19235	PA2299	PA14_34880		Probable transcriptional regulator		3.2E−04	−0.7
	IS492_26340	PA3391	PA14_20230	*nosR*	Regulatory protein NosR (denitrification)		3.2E−04	−0.6
	IS492_26345	PA3392	PA14_20200	*nosZ*	Nitrous oxide reductase (denitrification)		4.1E−05	−0.8
	IS492_26895	PA3519	PA14_18810		Iron-containing redox enzyme family protein		2.8E−05	−0.3
	IS492_26920	PA3523	PA14_18760	*mexP*	Resistance-nodulation-cell division (RND) efflux membrane fusion protein		3.2E−03	−0.2
	IS492_27180	PA3574	PA14_18080	*nalD*	Transcriptional regulator NalD (second repressor of MexAB-OprM)		1.5E−19	−1.3
	IS492_27185	PA3574a	PA14_18070	*copZ*	Copper chaperone CopZ (copper efflux)		9.1E−11	−1.0
	IS492_27760	PA3690	PA14_16660		Heavy metal-translocating P-type ATPase (efflux)		1.1E−08	−1.0
	IS492_28975	PA3920	PA14_13170	*copA*	Copper-translocating P-type ATPase CopA1 (copper efflux)		1.2E−27	−1.2
	IS492_04870	PA5100	PA14_67350	*hutU*	Urocanate hydratase (histidine catabolic process)		4.0E−04	−0.6

[a]TBDR, TonB-dependent receptor; SBP, soluble binding protein; ABC, ATP-binding cassette. Protein functions were inferred from the literature and PseudoCAP (https://www.Pseudomonas.com/pseudocap).
[b]ND, not determined.

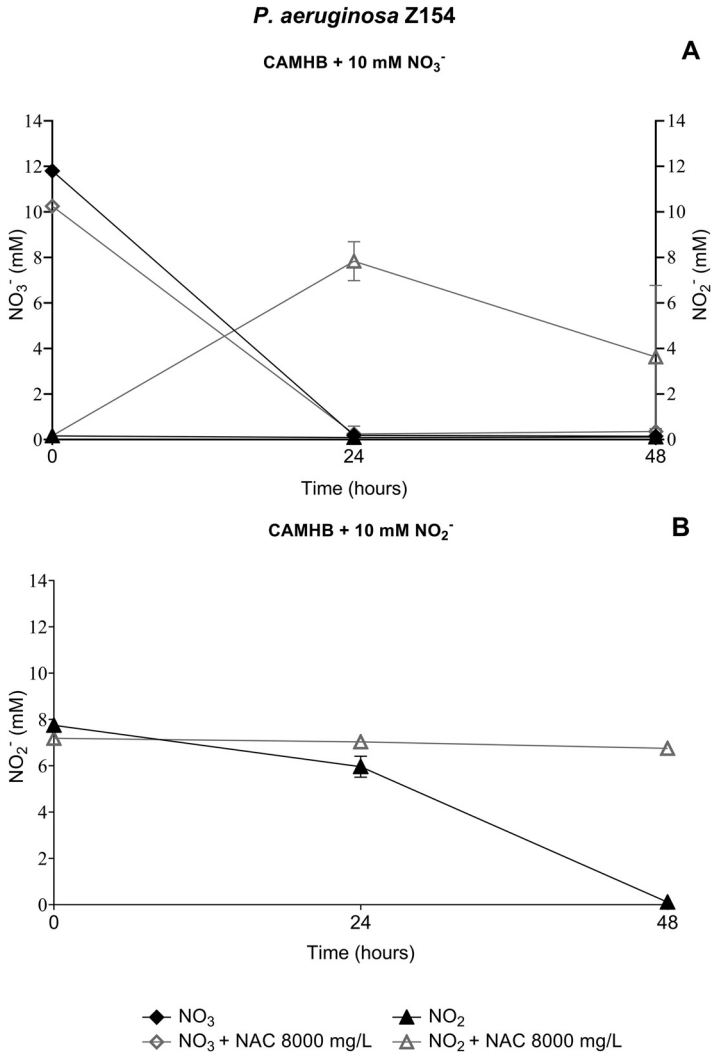

FIG 6 NAC-mediated inhibition of *P. aeruginosa* Z154 denitrification pathway. (A) NO_3^- and NO_2^- concentrations in anaerobic CAMHB supplemented with 10 mM NO_3^-, with or without NAC at 8,000 mg/L; (B) NO_2^- concentration in anaerobic CAMHB supplemented with 10 mM NO_2^-, with or without NAC at 8,000 mg/L. Data are plotted as the mean values of NO_3^- and/or NO_2^- levels detected at each time point.

Consistent with previous studies, anaerobic cultures were more susceptible to killing by colistin than aerobic cultures (34, 35) (Fig. 7A and B). Interestingly, a clear bactericidal effect of colistin at 0.25 mg/L (i.e., 1/8 MIC) in combination with NAC at 8,000 mg/L was observed in planktonic cultures grown under anaerobic conditions, with eradication achieved after 24 h of exposure (Fig. 7A). The wide error bars were due to the fact that in 2 out of 8 replicates (related to two independent experiments), no synergism was observed (Fig. 7A). This discrepancy was probably related to the low colistin concentration tested and the possible presence of heteroresistant subpopulations. On the contrary, cultures grown in the presence of oxygen were not affected by the NAC-colistin combination, demonstrating the influence of the growth conditions on the susceptibility of *P. aeruginosa* to such combination (Fig. 7B).

These results supported the hypothesis that, under anoxic conditions like those present in the deeper biofilm layers and in CF mucus, NAC-mediated inhibition of anaerobic respiration would prevent an adaptive response of *P. aeruginosa* to protect from colistin toxicity.

NAC-mediated inhibition of *P. aeruginosa* swimming and swarming motility. Transcriptomic results indicated that NAC downregulated two genes belonging to *P. aeruginosa* flagellar apparatus (i.e., *fliF* and *flhF*), which are necessary for the first step

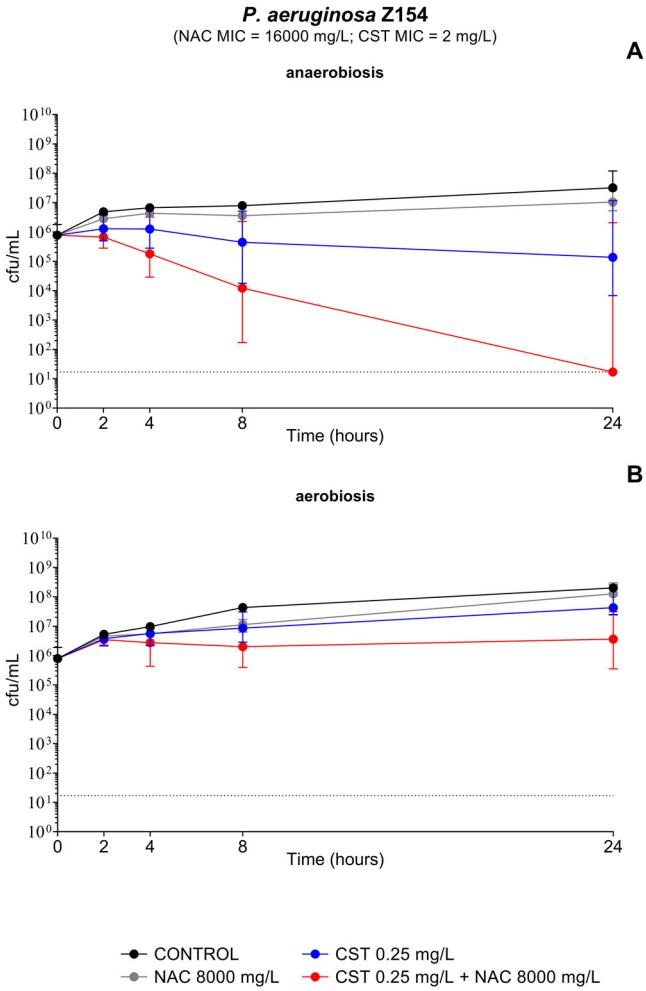

FIG 7 Time-kill curves of *P. aeruginosa* Z154 planktonic cultures exposed to *N*-acetylcysteine (NAC) at 8,000 mg/L, colistin (CST) at 0.25 mg/L, and the NAC-CST combination under anaerobic (A) and aerobic (B) conditions. NAC potentiated the bactericidal activity of colistin only under anaerobic conditions. Data are plotted as the median values of CFU per milliliter for each time point. Dotted lines indicate the detection limit (17 CFU/mL).

of flagellum assembly (36). In order to confirm the potential NAC-induced inhibition of flagellum-mediated motility, we performed classical swimming and swarming tests with the reference strain *P. aeruginosa* PAO1 and the CF strain *P. aeruginosa* Z154 (i.e., the strain used for transcriptomic analysis). *P. aeruginosa* Z154 was not capable of swarming motility under our laboratory conditions, so only the effect of NAC on swimming motility could be tested with this strain.

Overall, the results showed a clear inhibition of both swimming and swarming motility in the presence of NAC at 8,000 mg/L (Fig. 8 and 9). Such inhibition could be related to the downregulation of crucial genes of the flagellar apparatus and/or the induction of a zinc starvation response. Indeed, zinc starvation has been demonstrated to affect the ability of *P. aeruginosa* to express several virulence phenotypes, crucial for the ability of this pathogen to colonize CF lung, including motility, biofilm formation and siderophore synthesis (37).

Conclusions. In conclusion, the results of this study demonstrated a relevant antibiofilm synergism of NAC-colistin combinations (at the high concentrations achievable by inhalation) against *P. aeruginosa*, which would deserve further investigation for potential clinical applications of inhaled formulations. Transcriptomic and biological experiments suggested that NAC inhibited *P. aeruginosa* anaerobic respiration, which could be relevant for the observed antibiofilm synergism with colistin.

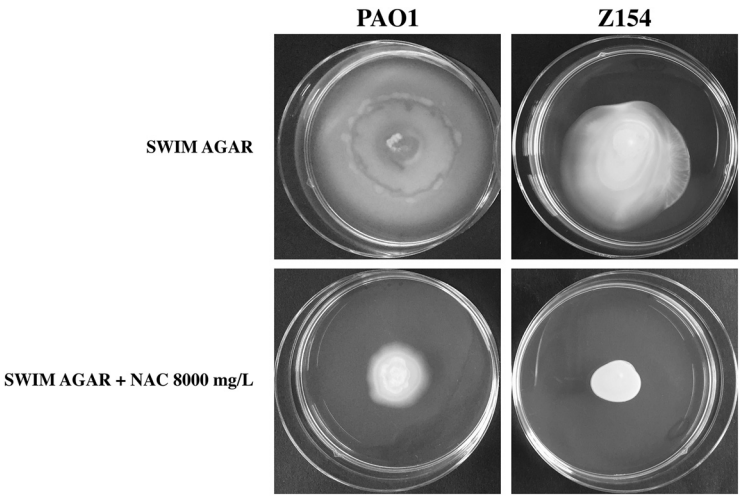

FIG 8 NAC-mediated inhibition of *P. aeruginosa* PAO1 and Z154 swimming motility. Assays were performed in at least three independent experiments (with three replicates per condition per experiment), and representative data are shown.

In addition, although NAC alone was not demonstrated to be effective against preformed *P. aeruginosa* biofilms, transcriptomic analysis of NAC-exposed planktonic cultures revealed that NAC could attenuate *P. aeruginosa* virulence, mainly by inducing a zinc starvation response, affecting anaerobic respiration and inhibiting flagellum-mediated motility (with the last two features confirmed experimentally). In this perspective, NAC, at the high concentrations achievable by inhalation, might have beneficial effects in the very first steps of lung infection, possibly preventing biofilm formation and the establishment of a chronic colonization, which should be further investigated.

MATERIALS AND METHODS

Bacterial strains. Seventeen strains were investigated, including 15 clinical isolates from CF patients, an MDR clinical isolate from a respiratory tract infection (RTI) from an intensive care unit (ICU), and the reference strain, *P. aeruginosa* PAO1 (Table 1). Identification was performed by matrix-assisted laser desorption ionization–time of flight mass spectrometry (MALDI-TOF MS) (Bruker, Shimadzu). Antimicrobial susceptibility was determined using the reference broth microdilution method (38). Whole-genome sequencing of clinical isolates was performed with the Illumina (San Diego, CA, USA) MiSeq platform, using a 2× 150-bp paired-end approach. Raw reads were assembled using SPAdes (39), and draft genomes were used to determine multilocus sequence types (MLSTs) and O types at the Oxford PubMLST site (https://pubmlst.org/) (40) and at the

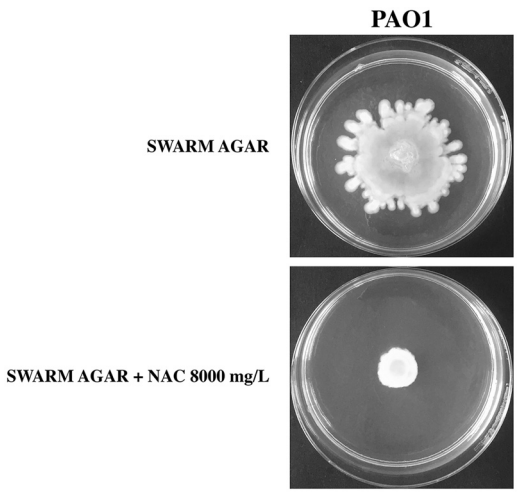

FIG 9 NAC-mediated inhibition of *P. aeruginosa* PAO1 swarming motility. Assays were performed in at least three independent experiments (with three replicates per condition per experiment), and representative data are shown.

Center for Genomic Epidemiology site (https://cge.food.dtu.dk/services/PAst/) (41), respectively. The complete genome of *P. aeruginosa* Z154 was obtained by combining results from Illumina with those obtained using the Oxford Nanopore Technologies (Oxford, United Kingdom) MinION platform, and *de novo* assembly was generated using Unicycler v0.4.4 as previously described (42).

Preparation of culture media. NAC stock solutions (100 g/L) were prepared immediately before use. NAC powder (Zambon, Bresso, Italy) was dissolved in sterile distilled water, the pH was adjusted to 6.5 to 6.8 with NaOH at 10 M, and the solution was filtered through a 0.22-μm-pore membrane filter. All experiments were performed in cation-adjusted Mueller-Hinton broth (CAMHB) (Becton Dickinson, Milan, Italy), unless otherwise specified, starting from an appropriately concentrated medium to avoid broth dilution when NAC solution was used. The artificial sputum medium (ASM) was also used in selected experiments and was prepared as previously described by Kirchner et al. (43).

***In vitro* biofilm susceptibility testing.** Biofilm susceptibility testing was first performed using the Nunc-TSP lid system (Thermo Fisher Scientific, Waltham, MA, USA), as described previously (44). Briefly, biofilms were grown for 24 h in CAMHB at 35°C under static conditions. Preformed biofilms were then exposed to NAC at 8,000 mg/L and colistin (colistin sulfate; Applichem, Darmstadt, Germany) at 2 to 32 mg/L, alone and in combination. The colistin concentration was selected according to preliminary results of antibiofilm susceptibility testing and the colistin MIC for each strain. After 24 h of exposure (i.e., 35°C, static conditions), biofilms were washed twice with 200 μL of phosphate-buffered saline (PBS) (Sigma-Aldrich, Milan, Italy) to remove loosely adherent bacteria, and sessile cells were removed from pegs by sonication for 30 min (Elma Transsonic T 460; Elma, Singen, Germany) in 200 μL of tryptic soy broth (TSB) (Oxoid, Milan, Italy) supplemented with 1% Tween 20 (Sigma-Aldrich) (i.e., the recovery medium). The median number of CFU per peg was then determined by plating 10 μL of appropriate dilutions of the recovery medium onto tryptic soy agar (TSA) (Oxoid) and incubating for 24 h at 35°C (detection limit, 20 CFU/peg). The colony count was also double-checked after 48 h of incubation.

The potential antibiofilm synergism of NAC-colistin combinations was further investigated using an *in vitro* ASM biofilm model (43) in order to mimic *P. aeruginosa* biofilm conditions within the CF mucus. The study was carried out with two selected CF strains (*P. aeruginosa* Z154 and Z34), exhibiting different features (i.e., mucoid/nonmucoid phenotype, antimicrobial susceptibility pattern, MLST, and O type) (Table 1). In brief, biofilms were grown in 2 mL ASM in 24-well plates (Sarstedt, Nümbrecht, Germany), for 72 h at 35°C under static conditions. Preformed biofilms were then exposed to NAC at 8,000 mg/L and colistin at 64 mg/L, alone and in combination. Preliminary experiments carried out with lower colistin concentrations (i.e., 2 to 32 mg/L) did not show evident synergistic antibiofilm activity, while higher colistin concentrations (i.e., >64 mg/L) led to eradication of the biofilm cultures even in the absence of NAC (data not shown). After 24 h of exposure (i.e., 35°C, static conditions), bacterial biofilms were disrupted by 30 min of sonication followed by manual pipetting, and the median number of CFU per milliliter was determined following the same protocol described for the Nunc-TSP lid assay.

Data from both biofilm models were obtained in at least three independent experiments, with at least 12 replicates per condition per experiment.

RNA-seq and transcriptomic analysis. *P. aeruginosa* Z154 (i.e., colistin-susceptible CF strain, mucoid, MDR, ST412, O6) (Table 1) was selected for studies aimed at investigating the transcriptomic response of *P. aeruginosa* to NAC exposure. A CF strain, rather than a reference strain (such as *P. aeruginosa* PAO1), was selected for this analysis because of the known adaptive diversification of *P. aeruginosa* into "specialized" types during chronic/recurrent infections in CF patients (3).

Because these represented the first data on the transcriptomic response of *P. aeruginosa* to NAC exposure, and considering the complex and still largely unknown effects of NAC on microbial physiology, we decided to perform the experiments with planktonic cultures, which represent a more homogenous and better standardized model for transcriptomic studies.

Overnight cultures in CAMHB were diluted at 1:50 in the same medium and incubated at 35°C with agitation to achieve an optical density at 600 nm (OD_{600}) of 1.0. The cells were then exposed to NAC at 8,000 mg/L for 30 min at 35°C under static conditions. Cultures treated in the same way but not exposed to NAC represented the control. Total RNA extraction was performed using the SV total RNA isolation system (Promega, Madison, WI, USA) following the manufacturer's instructions. rRNA depletion, cDNA library construction, and Illumina HiSeq 4000 platform-based transcriptome sequencing (RNA-seq) were performed by Eurofins Genomics Europe Sequencing (Constance, Germany). The transcriptome libraries were single-end sequenced with 50-bp reads for a total of 10 million reads per sample. Bioinformatic analysis was performed using the SeqMan NGen v17.3 software tool (DNASTAR Lasergene, Madison, WI, USA), with default parameters. Reads were aligned using *P. aeruginosa* Z154 complete genome (n = 6,344 coding DNA sequences [CDSs]) as a reference. Differentially expressed genes (DEGs) of the NAC-exposed cultures compared to the control were analyzed considering false-discovery rate (FDR) adjusted P values of <0.05 from DeSeq2. DEGs with a 99% confidence interval (CI) were discussed. Results were obtained from two independent experiments. In order to favor comparison with data present in the literature, genes without a univocal name have been indicated as *P. aeruginosa* PAO1 locus tags throughout the text and reported in Table 2 also as *P. aeruginosa* UCBPP-PA14 locus tags.

NO_3^- and NO_2^- quantification. NAC-mediated inhibition of the denitrification pathway was investigated by measuring the concentration of NO_3^- and NO_2^- in anaerobic cultures of *P. aeruginosa* Z154 (i.e., the strain used for transcriptomic analysis). For this purpose, the Griess nitrite/nitrate colorimetric assay (Cayman Chemicals, Ann Arbor, MI, USA) was used according to the manufacturer's recommendations and as previously described, with some modification (33). CAMHB was supplemented with 10 mM $NaNO_3$ or KNO_2 and allowed to equilibrate for 3 days at 35°C in an anaerobic atmosphere by using the AnaeroGen kit (Oxoid). Overnight cultures were then diluted in 20 mL of each anoxic culture medium to reach a concentration of 10^6 CFU/mL and challenged with NAC at 8,000 mg/L. At times 0, 24, and 48 h of incubation under

anoxic conditions at 35°C, supernatants were harvested and subjected to Griess colorimetric reaction in order to detect NO_3^- and NO_2^- levels. NAC-free cultures represented the control. Experiments were carried out in triplicate with one replicate per time point per condition.

Time-kill assays. Time-kill assays were performed according to CLSI guidelines (45) with the colistin-susceptible strain *P. aeruginosa* Z154 (i.e., the strain used for transcriptomic analysis). Colistin at 0.25 mg/L was tested alone and in combination with NAC at 8,000 mg/L under both aerobic and anaerobic conditions. We decided to use this colistin concentration since a higher concentration led to eradication of the planktonic cultures (data not shown). The medium (CAMHB) used to obtain anoxic cultures was placed under an anaerobic atmosphere by using the AnaeroGen kit (Oxoid) for 3 days prior to use and during the whole experiment. The killing curves were carried out in borosilicate glass bottles with a final volume of 20 mL of CAMHB. At 0, 2, 4, 8, and 24 h of exposure, CFU per milliliter were determined by plating 60 μL of appropriate dilutions of each condition onto TSA and incubating for 24 h at 35°C (detection limit, 17 CFU/mL). Data were obtained from at least four independent experiments with two replicates per condition per experiment.

Motility tests. NAC-induced inhibition of flagellum-mediated motility (i.e., both swimming and swarming motility) was investigated with the reference strain *P. aeruginosa* PAO1, which has been used for similar motility experiments in several previous studies (46), and *P. aeruginosa* Z154 (i.e., the strain used for transcriptomic analysis). *P. aeruginosa* Z154 was not capable of swarming motility under our laboratory conditions (perhaps due to the known reduction of flagellar expression in mucoid CF-adapted strains) (47), so only the effect of NAC on swimming motility could be tested with this strain. Swim plates consisted of Luria-Bertani (LB) broth (Oxoid) containing 0.3% agar (46). Swarm plates consisted of nutrient broth (Oxoid) with 0.5% glucose and 0.5% agar (46). Overnight cultures in CAMHB were diluted in the same medium to a final OD_{600} of 3.0, and 5 μL was spotted onto swim and swarm plates, with or without NAC at 8,000 mg/L. Results were observed after incubation at 35°C for 48 h. Assays were performed in at least three independent experiments with three replicates per condition per experiment.

Statistical analysis. Statistical analysis of biofilm susceptibility assays was performed using GraphPad Prism version 8.0 (San Diego, CA, USA). Multiple-comparison tests were performed by the Kruskal-Wallis test with Dunn's correction. A P value of ≤ 0.05 was considered significant. RNA-seq statistical analysis was performed using the SeqMan NGen v17.3 software tool.

Data availability. The complete genome sequence of *P. aeruginosa* Z154 was deposited in GenBank under accession no. CP069177. RNA-seq data were also deposited in the NCBI Gene Expression Omnibus (GEO) database under accession no. GSE190946.

ACKNOWLEDGMENTS

This work was supported by a research grant from Zambon S.p.A. G.M.R. and L.P. have been Advisory Board members for Zambon S.p.A. and have participated in scientific events financed by Zambon. The remaining authors declare no conflict of interest.

P. aeruginosa strains Z154 and Z152 were kindly provided by Lisa Cariani, Cystic Fibrosis Microbiology Laboratory, IRCCS Fondazione Cà Granda, Ospedale Maggiore Policlinico, Milan, Italy.

REFERENCES

1. Malhotra S, Hayes D, Wozniak DJ. 2019. Cystic fibrosis and *Pseudomonas aeruginosa*: the host-microbe interface. Clin Microbiol Rev 32:e00138-18. https://doi.org/10.1128/CMR.00138-18.
2. Parkins MD, Somayaji R, Waters VJ. 2018. Epidemiology, biology, and impact of clonal *Pseudomonas aeruginosa* infections in cystic fibrosis. Clin Microbiol Rev 31:e00019-18. https://doi.org/10.1128/CMR.00019-18.
3. Rossi E, La Rosa R, Bartell JA, Marvig RL, Haagensen JAJ, Sommer LM, Molin S, Johansen HK. 2021. *Pseudomonas aeruginosa* adaptation and evolution in patients with cystic fibrosis. Nat Rev Microbiol 19:331–342. https://doi.org/10.1038/s41579-020-00477-5.
4. Karaiskos I, Souli M, Galani I, Giamarellou H. 2017. Colistin: still a lifesaver for the 21st century? Expert Opin Drug Metab Toxicol 13:59–71. https://doi.org/10.1080/17425255.2017.1230200.
5. Ding L, Wang J, Cai S, Smyth H, Cui Z. 2021. Pulmonary biofilm-based chronic infections and inhaled treatment strategies. Int J Pharm 604:120768. https://doi.org/10.1016/j.ijpharm.2021.120768.
6. Manos J. 2021. Current and emerging therapies to combat cystic fibrosis lung infections. Microorganisms 9:1874. https://doi.org/10.3390/microorganisms9091874.
7. Pollini S, Di Pilato V, Landini G, Di Maggio T, Cannatelli A, Sottotetti S, Cariani L, Aliberti S, Blasi F, Sergio F, Rossolini GM, Pallecchi L. 2018. *In vitro* activity of *N*-acetylcysteine against *Stenotrophomonas maltophilia* and *Burkholderia cepacia* complex grown in planktonic phase and biofilm. PLoS One 13:e0203941. https://doi.org/10.1371/journal.pone.0203941.
8. Blasi F, Page C, Rossolini GM, Pallecchi L, Matera MG, Rogliani P, Cazzola M. 2016. The effect of *N*-acetylcysteine on biofilms: implications for the treatment of respiratory tract infections. Respir Med 117:190–197. https://doi.org/10.1016/j.rmed.2016.06.015.
9. Pollini S, Boncompagni S, Di Maggio T, Di Pilato V, Spanu T, Fiori B, Blasi F, Aliberti S, Sergio F, Rossolini GM, Pallecchi L. 2018. *In vitro* synergism of colistin in combination with *N*-acetylcysteine against *Acinetobacter baumannii* grown in planktonic phase and in biofilms. J Antimicrob Chemother 73:2388–2395. https://doi.org/10.1093/jac/dky185.
10. Ciacci N, Boncompagni S, Valzano F, Cariani L, Aliberti S, Blasi F, Pollini S, Rossolini GM, Pallecchi L. 2019. *In vitro* synergism of colistin and *N*-acetylcysteine against *Stenotrophomonas maltophilia*. Antibiotics 8:101. https://doi.org/10.3390/antibiotics8030101.
11. Tenório MCDS, Graciliano NG, Moura FA, de Oliveira ACM, Goulart MOF. 2021. *N*-Acetylcysteine (NAC): impacts on human health. Antioxidants 10:967. https://doi.org/10.3390/antiox10060967.
12. Boisson M, Jacobs M, Grégoire N, Gobin P, Marchand S, Couet W, Mimoz O. 2014. Comparison of intrapulmonary and systemic pharmacokinetics of colistin methanesulfonate (CMS) and colistin after aerosol delivery and intravenous administration of CMS in critically ill patients. Antimicrob Agents Chemother 58:7331–7339. https://doi.org/10.1128/AAC.03510-14.
13. Shen Y, Li P, Chen X, Zou Y, Li H, Yuan G, Hu H. 2020. Activity of sodium lauryl sulfate, rhamnolipids, and *N*-acetylcysteine against biofilms of five common pathogens. Microb Drug Resist 26:290–299. https://doi.org/10.1089/mdr.2018.0385.

14. Belfield K, Bayston R, Hajduk N, Levell G, Birchall JP, Daniel M. 2017. Evaluation of combinations of putative anti-biofilm agents and antibiotics to eradicate biofilms of *Staphylococcus aureus* and *Pseudomonas aeruginosa*. J Antimicrob Chemother 72:2531–2538. https://doi.org/10.1093/jac/dkx192.
15. Huang JX, Blaskovich MAT, Pelingon R, Ramu S, Kavanagh A, Elliott AG, Butler MS, Montgomery AB, Cooper MA. 2015. Mucin binding reduces colistin antimicrobial activity. Antimicrob Agents Chemother 59:5925–5931. https://doi.org/10.1128/AAC.00808-15.
16. Diaz Iglesias Y, Van Bambeke F. 2020. Activity of antibiotics against *Pseudomonas aeruginosa* in an *in vitro* model of biofilms in the context of cystic fibrosis: influence of the culture medium. Antimicrob Agents Chemother 64:e02204-19. https://doi.org/10.1128/AAC.02204-19.
17. Kandari D, Joshi H, Bhatnagar R. 2021. Zur: zinc-sensing transcriptional regulator in a diverse set of bacterial species. Pathogens 10:344. https://doi.org/10.3390/pathogens10030344.
18. Ducret V, Abdou M, Goncalves MC, Leoni S, Martin-Pelaud O, Sandoz A, Segovia CI, Tercier-Waeber M-L, Valentini M, Perron K. 2021. Global analysis of the zinc homeostasis network in *Pseudomonas aeruginosa* and its gene expression dynamics. Front Microbiol 12:739988. https://doi.org/10.3389/fmicb.2021.739988.
19. Lhospice S, Gomez NO, Ouerdane L, Brutesco C, Ghssein G, Hajjar C, Liratni A, Wang S, Richaud P, Bleves S, Ball G, Borezée-Durant E, Lobinski R, Pignol D, Arnoux P, Voulhoux R. 2017. *Pseudomonas aeruginosa* zinc uptake in chelating environment is primarily mediated by the metallophore pseudopaline. Sci Rep 7:17132. https://doi.org/10.1038/s41598-017-16765-9.
20. Schalk IJ, Cunrath O. 2016. An overview of the biological metal uptake pathways in *Pseudomonas aeruginosa*. Environ Microbiol 18:3227–3246. https://doi.org/10.1111/1462-2920.13525.
21. Pederick VG, Eijkelkamp BA, Begg SL, Ween MP, McAllister LJ, Paton JC, McDevitt CA. 2015. ZnuA and zinc homeostasis in *Pseudomonas aeruginosa*. Sci Rep 5:13139. https://doi.org/10.1038/srep13139.
22. Haas CE, Rodionov DA, Kropat J, Malasarn D, Merchant SS, de Crécy-Lagard V. 2009. A subset of the diverse COG0523 family of putative metal chaperones is linked to zinc homeostasis in all kingdoms of life. BMC Genomics 10:470. https://doi.org/10.1186/1471-2164-10-470.
23. Kamal SM, Rybtke ML, Nimtz M, Sperlein S, Giske C, Trček J, Deschamps J, Briandet R, Dini L, Jänsch L, Tolker-Nielsen T, Lee C, Römling U. 2019. Two FtsH proteases contribute to fitness and adaptation of *Pseudomonas aeruginosa* clone C strains. Front Microbiol 10:1372. https://doi.org/10.3389/fmicb.2019.01372.
24. Heacock-Kang Y, Sun Z, Zarzycki-Siek J, Poonsuk K, McMillan IA, Chuanchuen R, Hoang TT. 2018. Two regulators, PA3898 and PA2100, modulate the *Pseudomonas aeruginosa* multidrug resistance MexAB-OprM and EmrAB efflux pumps and biofilm formation. Antimicrob Agents Chemother 62:e01459-18. https://doi.org/10.1128/AAC.01459-18.
25. Hare NJ, Scott NE, Shin EHH, Connolly AM, Larsen MR, Palmisano G, Cordwell SJ. 2011. Proteomics of the oxidative stress response induced by hydrogen peroxide and paraquat reveals a novel AhpC-like protein in *Pseudomonas aeruginosa*. Proteomics 11:3056–3069. https://doi.org/10.1002/pmic.201000807.
26. Landini G, Di Maggio T, Sergio F, Docquier J-D, Rossolini GM, Pallecchi L. 2016. Effect of high *N*-acetylcysteine concentrations on antibiotic activity against a large collection of respiratory pathogens. Antimicrob Agents Chemother 60:7513–7517. https://doi.org/10.1128/AAC.01334-16.
27. Rossi E, Falcone M, Molin S, Johansen HK. 2018. High-resolution *in situ* transcriptomics of *Pseudomonas aeruginosa* unveils genotype independent patho-phenotypes in cystic fibrosis lungs. Nat Commun 9:3459. https://doi.org/10.1038/s41467-018-05944-5.
28. Borrero-de Acuña JM, Rohde M, Wissing J, Jänsch L, Schobert M, Molinari G, Timmis KN, Jahn M, Jahn D. 2016. Protein network of the *Pseudomonas aeruginosa* denitrification apparatus. J Bacteriol 198:1401–1413. https://doi.org/10.1128/JB.00055-16.
29. Kolpen M, Appeldorff CF, Brandt S, Mousavi N, Kragh KN, Aydogan S, Uppal HA, Bjarnsholt T, Ciofu O, Høiby N, Jensen PØ. 2016. Increased bactericidal activity of colistin on *Pseudomonas aeruginosa* biofilms in anaerobic conditions. Pathog Dis 74:ftv086. https://doi.org/10.1093/femspd/ftv086.
30. Thöming JG, Tomasch J, Preusse M, Koska M, Grahl N, Pohl S, Willger SD, Kaever V, Müsken M, Häussler S. 2020. Parallel evolutionary paths to produce more than one *Pseudomonas aeruginosa* biofilm phenotype. NPJ Biofilms Microbiomes 6:2. https://doi.org/10.1038/s41522-019-0113-6.
31. Morita Y, Cao L, Gould VC, Avison MB, Poole K. 2006. *nalD* encodes a second repressor of the *mexAB-oprM* multidrug efflux operon of *Pseudomonas aeruginosa*. J Bacteriol 188:8649–8654. https://doi.org/10.1128/JB.01342-06.
32. Lim CK, Hassan KA, Penesyan A, Loper JE, Paulsen IT. 2013. The effect of zinc limitation on the transcriptome of *Pseudomonas protegens* Pf-5. Environ Microbiol 15:702–715. https://doi.org/10.1111/j.1462-2920.2012.02849.x.
33. Kolpen M, Kragh KN, Bjarnsholt T, Line L, Hansen CR, Dalbøge CS, Hansen N, Kühl M, Høiby N, Jensen PØ. 2015. Denitrification by cystic fibrosis pathogens—*Stenotrophomonas maltophilia* is dormant in sputum. Int J Med Microbiol 305:1–10. https://doi.org/10.1016/j.ijmm.2014.07.002.
34. Pompilio A, Crocetta V, Pomponio S, Fiscarelli E, Di Bonaventura G. 2015. *In vitro* activity of colistin against biofilm by *Pseudomonas aeruginosa* is significantly improved under "cystic fibrosis-like" physicochemical conditions. Diagn Microbiol Infect Dis 82:318–325. https://doi.org/10.1016/j.diagmicrobio.2015.01.006.
35. Brochmann RP, Toft A, Ciofu O, Briales A, Kolpen M, Hempel C, Bjarnsholt T, Høiby N, Jensen PØ. 2014. Bactericidal effect of colistin on planktonic *Pseudomonas aeruginosa* is independent of hydroxyl radical formation. Int J Antimicrob Agents 43:140–147. https://doi.org/10.1016/j.ijantimicag.2013.10.015.
36. Bouteiller M, Dupont C, Bourigault Y, Latour X, Barbey C, Konto-Ghiorghi Y, Merieau A. 2021. *Pseudomonas* flagella: generalities and specificities. Int J Mol Sci 22:3337. https://doi.org/10.3390/ijms22073337.
37. Mastropasqua MC, Lamont I, Martin LW, Reid DW, D'Orazio M, Battistoni A. 2018. Efficient zinc uptake is critical for the ability of *Pseudomonas aeruginosa* to express virulence traits and colonize the human lung. J Trace Elem Med Biol 48:74–80. https://doi.org/10.1016/j.jtemb.2018.03.009.
38. Clinical and Laboratory Standards Institute. 2018. Methods for dilution antimicrobial susceptibility tests for bacteria that grow aerobically: M07-A1111. Committee for Clinical Laboratory Standards, Wayne, PA.
39. Bankevich A, Nurk S, Antipov D, Gurevich AA, Dvorkin M, Kulikov AS, Lesin VM, Nikolenko SI, Pham S, Prjibelski AD, Pyshkin AV, Sirotkin AV, Vyahhi N, Tesler G, Alekseyev MA, Pevzner PA. 2012. SPAdes: a new genome assembly algorithm and its applications to single-cell sequencing. J Comput Biol 19:455–477. https://doi.org/10.1089/cmb.2012.0021.
40. Jolley KA, Bray JE, Maiden MCJ. 2018. Open-access bacterial population genomics: BIGSdb software, the PubMLST.org website and their applications. Wellcome Open Res 3:124. https://doi.org/10.12688/wellcomeopenres.14826.1.
41. Thrane SW, Taylor VL, Lund O, Lam JS, Jelsbak L. 2016. Application of whole-genome sequencing data for O-specific antigen analysis and *in silico* serotyping of *Pseudomonas aeruginosa* isolates. J Clin Microbiol 54:1782–1788. https://doi.org/10.1128/JCM.00349-16.
42. Di Pilato V, Aiezza N, Viaggi V, Antonelli A, Principe L, Giani T, Luzzaro F, Rossolini GM. 2020. KPC-53, a KPC-3 variant of clinical origin associated with reduced susceptibility to ceftazidime-avibactam. Antimicrob Agents Chemother 65:e01429-20. https://doi.org/10.1128/AAC.01429-20.
43. Kirchner S, Fothergill JL, Wright EA, James CE, Mowat E, Winstanley C. 2012. Use of artificial sputum medium to test antibiotic efficacy against *Pseudomonas aeruginosa* in conditions more relevant to the cystic fibrosis lung. J Vis Exp https://doi.org/10.3791/3857.
44. Harrison JJ, Stremick CA, Turner RJ, Allan ND, Olson ME, Ceri H. 2010. Microtiter susceptibility testing of microbes growing on peg lids: a miniaturized biofilm model for high-throughput screening. Nat Protoc 5:1236–1254. https://doi.org/10.1038/nprot.2010.71.
45. National Committee for Clinical Laboratory Standards, Barry AL. 1999. Methods for determining bactericidal activity of antimicrobial agents: approved guideline. National Committee for Clinical Laboratory Standards, Wayne, PA.
46. Rashid MH, Kornberg A. 2000. Inorganic polyphosphate is needed for swimming, swarming, and twitching motilities of *Pseudomonas aeruginosa*. Proc Natl Acad Sci U S A 97:4885–4890. https://doi.org/10.1073/pnas.060030097.
47. Folkesson A, Jelsbak L, Yang L, Johansen HK, Ciofu O, Høiby N, Molin S. 2012. Adaptation of *Pseudomonas aeruginosa* to the cystic fibrosis airway: an evolutionary perspective. Nat Rev Microbiol 10:841–851. https://doi.org/10.1038/nrmicro2907.